Homeomorphism Groups of Fractals

A Senior Project submitted to
The Division of Science, Mathematics, and Computing
of
Bard College

by
Shuyi Weng
翁舒逸

Annandale-on-Hudson, New York
May, 2015

Abstract

Fractals are geometric objects that often arise from the study of dynamical systems. Besides their beautiful structures, they have unusual geometric properties that mathematicians are interested in. People have studied the homeomorphism groups of various fractals. In 1965, Thompson introduced the Thompson groups $F \subseteq T \subseteq V$, which are groups of piecewise-linear homeomorphisms on the unit interval, the unit circle, and the Cantor set, respectively. Louwsma has shown that the homeomorphism group of the Sierpinski gasket is D_3. More recently, Belk and Forrest investigated a group of piecewise-linear homeomorphisms on the Basilica, which is the Julia set associated with the quadratic polynomial $z^2 - 1$. Weinrich-Burd and Smith, respectively, have studied the Julia sets for the maps $\phi(z) = z^{-2} - 1$ and $\psi(z) = z^2 + i$, and presented Thompson-like groups acting on these Julia sets.

In this project, we study the Julia set associated with the rational function $f(z) = (z^2 + 1)/(z^2 - 1)$. We construct a fractal E_4 that has the same geometric structure as the Julia set, and show that the homeomorphism group of E_4 is $D_4 \times \mathbb{Z}/2$. We construct another fractal E_3 with the same local structure as E_4. We prove that the homeomorphism group of E_3 is finitely generated, and show a finite presentation for this group. Furthermore, we show that this group contains an index-2 Kleinian subgroup. Finally, we give a geometric presentation of this group, and describe the limit set of this group acting on the Riemann sphere. The limit set appears to be homeomorphic to the E_3 fractal.

Contents

List of Figures

Dedication

To My Parents

致父母

Acknowledgments

I would like to offer my greatest gratitude to my project advisor, Jim Belk, without whom this project would never become a reality. With his contagious passion in mathematics, Jim has got me interested in fractals since my sophomore year. Jim's enthusiasm, encouragement, and clarity has been a great motive force to keep me moving forward on research throughout this project.

The rest of the mathematics program has been an irreplaceable part of my experience as a Bardian. I want to acknowledge their support, especially in my senior year. I want to thank John for the amazing courses and conversations we had together. Thanks to Ethan, who instructed my first proof-based course in mathematics and settled my aspiration to become a math major. Many thanks goes to Maria for generously lending me Jim for project advising. I wish I had a course with you in the past four years. The mutual support from my classmates has been a great encouragement. Thanks to all my classmates, especially Galen, Noah, Nicole, and Xingye.

Although this is not a chemistry project, I still want to acknowledge my friends in the chemistry department. You make up an important part of my undergraduate experience. I would especially like to thank Emily McLaughlin, my academic advisor, who has been encouraging me throughout the past month when the extreme tension strikes. Thanks to Olja, Seoyoung, Anuska, and Kody for being a productive company striving for senior projects in the cheminar room.

Special thanks goes to my housemates, Zhe Mei and Zexi Song. I would not be able to generate the nice figures in my senior project without your technical support, given that the graphing software on my computer broke down five days before the due date.

I can keep going on and on for the list of people I would like to acknowledge. There have been so many awesome souls that I came across in the past four years, but I need to stop at some point. Last but not least, thanks to my parents, for their constant support in the past 22 years. I love you both.

Introduction

To see a world in a grain of sand,
And a heaven in a wild flower,
Hold infinity in the palm of your hand,
And eternity in an hour.

William Blake, *Auguries of Innocence*

Fractals are geometric objects that exhibit repeating patterns at every scale. In this project, we study the symmetry of several related fractals. There are many ways to construct a fractal. The fractals we consider are constructed through *iterated function systems*, *Julia sets* of rational functions, and *limit sets* of Kleinian groups.

A *homeomorphism* is a continuous bijection between topological spaces whose inverse is also continuous. A homeomorphism defined from a topological space T to itself can be viewed as a symmetry of T. The *homeomorphism group* of a topological space T is the group of all homeomorphisms $\varphi\colon T \to T$ under function composition. Mathematicians have been interested in the homeomorphisms and homeomorphism groups of fractals because of the unusual geometric and topological properties they possess. In particular, new group structures have been emerging from the homeomorphism groups of fractals. Richard Thompson introduced the Thompson

groups $F \subseteq T \subseteq V$ in 1965. The Thompson groups F, T, and V are piecewise linear homeomorphisms of the unit interval, the unit circle, and the Cantor set, respectively [7]. The Thompson group V is an early case of an interesting subgroup of the homeomorphism group of a fractal structure. It is then natural to apply this idea to some other fractals. More recently, Belk and Forrest [4] have studied the Basilica in detail, which is the Julia set associated with the complex analytic map $f(z) = z^2 - 1$. They defined a group T_B analogous to the Thompson groups, which acts as "piecewise linear" homeomorphisms of the Basilica. They proved that the group T_B they constructed is finitely generated, and the commutator subgroup is simple. Similar to Belk and Forrest's work, Weinrich-Burd [26] and Smith [25] have also described Thompson-like groups acting on the Bubble Bath Julia set and the dendrite Julia sets. In each case, the Thompson-like groups are countable, even though the full homeomorphism group of the fractals are uncountable.

There are yet countable homeomorphism groups of fractals. These types of fractals are "rigid" in the sense that they usually have rigid local connection patterns. One of these fractals is the Sierpinski gasket. In 2004, Louwsma has shown in an unpublished paper [16] that the full homeomorphism group of the Sierpinski gasket is the dihedral group D_3. However, the Apollonian gasket, with the same local structure as the Sierpinski gasket but having a different global structure, was well-known to mathematicians as the limit set of a Kleinian group [20]. A Kleinian group acts on its own limit set by homeomorphisms. We show in Chapter 3 of this project that

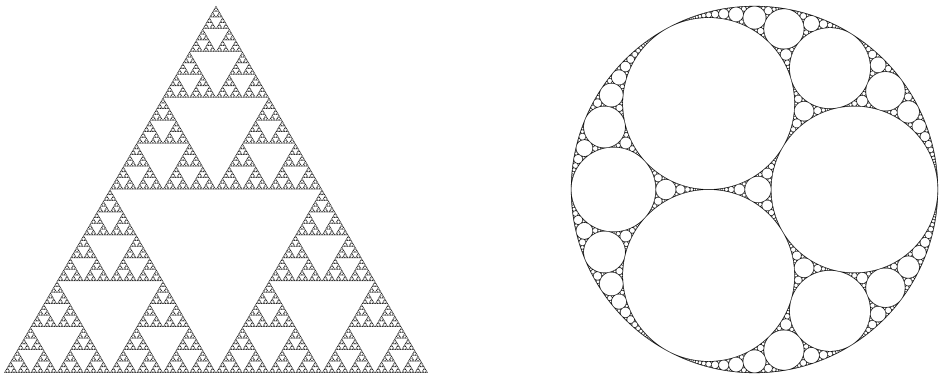

Figure 0.0.1: The Sierpinski Gasket and the Apollonian Gasket

the full homeomorphism group of the Apollonian gasket is countable, and it contains an index-2 Kleinian subgroup. This is an interesting phenomenon, where two fractals with the same local structure have completely different homeomorphism groups. We will address this phenomenon in this project.

There exists a rational function Julia set homeomorphic to the Sierpinski gasket [9, 13]. A modification on the global structure of the Sierpinski gasket makes the Apollonian gasket, whose full homeomorphism group becomes countably infinite. Does this phenomenon happen with other rational Julia sets with finite homeomorphism groups? In Chapter 4 of [26], Weinrich-Burd investigated several rational Julia sets that he conjectured to have finite full homeomorphism groups. Among these Julia sets, the one associated with the rational map $f(z) = (z^2+1)/(z^2-1)$ attracts our attention. This Julia set is shown in Figure 0.0.2, and we refer to this Julia set as E_4. In this project, we describe the structure of E_4 using a hypergraph replacement system with a base graph (global structure) and a replacement rule (local structure). Then we construct another fractal E_3, which has the same replacement rule as E_4 but a modified base graph. We show that the homeomorphism group of E_3 is infinite, and we show finite generation of the homeomorphism group of E_3 by a set of four generators. In addition, we prove that full homeomorphism group of E_4 is isomorphic to the finite group $D_4 \times \mathbb{Z}/2$.

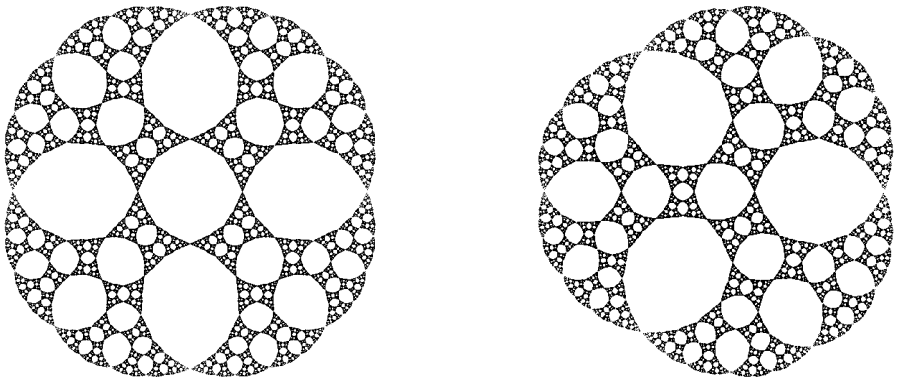

Figure 0.0.2: The E_4 and E_3 Fractals

In order to find a presentation of the homeomorphism group of E_3, we construct a polyhedral complex that represents the structure of E_3. We then consider the dual tree of the polyhedral complex, which we refer to as the structural tree of E_3. The homeomorphism group of E_3 acts on the tree, which allows us to use Bass-Serre theory [18] to find a presentation for the homeomorphism group of E_3.

The Apollonian gasket is a limit set of a Kleinian group [20]. Because the Julia set associated with the rational function $f(z) = (z^2+1)/(z^2-1)$ also appears to have tangent complementary regions, we propose the question whether the E_3 fractal is homeomorphic to a limit set. We attempt to find a group of Möbius transformations and anti-Möbius transformations isomorphic to a quotient the homeomorphism group of E_3. There turns out to be a one-parameter family of groups with such properties. We show that, up to conjugacy, there is a unique group K_+ in this family, whose limit set appear to be homeomorphic to the E_3 fractal. Furthermore, we find a nice conjugator acting on this group so that the generators of this group have well-understood geometric interpretations on the Riemann sphere.

Note that the visual structure of the rational function Julia set associated with $f(z) = (z^2 + 1)/(z^2 - 1)$ is described by the hypergraph replacement system. We have not proved that the actual Julia set is homeomorphic to the E_4 fractal. It is generally a hard thing to show any geometric structure is homeomorphic to a Julia set, which is an abstractly defined object in

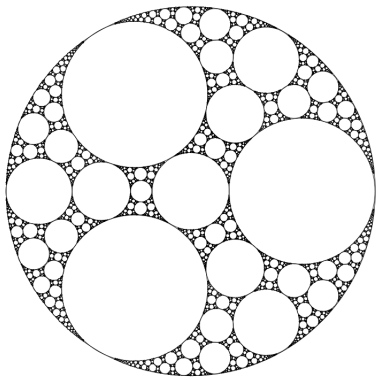

Figure 0.0.3: The Limit Set of the Kleinian Group K_+

complex dynamical systems. One can use techniques provided in Chapter 2 of [26] to accomplish that. The E_3 fractal is a global modification of E_4, and it appears to have the same structure as the Julia set associated with algebraic function $g(z) = f(z^{3/4})^{4/3}$. However, this algebraic function is multi-valued on the Riemann sphere. We do not understand the dynamics of this function well, neither is its associated Julia set well-understood. There are rational functions defined on the Riemann sphere that have associated Julia sets homeomorphic to the Sierpinski gasket and the Apollonian gasket [9,13,15]. The inverse problem for the E_3 fractal is not resolved yet. One may conjecture that there exist a rational function whose Julia set is isomorphic to the E_3 fractal.

This project is organized into six chapters. In Chapter 1, we present preliminaries about dynamical systems, general topology, and Kleinian groups. Chapter 2 gives more background on fractals. We introduce the construction and some of the properties of the Cantor set, the Sierpinski gasket, and Julia sets. In Chapter 3, we present a hypergraph replacement system to define the Apollonian gasket, and show finite generation of its homeomorphism group. Similar to the structure of Chapter 3, we define the E_4 and the E_3 fractals in Chapter 4, and show finite generation of the homeomorphism group of E_3. In Chapter 5, we present some useful background of Bass-Serre theory. We define structural complexes and structural trees of the Apollonian gasket and the E_3 fractal, respectively, and find presentations for their homeomorphism groups using Bass-Serre theory. Furthermore, a structural complex of the E_4 is constructed and used to show that the homeomorphism group of E_4 is a finite group $D_4 \times \mathbb{Z}/2$. The final chapter investigates the geometric representation of the homeomorphism group of E_3. We show that this group has an index-2 Kleinian subgroup, and give the limit set of this group acting on the Riemann sphere. Furthermore, we present a conjugated version of this homeomorphism group, whose geometric interpretation appears to be more intuitive. The limit set of the conjugated Kleinian group is also shown in the last chapter, and these two limit sets are homeomorphic to each other.

1
Preliminaries and Background

1.1 Dynamical Systems

Dynamical systems is a study on the evolution of different systems over time. It started as a science aiming to describe the change of physical systems. The n-body problem is a classical example of a dynamical system. It is widely applied in predicting the motions of celestial objects under their gravitational influences. Solving the problem has been motivated by the desire to understand the relative motions within the solar system as well as multiple star systems and galaxies. In the late 19th century, King Oscar II of Sweden established a prize for anyone who could find the solution to the n-body problem. The prize was awarded to Henri Poincaré in 1887, even though he did not solve the problem. Instead, he showed that there is no analytical solution to the three-body problem. He further discovered that a small perturbation in initial conditions can lead to dramatic difference in the motion of the bodies, even though the system is governed solely by motion and gravitation. Poincaré's contributions on the n-body problem eventually lead to the development of *chaos theory*. Sensitivity to initial conditions, popularly referred to as the "butterfly effect", is a characteristic of dynamical systems. Generally speaking,

a *dynamical system* is a set of deterministic rules acting on a collection of objects that leads to chaotic behaviors.

Definition 1.1.1. A **dynamical system** is an ordered pair (X, ϕ), where X is a topological space and ϕ is a map $\phi : X \longrightarrow X$. The topological space X is called the **state space** of the dynamical system.

To deliver mathematical intuition on dynamical system, we consider the squaring of numbers. If we start with the number 1, and keeps squaring it, we will always get 1 back no matter how many times we apply the squaring function. However, if, instead of starting at 1, we start with the number 1.01, which is only slightly different, we would obtain 26612.6 after ten times of squaring. In this example, the state space of the squaring system is the real numbers $\mathbb{R}$, and the map for the dynamical system is clearly the function $\phi(x) = x^2$ defined on $\mathbb{R}$.

Definition 1.1.2. Given a dynamical system (X, ϕ) and a point $x_0 \in X$, the **orbit** of x_0 is the set

$$\{x_0, \phi(x_0), \phi^2(x_0), \phi^3(x_0), \dots\}.$$

The starting point x_0 of an orbit is the **initial value**, and the n-th iteration of the map ϕ applied to the initial value is often referred to as $x_n = \phi^n(x_0)$.

In the example of the squaring dynamical system, the orbits of the initial values 1 and 1.01 are examined and listed below.

$$\text{orbit of } 1 = \{1, 1, 1, 1, 1, 1, 1, 1, 1, 1, 1, \dots\}$$

$$\text{orbit of } 1.01 = \{1.01, 1.0201, 1.0406, 1.08286, 1.17258, 1.37494, 1.89046,$$

$$3.57385, 12.7724, 163.134, 26612.6, \dots\}$$

We observe that the difference in the orbits of 1 and 1.01 starts to be prominent after seven iterations of the squaring function, and after that point, the difference grows larger and larger. In fact, the orbits of 1 and 1.01 have different behaviors. If we make the orbit into a sequence

$\{x_0, x_1, x_2, \dots\}$, the orbit of 1 is a *converging* sequence, and the limit of the orbit is 1. On the other hand, the orbit of 1.01 is *diverging* to infinity.

We also notice that the orbit of 1 is simply repeating 1's, which is very special. We define the points that map to themselves in a dynamical system *fixed points*.

Definition 1.1.3. Given a dynamical system (X, ϕ), a point $x_0 \in X$ is a **fixed point** if $\phi(x_0) = x_0$.

Example 1.1.4. We extend the squaring map to the complex plane $\mathbb{C}$. Let $f : \mathbb{C} \longrightarrow \mathbb{C}$ be the map defined by $f(z) = z^2$ for all $z \in \mathbb{C}$. The map f takes in a complex number z, squares its norm and doubles its angle as the output. There are two fixed points of the map f, namely 0 and 1. We may investigate some more orbits under the map f.

Let $\alpha = e^{2i\pi/5}$, $\beta = i$, and $\gamma = e^{\pi/12}$. The orbits of them, respectively, are

$$\text{orbit of } \alpha = \{e^{2i\pi/5}, e^{4i\pi/5}, e^{8i\pi/5}, e^{6i\pi/5}, e^{2i\pi/5}, e^{4i\pi/5}, e^{8i\pi/5}, e^{6i\pi/5}, \dots\}$$

$$\text{orbit of } \beta = \{i, -1, 1, 1, 1, 1, 1, \dots\}$$

$$\text{orbit of } \gamma = \{e^{\pi/12}, e^{\pi/6}, e^{\pi/3}, e^{2\pi/3}, e^{4\pi/3}, e^{2\pi/3}, e^{4\pi/3}, e^{2\pi/3}, e^{4\pi/3}, \dots\}$$

In the orbit of α, we see four points repeating themselves under the map f. The orbit of β falls on a fixed point and keeps repeating that fixed point. Similarly, the orbit of γ falls in a cycle of two points and repeats them.

Definition 1.1.5. Given a dynamical system (X, ϕ), a **periodic point** is a point $p \in X$ such that $\phi^n(p) = p$ for some $n \in \mathbb{N}$. The number n is the **period** of p. The orbit $\{p, \phi(p), \dots, \phi^{n-1}(p)\}$ of a periodic point with period n is an n**-cycle**.

Definition 1.1.6. Given a dynamical system (X, ϕ), a point $p \in X$ is **pre-fixed** if there exist $k \in \mathbb{N}$ such that $\phi^k(p)$ is a fixed point of ϕ; a point $q \in X$ is **pre-periodic** if there exist $j \in \mathbb{N}$ such that $\phi^j(q)$ is a periodic point of ϕ.

In Example 1.1.4, the points $\alpha = e^{2i\pi/5}$, $\beta = i$, and $\gamma = e^{\pi/12}$ are, periodic with period 4, pre-fixed, and pre-periodic, respectively.

Definition 1.1.7. Given a dynamical system (X, ϕ), and let p be a fixed point of ϕ. We say p is **attracting** if there exist a deleted neighborhood P of p such that for all $x \in P$, the orbit of x converges to p, and p is **repelling** if there exist an neighborhood U of p such that every neighborhood $V \subseteq U$ of p contains a point $x \in V$ such that the orbit of x is not bounded by U. The definitions naturally extend to cycles.

In Example 1.1.4, we know that the point 1.01 has an orbit that diverges to infinity. We investigate a deleted neighborhood S of the fixed point 1. For $z \in S$ such that $\|z\| < 1$, the orbit converges to the other fixed point 0 because the norm gets squared in each iteration; for $z \in S$ such that $\|z\| > 1$, the orbit diverges to infinity; for $z \in S$ such that $\|z\| = 1$, the situation is slightly more complicated (explain the pre-fixed points in the neighborhood...). We may now conclude that 1 is a repelling fixed point.

Definition 1.1.8. The **basin of attraction** of an attracting fixed point p is an open set U such that every $x \in U$ has an orbit converging to p.

1.2 Homeomorphisms

Homeomorphism is a central topic of this paper. We will primarily use [21] to build the basic ideas of continuous functions and homeomorphisms in this section, and then the quotient topology in the next section. Readers are assumed to have familiarity with the basics of topological spaces.

We consider a function $f : \mathbb{R} \to \mathbb{R}$. In analysis, the continuity of a real-valued function is given by the "ϵ-δ definition". The continuity of a function in topology is, however, defined via open sets.

Definition 1.2.1. Let X and Y be topological spaces. A function $f : X \to Y$ is **continuous** if for each open subset V of Y, its preimage $f^{-1}(V)$ is open in X.

The following lemma shows that this definition is equivalent to the "ϵ-δ definition" in analysis, and therefore, common continuous functions in analysis are also continuous functions in topology.

Lemma 1.2.2. *Let $f : \mathbb{R} \to \mathbb{R}$ be a real-valued function of one real variable. Then f is a continuous function if and only if for all $x_0 \in \mathbb{R}$ and for any given $\epsilon > 0$, there exist $\delta > 0$ such that $|x - x_0| < \delta$ implies $|f(x) - f(x_0)| < \epsilon$.*

Proof. Suppose that f is continuous. Let $x_0 \in \mathbb{R}$, and let $\epsilon > 0$. Let V be the open interval $(f(x_0) - \epsilon, f(x_0) + \epsilon)$. By continuity, $U = f^{-1}(V)$ is an open set containing x_0. Thus there exist $\delta > 0$ such that the interval $(x_0 - \delta, x_0 + \delta)$ is contained in U. Therefore, $|x - x_0| < \delta$ implies that $|f(x) - f(x_0)| < \epsilon$.

Suppose that for all $x_0 \in \mathbb{R}$ and for any given $\epsilon > 0$, there exist $\delta > 0$ such that $|x - x_0| < \delta$ implies $|f(x) - f(x_0)| < \epsilon$. Let V be an open set of $\mathbb{R}$, and let $U = f^{-1}(V)$. If $U = \varnothing$, it follows that U is open. Suppose that U is not empty. Let $x_0 \in U$. Then there exist $\delta > 0$ such that the interval $X = (x_0 - \delta, x_0 + \delta)$ is entirely contained in U. Thus $f(X)$ is contained in V. Let $\mathcal{A} = \{(x_0 - \delta, x_0 + \delta) \mid x_0 \in U, \delta > 0 \text{ such that } (x_0 - \delta, x_0 + \delta) \subseteq U\}$, and let $S = \bigcup_{X \in \mathcal{A}} X$. It follows that S is open in $\mathbb{R}$, and $S \subseteq U$. Because S contains all $x_0 \in U$, it follows that $U \subseteq S$. Therefore, $U = S$ is open, and f is continuous. □

The "ϵ-δ definition" of continuity in analysis can also apply to continuity at a single point. There is an analogous definition in topology.

Definition 1.2.3. Let X and Y be topological spaces, and let $f : X \to Y$ be a function. Let x be a point in X. We say that f is **continuous at the point** x if for any neighborhood V of $f(x)$, there exist a neighborhood U of x such that $f(U) \subseteq V$.

With the notion of continuous functions, we are now ready to define homeomorphisms.

Definition 1.2.4. Let X and Y be topological spaces, and let $f : X \longrightarrow Y$ be a bijective function. If both the function f and its inverse function $f^{-1} : Y \longrightarrow X$ are continuous, then we say that f is a **homeomorphism**. The spaces X and Y are said to be **homeomorphic** if there exist a homeomorphism between them.

If two topological spaces are homeomorphic, they are considered the same from a topological point of view.

Example 1.2.5. The open interval $(0, 1)$ and the real line $\mathbb{R}$ are homeomorphic with the homeomorphism $f : (0, 1) \longrightarrow \mathbb{R}$ defined by

$$f(x) = \tan(\pi x - \pi/2).$$

The continuity of f is guaranteed by the continuity of the tangent function within each of its periods. Its inverse function $f^{-1} : \mathbb{R} \longrightarrow (0, 1)$ given by

$$f^{-1}(x) = \frac{\tan^{-1}(x) + \pi/2}{\pi}$$

is also continuous because the inverse tangent function is continuous over $\mathbb{R}$. In addition, both functions f and f^{-1} are bijective.

A continuous bijective function $f : X \longrightarrow Y$ is not necessarily a homeomorphism. The continuity of both the original function and its inverse function is required for the function to be a homeomorphism. The following is an example of such type of function.

Example 1.2.6. Let S^1 denote the unit circle

$$S^1 = \{(x, y) \in \mathbb{R}^2 \mid x^2 + y^2 = 1\}$$

as a subspace of the plane $\mathbb{R}^2$. Let $f : [0, 1) \longrightarrow S^1$ be the function defined by

$$f(t) = (\cos(2\pi t), \sin(2\pi t))$$

The properties of trigonometric functions guarantees the continuity of f. However, the inverse function $f^{-1} : S^1 \longrightarrow [0, 1)$ is not continuous. Consider the open subset $U = [0, 1/2)$ of $[0, 1)$.

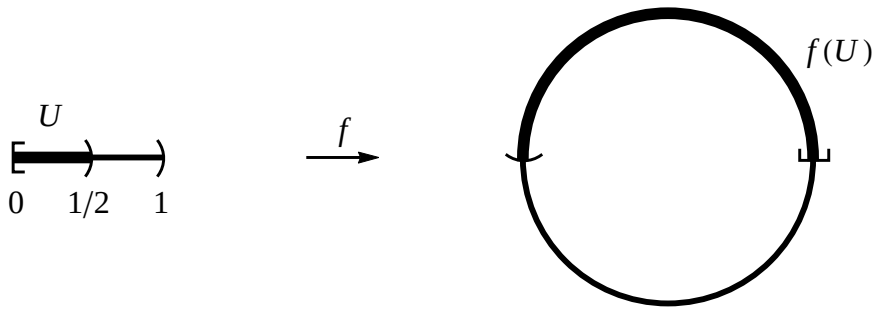

Figure 1.2.1: A Continuous Bijection that is not a Homeomorphism

Its preimage under f^{-1} is $f(U)$, and it is not an open set of S^1 (Figure 1.2.1). Thus f^{-1} is not continuous, and f is not a homeomorphism.

In order for a function between spaces to be a homeomorphism, both the function and its inverse are required to be bijective and continuous. Thus both the original function and its inverse function are homeomorphisms. The following theorem gives another criterion for a continuous bijection to be a homeomorphism.

Theorem 1.2.7. *Let X be a compact space and Y be a Hausdorff space. If $f : X \longrightarrow Y$ is a continuous bijection, then f is a homeomorphism.*

Proof. See Theorem 26.6 in [21]. □

Given a topological space, the set of all homeomorphisms from the space to itself forms a group under function composition. Two homeomorphisms can compose together to form another homeomorphism. Associativity follows from the property of function composition. The identity function is clearly a homeomorphism, and the inverse function of a homeomorphism is, once again, a homeomorphism.

Definition 1.2.8. Let X be a topological space. The **homeomorphism group** of X, denoted Homeo(X), is the group of all homeomorphisms from X to itself with function composition as the group operation.

Example 1.2.9. Consider the topological space $X = \{1, 2, 3, \ldots, n\}$ with discrete topology. Then any permutation of X gives a homeomorphism from X to itself. In fact, the homeomorphism group $\mathrm{Homeo}(X)$ is simply the permutation group S_n.

Example 1.2.10. Let $I = [0, 1]$ be the topological space with subspace topology inherited from $\mathbb{R}$. The homeomorphism group of I can be described as the set of continuous bijective functions $f : I \to I$ such that $f(0) = 0$ and $f(1) = 1$, or $f(0) = 1$ and $f(1) = 0$. Define the functions $f, g, h : I \to I$ by

$$f(x) = x^2, \quad g(x) = \begin{cases} 2x, & \text{if } 0 \le x < 1/4, \\ x + 1/4, & \text{if } 1/4 \le x < 1/2, \\ x/2 + 1/2, & \text{if } 1/2 \le x \le 1, \end{cases} \quad \text{and} \quad h(x) = 1 - x.$$

The graphs of these functions, their inverses, and some of their compositions are shown in Figure 1.2.2. Additionally, we notice that the homeomorphisms of I are either monotone increasing

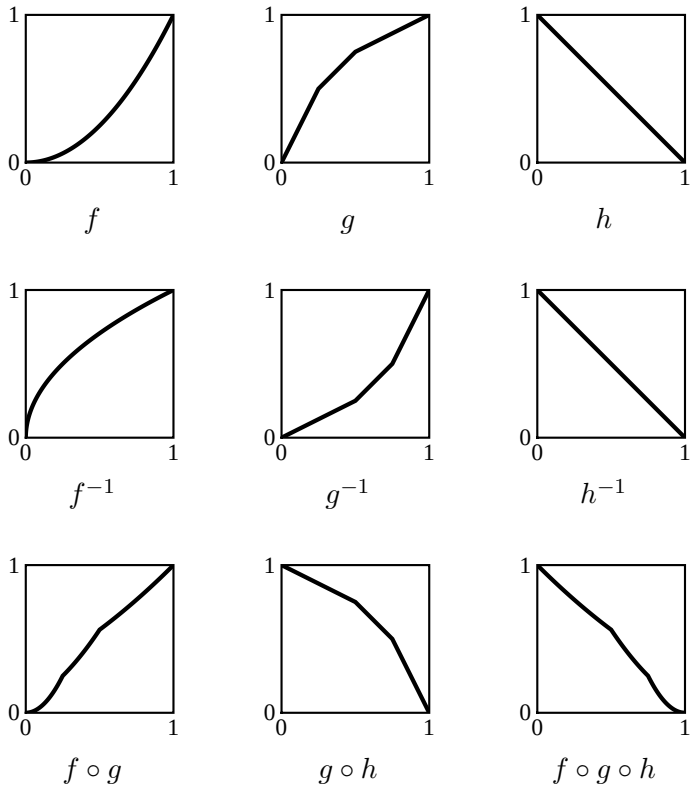

Figure 1.2.2: Some Homeomorphisms of $[0, 1]$

from 0 to 1 or monotone decreasing from 1 to 0. The identity map is monotone increasing. The inverses and compositions of monotone increasing homeomorphisms are also monotone increasing. In fact, the set of monotone increasing homeomorphisms of I forms an index 2 subgroup of Homeo(I).

The following theorem provides a powerful tool to construct new continuous functions with existing continuous functions.

Theorem 1.2.11 (The Pasting Lemma)**.** *Let $X = A \cup B$, where A and B are closed subsets of X. Let $f : A \longrightarrow Y$ and $g : B \longrightarrow Y$ be continuous functions. If $f(x) = g(x)$ for all $x \in A \cap B$, the the function $h : X \longrightarrow Y$ defined by*

$$h(x) = \begin{cases} f(x), & \text{if } x \in A, \\ g(x), & \text{if } x \in B \end{cases}$$

is continuous.

Proof. Let U be an open subset of Y. Let $C = Y - U$. Then C is closed. Thus

$$\begin{aligned} h^{-1}(C) &= f^{-1}(C) \cup g^{-1}(C) = (f^{-1}(Y) - f^{-1}(U)) \cup (g^{-1}(Y) - g^{-1}(U)) \\ &= (A - f^{-1}(U)) \cup (B - g^{-1}(U)). \end{aligned}$$

Because both f and g are continuous, it follows that $f^{-1}(U)$ and $g^{-1}(U)$ are open in A and B, respectively. Then $(A - f^{-1}(U))$ and $(B - g^{-1}(U))$ are closed in A and B, respectively, and thus both closed in X because A and B are closed sets. Thus $h^{-1}(C)$ is closed in X. Therefore, $h^{-1}(U) = X - h^{-1}(C)$ is open in X, and thus h is continuous. □

1.3 The Quotient Topology

It would be helpful to introduce the idea of the *quotient topology* for studying the topological structures and properties of fractals. In the coming sections and chapters, we will introduce the Cantor set C, which can be thought to be the blueprint of fractals, and view some of the fractals that we will study as a *quotient space* of C.

Definition 1.3.1. Let X and Y be topological space. Let $p : X \longrightarrow Y$ be a surjective map. The map p is said to be a **quotient map** provided that a subset U of Y is open in Y if and only if $p^{-1}(U)$ is open in X.

Notice that the condition for a map to be a quotient map is stronger than that for continuity. Hence, every quotient map between two spaces is a continuous map. Similar with continuity, quotient maps can also be defined with closed set. The equivalent condition in terms of closed set is to require that a subset C of Y be closed in Y if and only if $p^{-1}(C)$ is closed in X. The equivalence follows from the relation

$$f^{-1}(Y - U) = f^{-1}(Y) - f^{-1}(U) = X - f^{-1}(U).$$

The next two definitions show two special kinds of quotient maps.

Definition 1.3.2. Let X and Y be topological spaces. A map $f : X \longrightarrow Y$ is an **open map** if for each open set U of X, its image $f(U)$ is open in Y. A map $g : X \longrightarrow Y$ is a **closed map** if for each closed set C of X, its image $f(C)$ is closed in Y.

It follows that a surjective continuous open map between two spaces is a quotient map, so is a surjective continuous closed map. However, there are quotient maps that are neither open nor closed.

Lemma 1.3.3. *Let X be a topological space, and let A be a set. If $p : X \longrightarrow A$ is a surjective map, then there exist exactly one topology $\mathcal{T}$ on A such that p is a quotient map. This topology $\mathcal{T}$ on A is called the **quotient topology** induced by p.*

Proof. Let $\mathcal{T}$ be the topology on A defined by

$$\mathcal{T} = \{U \subseteq A \mid p^{-1}(U) \text{ is open in } X\}.$$

We verify that $\mathcal{T}$ is a topology. First of all, $\varnothing = p^{-1}(\varnothing)$ and $A = p^{-1}(X)$ are open. An arbitrary union of open sets

$$\bigcup_{\alpha\in\mathcal{A}} p^{-1}(U_\alpha) = p^{-1}\Big(\bigcup_{\alpha\in\mathcal{A}} U_\alpha\Big),$$

which is an open set. A finite intersection of open sets

$$\bigcap_{i=1}^{n} p^{-1}(U) = p^{-1}\Big(\bigcap_{i=1}^{n} U_i\Big),$$

which, once again, is an open set. Thus $\mathcal{T}$ is a topology on A. □

Definition 1.3.4. Let X be a topological space, and let $\sim$ be an equivalence relation defined on X. Let X^* be the partition of X corresponding to the equivalence relation $\sim$. Let $p : X \longrightarrow X^*$ be the surjective map defined by

$$p(x) = [x],$$

where $[x]$ is the equivalence class containing x. In the quotient topology induced by p, the space X^* is a **quotient space** of X.

Example 1.3.5. Let X be the rectangle $[0,1] \times [0,1]$. Define an equivalence relation $\sim$ on X by

$$(x_1, y_1) \sim (x_2, y_2) \text{ if } x_1 = x_2 \text{ and } y_1 = y_2 = 0, \text{ or } y_1 = y_2 \text{ and } x_1 = x_2 = 0.$$

The partition X^*corresponding to this equivalence relation consists of all singleton sets $\{(x, y)\}$ where $0 < x < 1$ and $0 < y < 1$, the following two-point sets

$$\{(x, 0), (x, 1)\}, \text{ where } 0 < x < 1,$$

$$\{(0, y), (1, y)\}, \text{ where } 0 < y < 1,$$

and the four-point set

$$\{(0, 0), (0, 1), (1, 0), (1, 1)\}.$$

The resulting quotient space is a *torus*. Three typical open sets of this quotient space are shown in the rectangle as well as the torus in Figure 1.3.1.

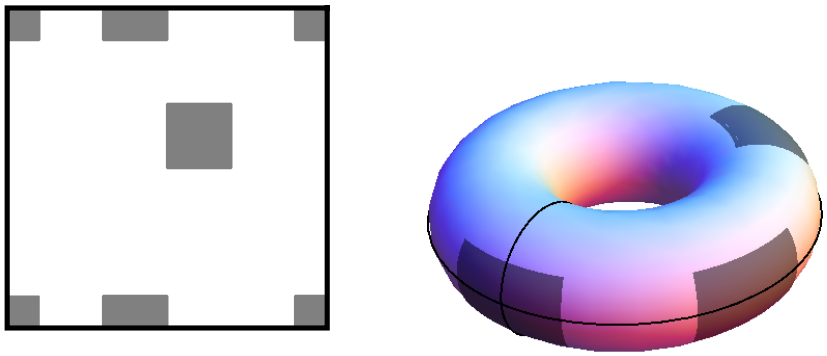

Figure 1.3.1: Open Sets in the Quotient Space of $[0,1] \times [0,1]$

1.4 Möbius Transformations and Anti-Möbius Transformations

In this section, we introduce two important families of functions defined on the Riemann sphere $\hat{\mathbb{C}} = \mathbb{C} \cup \{\infty\}$, namely, the *Möbius transformations* and the *anti-Möbius transformations*.

Definition 1.4.1. A **Möbius transformation** is a map $f : \hat{\mathbb{C}} \to \hat{\mathbb{C}}$ of the form

$$f(z) = \frac{az + b}{cz + d},$$

where the coefficients $a, b, c, d \in \mathbb{C}$ satisfy that $ad - bc \neq 0$.

If we divide all coefficients by the complex square root $\sqrt{ad - bc}$, we can arrange that $ad - bc = 1$ without changing the map f. Thus the Möbius transformations can also be defined with the coefficients satisfying $ad - bc = 1$.

Möbius transformations are bijective holomorphic functions of the Riemann sphere. An inverse of a Möbius transformation is yet another Möbius transformation. If we have a Möbius transformation $f : \hat{\mathbb{C}} \to \hat{\mathbb{C}}$ defined by

$$f(z) = \frac{az + b}{cz + d},$$

its inverse has the formula

$$f^{-1}(z) = \frac{dz - b}{-cz + a}.$$

A composition of Möbius transformations is also a Möbius transformation. Let f and g be Möbius transformations defined by

$$f(z) = \frac{az+b}{cz+d} \quad \text{and} \quad g(z) = \frac{mz+n}{pz+q},$$

then the composition function of f and g has the formula

$$(g \circ f)(z) = \frac{m \cdot \frac{az+b}{cz+d} + n}{p \cdot \frac{az+b}{cz+d} + q} = \frac{(ma+nc)z + (mb+nd)}{(pa+qc)z + (pb+qd)}.$$

The composition of Möbius transformations is associative, inherited from the associativity of functions. In addition, the identity function is a special Möbius transformation with coefficients $a = d = 1$ and $b = c = 0$. Therefore, the set of Möbius transformations forms a group under function composition.

Definition 1.4.2. The **Möbius group**, denoted by Mob, is the group of Möbius transformations.

We notice that the coefficients of $g \circ f$ are exactly the entries of the product of two matrices, namely,

$$\begin{bmatrix} m & n \\ p & q \end{bmatrix} \begin{bmatrix} a & b \\ c & d \end{bmatrix} = \begin{bmatrix} ma+nc & mb+nd \\ pa+qc & pb+qd \end{bmatrix}.$$

The following theorem shows that such phenomenon is not merely coincidence. There is a correspondence between the Möbius group and matrix groups.

Theorem 1.4.3. *The Möbius group* Mob *is isomorphic to* $\mathrm{PSL}_2(\mathbb{C})$.

Proof. Let $\varphi : \mathrm{SL}_2(\mathbb{C}) \longrightarrow \mathrm{Mob}$ be a map defined by

$$\varphi(A) = f_A$$

where

$$A = \begin{bmatrix} a & b \\ c & d \end{bmatrix}$$

for any $a, b, c, d \in \mathbb{C}$ satisfying $ad - bc = 1$, and

$$f_A(z) = \frac{az + b}{cz + d}.$$

The map φ is clearly surjective. Thus we have $\varphi(\mathrm{SL}_2(\mathbb{C})) = \mathrm{Mob}$.

Let

$$A = \begin{bmatrix} a & b \\ c & d \end{bmatrix}, \quad \text{and} \quad M = \begin{bmatrix} m & n \\ p & q \end{bmatrix}.$$

Then

$$MA = \begin{bmatrix} m & n \\ p & q \end{bmatrix} \begin{bmatrix} a & b \\ c & d \end{bmatrix} = \begin{bmatrix} ma + nc & mb + nd \\ pa + qc & pb + qd \end{bmatrix}.$$

Thus

$$\varphi(M) \circ \varphi(A) = f_M \circ f_A,$$

where

$$(f_M \circ f_A)(z) = \frac{m \cdot \frac{az+b}{cz+d} + n}{p \cdot \frac{az+b}{cz+d} + q} = \frac{(ma + nc)z + (mb + nd)}{(pa + qc)z + (pb + qd)},$$

and

$$\varphi(MA) = f_{MA},$$

where

$$f_{MA}(z) = \frac{(ma + nc)z + (mb + nd)}{(pa + qc)z + (pb + qd)}.$$

It follows that φ is a homomorphism.

Now we look for the kernel of this homomorphism. Let

$$A = \begin{bmatrix} a & b \\ c & d \end{bmatrix}.$$

Suppose that $A \in \ker(\varphi)$. Then $\varphi(A) = 1_{\hat{\mathbb{C}}}$. Thus $ad - bc = 1$ and $(az + b)/(cz + d) = z$ for all $z \in \hat{\mathbb{C}}$. It follows that $\ker(\varphi) = \{\pm I\}$. By the First Isomorphism Theorem,

$$\mathrm{SL}_2(\mathbb{C})/\ker(\varphi) \cong \varphi(\mathrm{SL}_2(\mathbb{C})).$$

We know that $\varphi(\mathrm{SL}_2(\mathbb{C})) = \mathrm{Mob}$, and by definition, $\mathrm{PSL}_2(\mathbb{C}) \cong \mathrm{SL}_2(\mathbb{C})/\{\pm I\}$. Therefore, we conclude that $\mathrm{Mob} \cong \mathrm{PSL}_2(\mathbb{C})$. □

There are several natural representations of $\mathrm{PSL}_2(\mathbb{C})$ including conformal transformations of the Riemann sphere $\hat{\mathbb{C}}$, orientation-preserving isometries of hyperbolic 3-space $\mathbb{H}^3$, and orientation preserving conformal maps of the open unit ball $B^3 \subseteq \mathbb{R}^3$ to itself. The Möbius group can act on any of these spaces described.

Given two sets of three distinct points $\{z_1, z_2, z_3\}$ and $\{w_1, w_2, w_3\}$ on the Riemann sphere $\hat{\mathbb{C}}$, there exist a unique Möbius transformation under which z_1, z_2, z_3 map to w_1, w_2, w_3, respectively. It is easy to check that the Möbius transformation defined by

$$f_1(z) = \frac{(z - z_1)(z_2 - z_3)}{(z - z_3)(z_2 - z_1)}$$

maps z_1, z_2, z_3 to $0, 1, \infty$, respectively. Similarly, there exist another Möbius transformation $f_2(z)$ that maps w_1, w_2, w_3 to $0, 1, \infty$, respectively. The composition function $g = f_2^{-1} \circ f_1$ is then the desired Möbius transformation that maps z_1, z_2, z_3 to w_1, w_2, w_3, respectively.

Möbius transformations are orientation-preserving conformal mappings of the Riemann sphere. There is yet another important class of functions defined on the Riemann sphere – the *anti-Möbius transformations*. They are very similar to Möbius transformations, besides the fact that they are orientation-reversing mappings of the Riemann sphere.

Definition 1.4.4. An **anti-Möbius transformation** is a map $f^* : \hat{\mathbb{C}} \longrightarrow \hat{\mathbb{C}}$ of the form

$$f^*(z) = \frac{a\overline{z} + b}{c\overline{z} + d},$$

where the coefficients $a, b, c, d \in \mathbb{C}$ satisfy that $ad - bc \neq 0$.

It is clear that the complex conjugate of a Möbius transformation is an anti-Möbius transformation, and *vice versa*. Therefore, the collection of all Möbius transformations and anti-Möbius transformations form a group $\mathrm{Mob}_{\pm} = \mathrm{Mob} \rtimes \langle s \rangle$, where s is the complex conjugation function. The Möbius group is an index-2 normal subgroup of G, and the collection of all anti-Möbius transformations is the coset containing the complex conjugation function.

An important family of anti-Möbius transformations is the circle inversions.

Definition 1.4.5. Let C be a circle on the complex plane centered at z_0 with radius r. The **inverse** of $z \in \mathbb{C} - \{z_0\}$ with respect to the circle C is the point $w \in \mathbb{C} - \{z_0\}$ lying on the ray from z_0 through z satisfying that

$$\|w - z_0\| \cdot \|z - z_0\| = r^2.$$

We can write down an explicit expression of w in terms of z_0, r, and z:

$$w = z_0 + r^2 \cdot \frac{z - z_0}{\|z - z_0\|^2}.$$

We immediately run into problem when we compute the inverse of z_0. In order for every point to have an inverse, we introduce the point at infinity. The inverse of the center is defined to be the point at infinity, and *vice versa*. Now we can define circle inversions.

Definition 1.4.6. The **circle inversion** across C centered at z_0 is a map defined on $\hat{\mathbb{C}}$ that maps each point $z \in \mathbb{C} - \{z_0\}$ to its inverse with respect to C. Additionally, the inversion interchanges the center z_0 of C and the point at infinity.

Example 1.4.7. Let $c(z)$ be an anti-Möbius transformation with the expression

$$c(z) = \frac{1}{\overline{z}}.$$

Suppose $z = re^{i\theta}$ is an arbitrary complex number. Then

$$c(z) = \frac{1}{\overline{z}} = \frac{1}{\overline{re^{i\theta}}} = \frac{1}{re^{-i\theta}} = \frac{1}{r} \cdot e^{i\theta} = \frac{z}{\|z\|^2}.$$

It follows that $c(z)$ is a circle inversion of the Riemann sphere with respect to the unit circle.

Any circle inversion is an anti-Möbius transformation. Let $z(\theta) = z_0 + re^{i\theta}$ be an arbitrary circle on the Riemann sphere. Because three points determines a circle, we pick three distinct points $z_0 + r, z_0 + ir, z_0 - r$ on the circle. Then there exist a Möbius transformation f that sends these three points to 1, i, -1, respectively. In particular, this Möbius transformation is an affine linear transformation. The circle through the points 1, i, -1 is the unit circle, and

the inversion across the unit circle is the function c in Example 1.4.7, which is an anti-Möbius transformation. The composition of transformations $g = f^{-1} \circ c^* \circ f$ completes the circle inversion with respect to $z(\theta) = z_0 + re^{i\theta}$. Because f^{-1} and f are Möbius transformations, while c is an anti-Möbius transformation, it follows that the composition of these three functions gives an anti-Möbiustransformation.

A circle inversion always maps circles to circles on $\hat{\mathbb{C}}$. This property is very useful and helps in constructing Schottky groups of circle inversions in the following section.

1.5 Kleinian Groups and Schottky Groups

The matrix group $\mathrm{PSL}_2(\mathbb{C})$ has three complex dimensions, or equivalently, six real dimensions. We can impose a uniform topology on $\mathrm{PSL}_2(\mathbb{C})$ so that it becomes a topological group. We are particularly interested in the rich structure of subgroups of $\mathrm{PSL}_2(\mathbb{C})$.

Definition 1.5.1. A **Kleinian group** is a discrete subgroup of $\mathrm{PSL}_2(\mathbb{C})$.

Kleinian groups are discrete in a sense that they do not have limit points in $\mathrm{PSL}_2(\mathbb{C})$.

Definition 1.5.2. Let $C_1, C_2, \ldots, C_n$ be circles with disjoint interiors. Let $\gamma_1, \gamma_2, \ldots, \gamma_n$ be the circle inversions across the circles $C_1, C_2, \ldots, C_n$, respectively. The group, under function composition, generated by $\gamma_1, \gamma_2, \ldots, \gamma_n$, is a **Schottky group**.

The generators of a Schottky group are anti-Möbius transformations. Two anti-Möbius transformations compose together to give a Möbius transformation. Thus the Möbius transformations of a Schottky group forms an index-2 normal subgroup, which is a Kleinian group. The anti-Möbius transformations form the coset containing the generators of circle inversions.

Definition 1.5.3. Let K be a Kleinian group acting on the Riemann sphere $\hat{\mathbb{C}}$. Let $p \in \hat{\mathbb{C}}$ be a point. The orbit Kp of p typically accumulates on $\hat{\mathbb{C}}$. The set of accumulation points of Kp in $\hat{\mathbb{C}}$ is called the **limit set** of K, denoted by $\Lambda(K)$. The limit set of Schottky groups can be defined analogously.

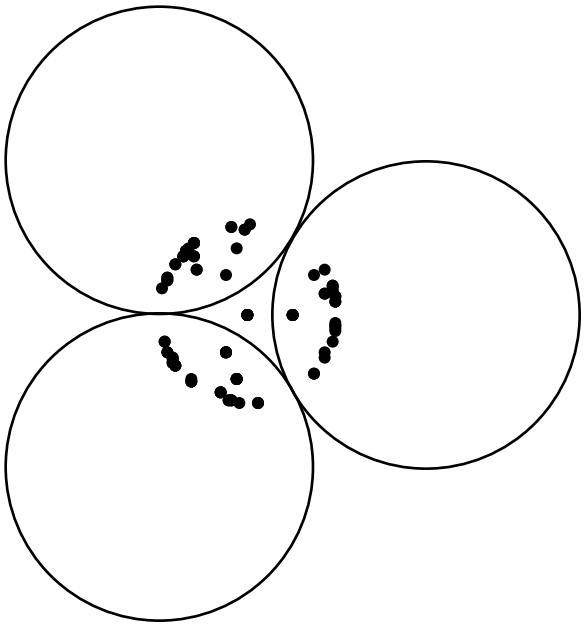

Figure 1.5.1: Circle Inversions and the Orbit of One Point

Notice that in the definition above, the choice of a starting point $p \in \hat{\mathbb{C}}$ is arbitrary. In fact, the limit set of a Kleinian group does not depend on the choice of the starting point p. Furthermore, we observe that the limit set is closed in the Riemann sphere $\hat{\mathbb{C}}$.

Example 1.5.4. Let C_1, C_2, and C_3 be three mutually tangent circles of the same size, and let γ_1, γ_2, and γ_3 be the circle inversions across C_1, C_2, and C_3, respectively. The limit set of the Schottky group generated by γ_1, γ_2, and γ_3 is the circle through the three tangent points. Figure 1.5.1 shows part of the orbit of one point under the action of this group. We can start to see the orbit converging to a circle.

We show more examples of Schottky group limit sets in Figure 1.5.2, in which the left circles correspond to the generating circle reflections for the Schottky groups. A lot of these limit sets have self-similar structures that resemble fractals.

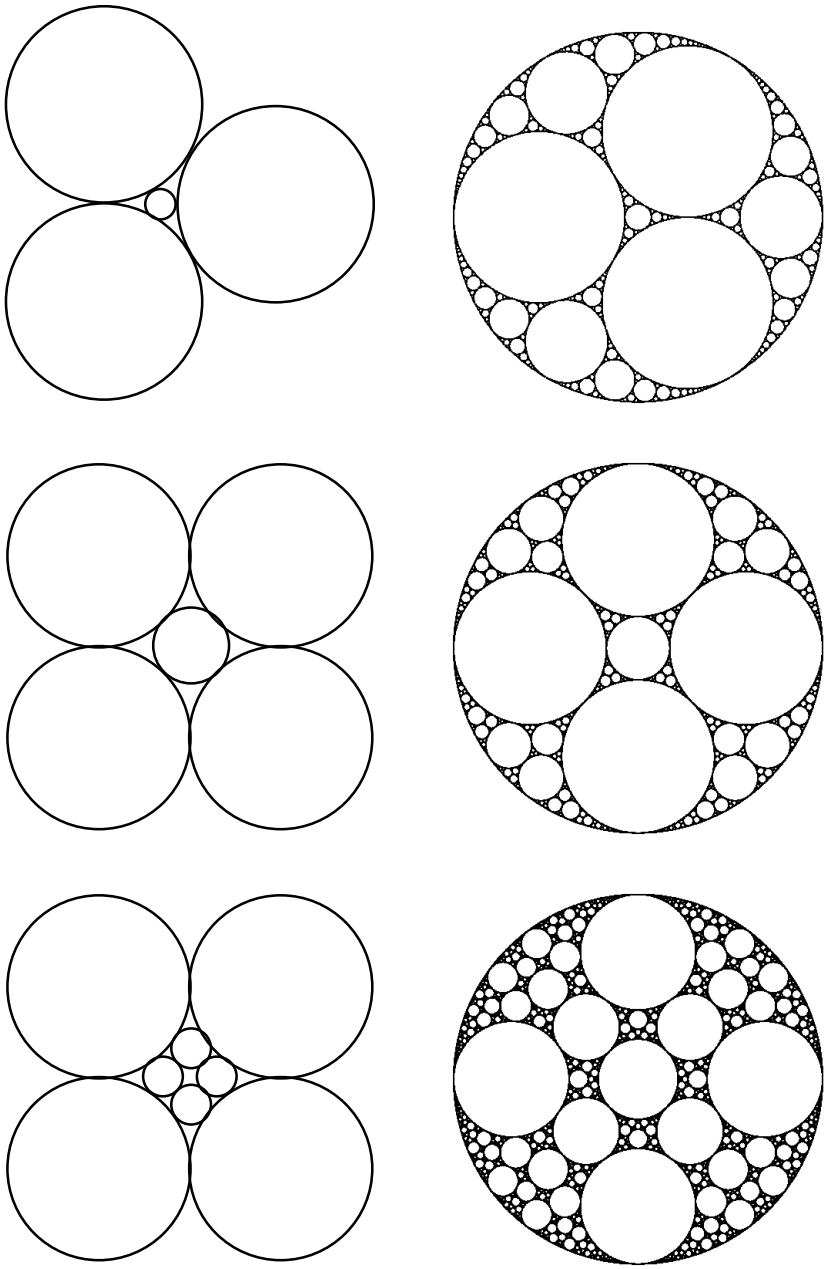

Figure 1.5.2: Limit Sets of Schottky Groups

2
Fractals

A fractal is a natural or mathematical object that exhibits a repeating pattern, formally called the *self-similar* property, that displays at different scales of the object. Fractals have been known for more than a century and have been observed in all branches of science. Fractal structures are ubiquitous in nature. The leaves of ferns demonstrates self-similarity – they show the same structure at different levels (Figure 2.0.1a). The clouds in the sky also presents self-similarity (Figure 2.0.1b). In meteorology, the demand for understanding the complex physics of the cloud motivated physicists and mathematicians to bring up the new field of fractal analysis in mathematics. The systematic study of fractals in mathematics started around the 1970s. In

(a) Fern Leaves (b) Clouds

Figure 2.0.1: Naturally-Occurring Fractal Structures

1967, mathematician Benoît Mandelbrot, by examining the coastline paradox [17], introduced several important concepts in fractal geometry. Later in 1975, Mandelbrot first used the term "fractal". With the development of modern computer graphics, more and more fractals show up in the field and enrich the study of fractals. In this chapter, we will walk through some basic properties of fractals, including self-similarity and ways to generate fractals. We will also briefly investigate several paradigms of fractals in mathematics, namely, the Cantor set, the Sierpinski gasket (SG), and Julia sets.

2.1 Basic Properties of Fractals

2.1.1 Self-similarity

An object is said to be *self-similar* if the whole object is exactly or approximately similar to part of itself. Fractals are usually self-similar objects. For example, if the Koch curve is magnified about a portion of itself, the shape is still the Koch curve (Figure 2.1.1).

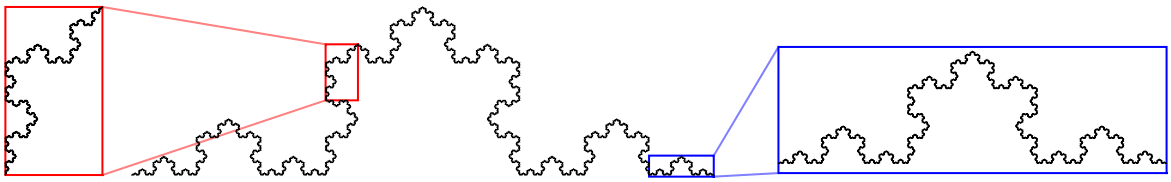

Figure 2.1.1: Zooming into the Koch Curve

Not only fractals are self-similar. A closed-up look of a portion of a line segment is simply a line segment. Thus any line segment is self-similar. In section 2.4, we will see that the line segment joining 2 and -2 on the complex plane is a Julia set.

2.1.2 Ways to generate fractals

There are numerous ways to generate fractals. The commonly-used methods include iterated function systems, escape-time method, strange attractors, L-systems, *etc.* We will mainly focus on iterated function systems and escape-time method. Among the examples in this chapter,

the Cantor set and the Sierpinski gasket are usually generated by iterated function systems, although there are other ways to give rise to these two fractals. The Julia sets are paradigms of fractals generated by escape-time method. Here, we introduce iterated function systems based on the set up given in [14]. In Section 2.4, we will give an expository introduction to escape-time method with the background given in [8].

Definition 2.1.1. Let (M, d) be a metric space. A map $f : M \longrightarrow M$ is a **contracting map** if there is a real number $\lambda \in (0, 1)$ such that

$$d(f(x), f(y)) \leq \lambda \cdot d(x, y) \text{ for all } x, y \in M.$$

Theorem 2.1.2 (Banach fixed-point theorem)**.** *Let M be a complete metric space and let $f : M \longrightarrow M$ a contracting map. Then there exist a unique fixed point for f in M.*

Proof. See [22]. □

Theorem 2.1.3. *Let M be a complete metric space and $\{f_1, \ldots, f_n\}$ a family of contracting maps on M. Denote the collection of all nonempty compact subsets of M by $\mathbb{K}(M)$. If we define the transformation $F : \mathbb{K}(M) \longrightarrow \mathbb{K}(M)$ by*

$$F(X) = \bigcup_{i=1}^{n} f_n(X).$$

Then there exist a unique compact subset $X \subseteq M$ such that $F(X) = X$.

Proof. See Theorem 2.6 in [10]. □

Definition 2.1.4. The set X given in Theorem 2.1.3 is called a **homogeneous self-similar fractal set**, and the family of functions $\{f_1, \ldots, f_n\}$ is usually called an **iterated function system** (i.f.s. for short).

The middle-third Cantor set and the Sierpinski gasket presented in the following two sections are classic examples of fractals generated from iterated function systems.

2.2 The Cantor Set

The Cantor set was introduced by German mathematician Georg Cantor in 1883 in an abstract way. The most commonly-referred Cantor set is the middle-third Cantor set. In this section, we construct the middle-third Cantor set, and show a remarkable topological property of the Cantor set.

2.2.1 The middle-third Cantor set

A classic way to obtain the Cantor set is by repetitively removing the middle thirds of line intervals. An iterated function system is used to generate the Cantor set.

Definition 2.2.1. Let $I \subseteq \mathbb{R}$ be the closed interval $[0, 1]$. Let $\gamma_1, \gamma_2 : I \longrightarrow I$ be maps defined by

$$\gamma_1(x) = \frac{x}{3}, \text{ and } \gamma_2 = \frac{x-1}{3} + 1$$

for all $x \in I$. Define $C_0 = I$, and inductively, $C_{n+1} = \gamma_1(C_n) \cup \gamma_2(C_n)$. Notice that the sets $\{C_n\}_{n\in\mathbb{N}}$ are nested, *i.e.*, $C_{n+1} \subseteq C_n$ for all $n \in \mathbb{N}$. The **Cantor set** C is defined to be the limit of the sequence of sets, *i.e.*,

$$C = \bigcap_{n\in\mathbb{N}} C_n.$$

Figure 2.2.1 shows the first few stages of approximation of the Cantor set.

2.2.2 $\{0, 1\}^\infty$

Definition 2.2.2. Let M be a metric space. We say M is a **Cantor space** if M is compact, non-empty, perfect, and totally disconnected.

Figure 2.2.1: The First Few Stages of Approximation of the Cantor Set

Theorem 2.2.3 (Moore-Kline Theorem)**.** *Every Cantor space is homeomorphic to the middle-third Cantor set.*

Proof. See Theorem 69 in [23]. □

The countable product $\{0,1\}^\infty$ is a Cantor space by definition, thus it is homeomorphic to the middle-third Cantor set. In fact, any countable product of finite discrete spaces is a Cantor space, and thus homeomorphic to the Cantor set.

2.3 The Sierpinski Gasket

The Sierpinski gasket is a fractal described by Polish mathematician Waclaw Sierpinski in 1915. It is alternatively called the Sierpinski triangle or the Sierpinski sieve. It has been a popular candidate for the study of fractals.

2.3.1 Construction

There are many different ways to construct the Sierpinski gasket. One of the most commonly used method is repeated triangle removals as shown in Figure 2.3.1. We start with the closed equilateral triangle (SG_0). The equilateral triangle is then subdivided into four identical congruent equilateral triangles. We remove the interior of the central one, which gives us the first stage of the construction (SG_1). This process of removing triangles is repeated for each of the remaining smaller triangles, and the result of each stage SG_n is a closed subspace of SG_0. The Sierpinski gasket (SG) is defined by

$$SG = \bigcap_{n \in \mathbb{Z}_{\geq 0}} SG_n. \tag{2.3.1}$$

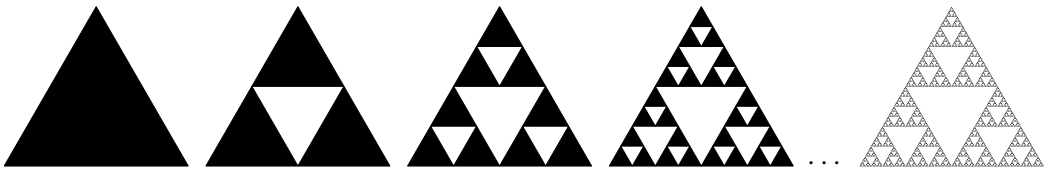

Figure 2.3.1: Construction of the Sierpinski Gasket

An alternative way to construct the Sierpinski gasket is through iterated function systems. Let f_1, f_2, and f_3 be the maps defined on the complex plane by

$$f_1(z) = z/2,$$

$$f_2(z) = (z-1)/2 + 1,$$

$$f_3(z) = (z-i)/2 + i,$$

for all $z \in \mathbb{C}$. The homogeneous self-similar fractal set of the iterated function system $\{f_1, f_2, f_3\}$ is a Sierpinski gasket embedded on the complex plane.

Theorem 2.3.1. *The Sierpinski gasket SG is a path-connected compact Hausdorff space.*

Proof. SG is Hausdorff follows from $SG \subseteq \mathbb{R}^2$, in which case $\mathbb{R}^2$ is Hausdorff. For all $n \in Z_{\geq 0}$, the subspace SG_n is closed. Then SG is closed by definition. Because SG is also bounded, it follows that SG is compact.

The path-connectedness of SG is shown in [16]. □

2.3.2 Address system

In order to describe points in the Sierpinski gasket (SG), we need an *address system* that assigns addresses. The address system described in this section is based on the visual geometry of the Sierpinski gasket. The basic components of the Sierpinski gasket are *cells*, and each cell is divided into three *subcells*. The complete Sierpinski gasket is built from one *main cell*.

The structure of the Sierpinski gasket is described by a *replacement system*. As shown in Figure 2.3.2, we may start with the main cell, and apply the replacement rule to components

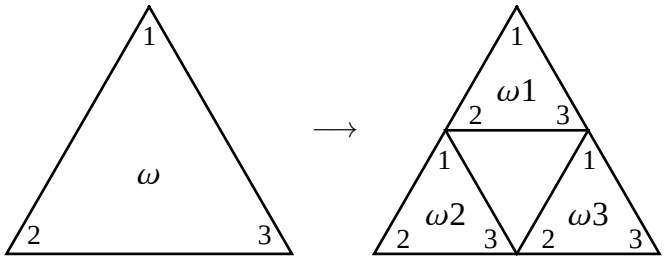

Figure 2.3.2: Replacement System of the Sierpinski Gasket

of the main cell. If we keep applying the replacement rule to subsequent cells, the limit of these graphs will eventually be the Sierpinski gasket. In addition, every point in the Sierpinski gasket can be described by an *address* – an infinite sequence of 1, 2, and 3. For example, if a cell has address ω, its three immediate subcells shall have addresses $\omega 1$, $\omega 2$, and $\omega 3$, respectively.

Definition 2.3.2. The **symbol space** of points in the Sierpinski gasket is the collection $\Omega_{SG} = \{1, 2, 3\}^\infty$ of infinite sequences with the alphabet $\{1, 2, 3\}$.

The collection $\Omega_{SG} = \{1, 2, 3\}^\infty$ is a topological space with product topology. It is homeomorphic to the Cantor set.

Definition 2.3.3. A **cell** of the Sierpinski gasket is the collection of all points with the same initial n digits in their addresses. Formally, a collection of points S is a **cell** if there exist $n \geq 1$ such that $S = \omega \times \{1, 2, 3\}^\infty$ for some finite word $\omega \in \{1, 2, 3\}^n$. The integer n is the **depth** of the cell S, and the finite word ω is the **address** of the cell S. The cell S is referred to as the ω-cell, or simply cell ω when there is no confusion.

Definition 2.3.4. The only cell with depth 1 in the Sierpinski gasket is the **main cell**.

It is clear that the complete Sierpinski gasket is the main cell.

There are points in the Sierpinski gasket with multiple addresses. The replacement rule tells us three types of points with two distinct addresses:

$$\omega 1\overline{2} = \omega 2\overline{1}, \qquad \omega 2\overline{3} = \omega 3\overline{2}, \qquad \omega 1\overline{3} = \omega 3\overline{1} \tag{2.3.2}$$

for any finite word $\omega \in \{A, B\} \times \{1, 2, 3\}^{k-1}$ of length k.

The equivalence relation in 2.3.2 defines a surjective map q from the symbol space Ω_{SG} to the Sierpinski gasket. Surjective continuous functions from a compact space to a Hausdorff space is a quotient map. Thus the Sierpinski gasket is homeomorphic to the quotient space of Ω_{SG} with quotient topology induced by q.

2.3.3 Homeomorphisms

It is clear that SG exhibits D_3 symmetry. It is not as clear that the only homeomorphisms of SG are the elements of D_3. This fact was previously proven by Joel Louwsma using the idea of *local cut points* [16]. In this section, we show the group structure of Homeo(SG) with the help of the following claim on the structure of SG.

Claim 2.3.5. *The points p_1, p_2, p_3 shown in the figure below form the only set of three points on SG whose removal results in the disconnection of SG into three mutually disjoint subsets.*

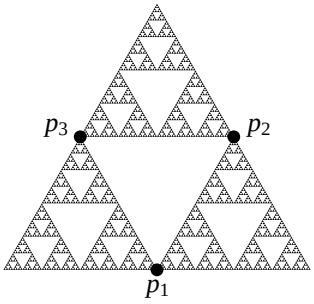

This claim was shown in a proof of Theorem 6.1 in [16].

Theorem 2.3.6. *The homeomorphism group* Homeo(SG) *of the Sierpinski gasket is the dihedral group D_3 of the triangle.*

Proof. Let $P = \{p_1, p_2, p_3\}$ be the collection of three points in Claim 2.3.5. Because P has the topological property stated in Claim 2.3.5, it follows that P is invariant under any homeomorphism of SG. Let $\varphi : SG \to SG$ be a homeomorphism. Then there exists a $\sigma \in D_3$ such that

$(\sigma \circ \varphi)(p_i) = i$ for $i \in \{1, 2, 3\}$. Let $\psi = \sigma \circ \varphi$. Notice that ψ is a homeomorphism of SG that fixes p_1, p_2, p_3. It suffices to show that ψ is the identity map on SG.

We look at the three components separated by the set P. The closure of each component is a sub-Sierpinski gasket. Let x be an arbitrary point in the cell with address 1. Because the Sierpinski gasket is path-connected, there exist paths γ_2 and γ_3 lying entirely in the cell with address 1, connecting x with p_2 and p_3, respectively. Then the images of γ_2 and γ_3 under the homeomorphism ψ must lie entirely within a single component of the Sierpinski gasket. Because ψ fixes p_2 and p_3, this component must be the cell with address 1. Thus $\psi(x)$ is in the same component as x is, *i.e.*, each cell of depth 1 is invariant under ψ.

Now we take a closer look at the cell with address 1. Because this cell has the structure of a Sierpinski gasket, it also has a set of three special points q_1, q_2, q_3, whose removal disconnects this cell into three disconnected components. By their special topological property, the set $\{q_1, q_2, q_3\}$ is invariant under the homeomorphism ψ. We show that ψ actually fixes all three of them.

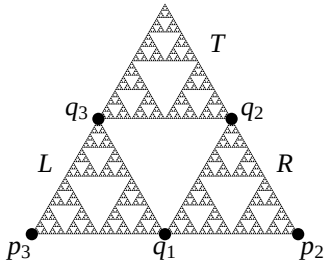

We call the three components of this cell T, L, and R. Each component is a sub-Sierpinski gasket. There exist a path α_1 lying entirely in the L component connecting p_3 to q_1, and a path α_2 lying entirely in the R component connecting p_2 to q_1. We have shown that $\psi(p_3) = p_3$ and $\psi(p_2) = p_2$. Suppose that $\psi(q_1) = q_2$. Then the image of the path α_1 cannot lie entirely in one single component, which contradicts that ϕ is a homeomorphism. Hence, $\psi(q_1) \neq q_2$. Similarly, we can show that $\psi(q_1) \neq q_3$. Thus ψ fixes q_1. There exist a path α_3 lying entirely in the L component connecting p_3 to q_3. Now suppose that $\psi(q_3) = q_2$. Then the image of the path α_3

cannot lie entirely in one single component. Hence, q_3 is also fixed by ψ, and q_2 is automatically fixed.

This process can be iterated to show that every point on the Sierpinski gasket where two cells meet each other is fixed by ψ. Such points form a dense subset of SG. Then ψ agrees with the identity map on a dense subset of SG. Because ψ is a homeomorphism, it follows that ψ is the identity map. Therefore, we conclude that the homeomorphism group of the Sierpinski gasket is the dihedral group D_3. □

2.4 Julia Sets

The notion of *Julia sets* arises from complex dynamical systems. The construction of a Julia set fractal uses *escape-time* method. In this section, we will give the definition of Julia sets and provide some examples of Julia sets.

Definition 2.4.1. Let Λ be a metric space with metric d, and let $f : \Lambda \longrightarrow \Lambda$ be a continuous map. We say f exhibits **sensitive dependence on initial conditions** if there exist $\epsilon > 0$ such that for any $x \in \Lambda$ and any neighborhood U of x, there exist $n > 0$ and $y \in U$ such that

$$d(f^n(x) - f^n(y)) > \epsilon.$$

The idea of sensitive dependence is the following. No matter how close we choose two points on the metric space as our initial conditions, the orbits of these two points diverges by at least ϵ units.

Definition 2.4.2. We say that $f : \Lambda \longrightarrow \Lambda$ is **chaotic** if f exhibits sensitive dependence on initial conditions at every point in Λ.

Definition 2.4.3. The **Julia set** of f, denoted by $J(f)$, is the set of all points at which f exhibits sensitive dependence. In another word, $J(f)$ is the chaotic set for f.

Example 2.4.4. The Julia set of the function $f(z) = z^2$ is the unit circle on the complex plane. For any values z with $\|z\| < 1$, the orbit converges to 0, and for any values z with $\|z\| > 1$, the orbit converges to ∞. For z on the unit circle, the function f doubles the argument of z modulo 2π, and such doubling function is a chaotic map.

Example 2.4.5. The Julia set of the function $f(z) = z^2 - 2$ is the line segment connecting 2 and -2 on the complex plane.

Julia sets usually have fractal structure. Figure 2.4.1 shows some Julia sets generated by Mathematica.

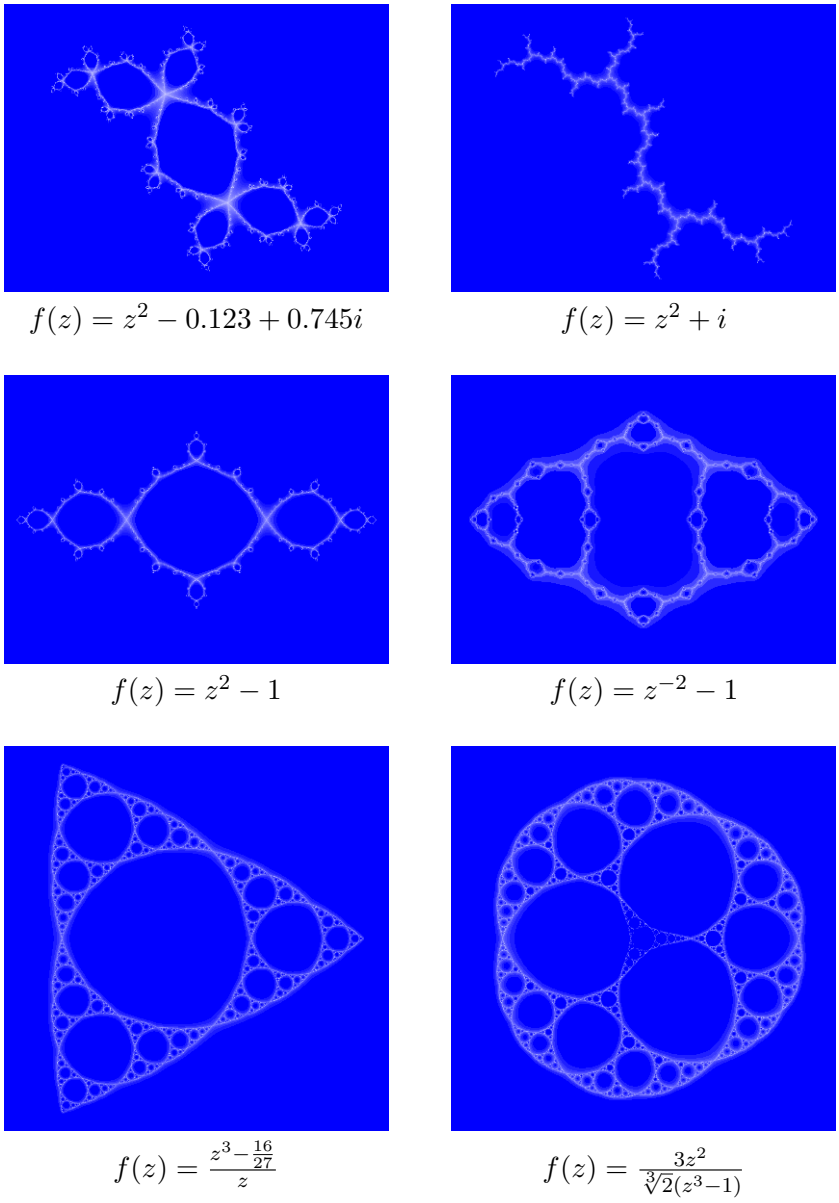

$f(z) = z^2 - 0.123 + 0.745i$ $\quad$ $f(z) = z^2 + i$

$f(z) = z^2 - 1$ $\quad$ $f(z) = z^{-2} - 1$

$f(z) = \frac{z^3 - \frac{16}{27}}{z}$ $\quad$ $f(z) = \frac{3z^2}{\sqrt[3]{2}(z^3-1)}$

Figure 2.4.1: Julia Sets of Complex-Valued Functions

3
The Apollonian Gasket

The first fractal structure we investigate is the *Apollonian gasket* (Figure 3.0.1). The Apollonian gasket is constructed by pasting the vertices of two Sierpinski gaskets together. The homeomorphism group for the Sierpinski gasket is finite, particularly, isomorphic to the dihedral group D_3 [16]. In this chapter, we show that the homeomorphism group for the Apollonian gasket is infinite and finitely generated by a set of three generators.

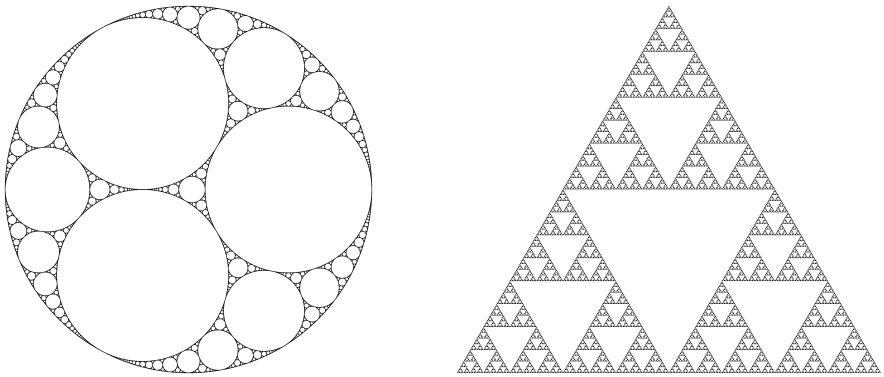

Figure 3.0.1: The Apollonian Gasket and the Sierpinski Gasket

3.1 Construction of the Apollonian Gasket

There are several equivalent constructions of the Apollonian gasket. In particular, the Apollonian gasket can be constructed by pasting the three vertices of two Sierpinski gaskets together. It can also be constructed by placing four Sierpinski gaskets on alternating faces of the octahedron. Figure 3.1.1 illustrates both of these two constructions.

The Apollonian gasket can also be constructed by Apollonian circles (Figure 3.1.2). To start, we draw three mutually tangent circles A, B, and C. Descartes' Theorem states that there are

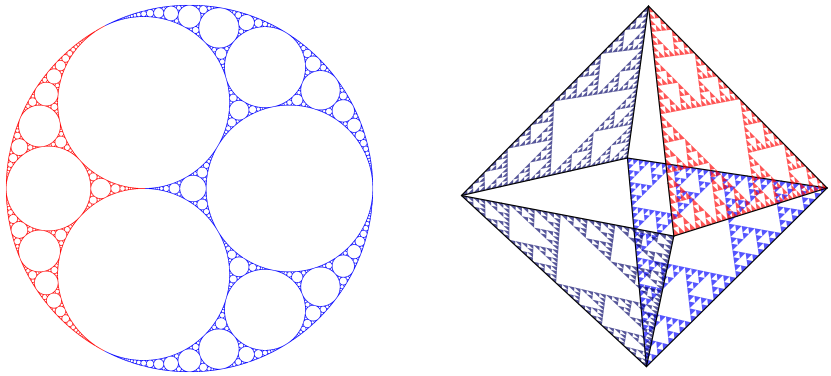

Figure 3.1.1: Two constructions of the Apollonian Gasket Using Sierpinski Gaskets

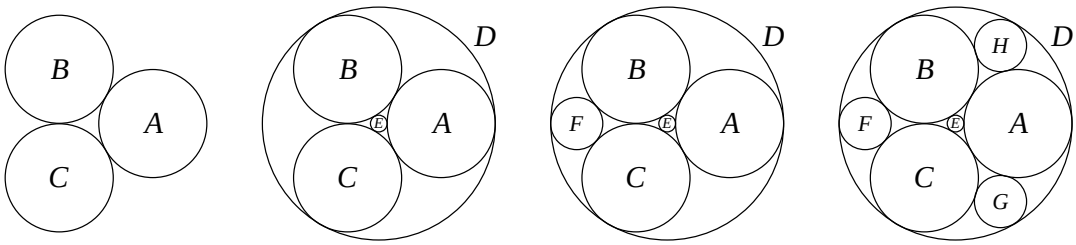

Figure 3.1.2: Construction of the Apollonian Gasket with Apollonian Circles

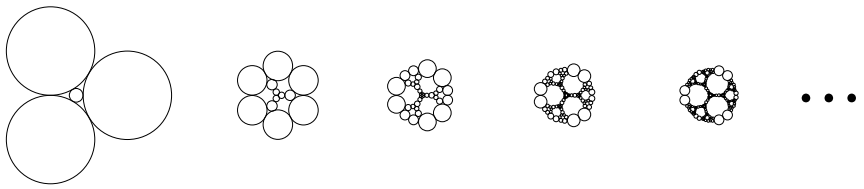

Figure 3.1.3: The Apollonian Gasket as a Limit Set

two other non-intersecting circles, D and E, that are tangent two all of the three starting circles, which are called *Apollonian circles*. If we choose three mutually tangent circles out of the five we have, B, C, and D for example, there are two Apollonian circles, one of them being the original circle A, and the other a new circle F. The addition of Apollonian circles can be continued in the same pattern indefinitely, and the limit of the set of circles is the Apollonian gasket.

The most useful construction of the Apollonian gasket is the Schottky groups and their limit sets. As defined in Section 1.5, Schottky groups are groups of functions defined on the Riemann sphere. They are generated by circle inversions on $\hat{\mathbb{C}}$. Readers should keep in mind that the planar structure of Schottky groups can be realized through stereographic projection of $\hat{\mathbb{C}}$ onto $\mathbb{R}^2$.

If we look at the Schottky group starting with three mutually tangent identical circles together with a little circle in the middle tangent to all the other three, and we apply the circle inversions, the limit set we obtain for this Schottky group turns out to be the Apollonian gasket (Figure 3.1.3). This construction of the Apollonian gasket is very convenient for finding homeomorphisms, in which case the corresponding Schottky group has provided abundant homeomorphisms of the fractal.

3.2 Addresses and Cells

Most of the definitions in this section will be analogous to those of the Sierpinski gasket given in Section 2.3.

In order to describe points in the Apollonian gasket (AG), we need and *address system* that assigns addresses. The address system described in this section is based on the visual geometry of the Apollonian gasket. The basic components of the Apollonian gasket are *cells*, and each cell is divided into three *subcells*. The complete Apollonian gasket is composed of two *main cells* as illustrated in Figure 3.2.1.

The structure of the Apollonian gasket is described by a *hypergraph replacement system*. As shown in Figure 3.2.2, we may start with a *base graph*, and apply the *replacement rule* to

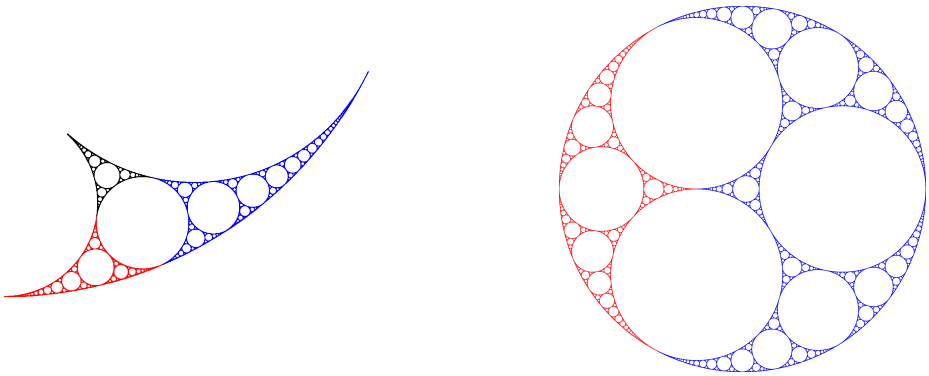

Figure 3.2.1: Cells, Subcells, and Main Cells of the Apollonian Gasket

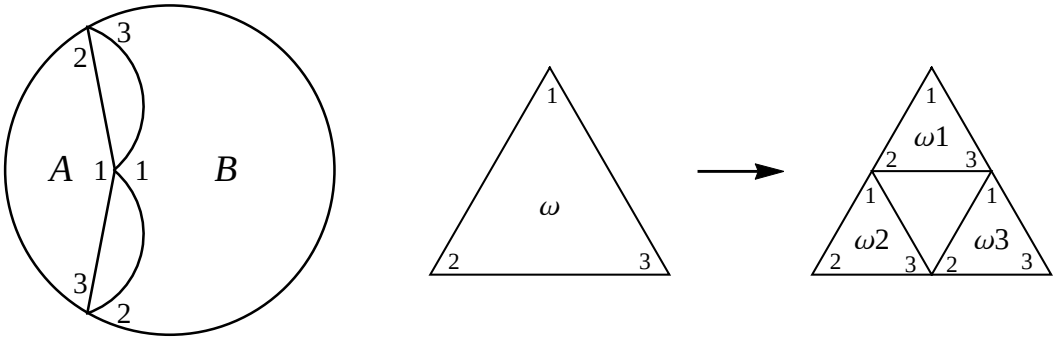

Figure 3.2.2: Base Graph and Replacement Rule for the Apollonian Gasket

components of the base graph. If we keep applying the replacement rule to subsequent graphs, the limit of these graphs will eventually be homeomorphic to the Apollonian gasket. In addition, every point in the Apollonian gasket can be described by an *address* – an infinite sequence of $\{0, 1, 2\}$ with one of $\{A, B\}$ at the beginning.

Definition 3.2.1. The **symbol space** of the Apollonian gasket is the set of infinite sequences $\Omega_{AG} = \{A, B\} \times \{1, 2, 3\}^{\infty}$.

The set $\Omega_{AG} = \{A, B\} \times \{1, 2, 3\}^{\infty}$ is a topological space with product topology. It is homeomorphic to the Cantor set.

There are points in the Apollonian gasket with multiple addresses. For example, the junction points between the main cells A and B can be viewed as in either A or B. The address $A\bar{1}$

refers to the same point in the Apollonian gasket as the address $B\overline{1}$ does. We give the following proposition for equivalent addresses on the Apollonian gasket.

Proposition 3.2.2. *The following addresses are identified*

$$A\overline{1} = B\overline{1}, \qquad A\overline{2} = B\overline{3}, \qquad A\overline{3} = B\overline{2}. \tag{3.2.1}$$

In addition, given any finite word $\omega \in \{A, B\} \times \{1, 2, 3\}^{k-1}$ of length k, the following addresses are identified

$$\omega 1\overline{2} = \omega 2\overline{1}, \qquad \omega 2\overline{3} = \omega 3\overline{2}, \qquad \omega 1\overline{3} = \omega 3\overline{1}. \tag{3.2.2}$$

The rules defined in this proposition induces a quotient map $q\colon \Omega_{AG} \to AG$. The Apollonian gasket is homeomorphic to the quotient space of Ω_{AG} with the quotient topology induced by q.

Definition 3.2.3. A cell of the Apollonian gasket is the collection of all the points with the same initial n digits in their addresses. Formally, a set of points S is a **cell** if there exist $n \geq 1$ such that $S = \omega \times \{1, 2, 3\}^{\infty}$ for some finite word $\omega \in \{A, B\} \times \{1, 2, 3\}^{n-1}$. The integer n is the **depth** of the cell S, and the finite word ω is the **address** of the cell S. The cell S is referred to as the ω-cell, or simply cell ω when there is no confusion.

Definition 3.2.4. A cell of depth 1 is a **main cell** of the Apollonian gasket. There are two main cells of the Apollonian gasket, namely, the A-cell and the B-cell.

The following claim helps us understand the connection pattern of the Apollonian gasket.

Claim 3.2.5. *The removal of a set of three points from the Apollonian gasket disconnects the Apollonian gasket if and only if at least one of the disconnected component is a cell.*

If we pick a cell with address ω, and we remove the three boundary points, namely the ones with addresses $\omega\overline{1}$, $\omega\overline{2}$, and $\omega\overline{3}$, the ω-cell is naturally disconnected from its complement in the Apollonian gasket. The converse is rather clear from the geometry of the Apollonian gasket.

We introduce a useful notation for the manipulation of addresses. Let $\omega \in \{1, 2, 3\}^{\infty}$ be an infinite word, and let a be an element of the permutation group. The infinite word obtained by

replacing each letter of ω according to the permutation a is denoted $\pi_a\omega$. Notice that for any word ω and any two permutations a, b, we have $\pi_b\pi_a\omega = \pi_{ba}\omega$.

3.3 Generators

In this section, we present several homeomorphisms in terms of the addresses. In the section following, we will show that three of these homeomorphisms generate the homeomorphism group Homeo(AG) of the Apollonian gasket.

Definition 3.3.1. Let r be the counterclockwise 120° rotation of the Apollonian gasket. Symbolically, we have $r : \Omega_{AG} \longrightarrow \Omega_{AG}$ with

$$r(A\omega) = B2\omega, \quad r(B2\omega) = B3\omega, \quad r(B3\omega) = A\omega, \quad r(B1\omega) = B1\pi_{(1\ 2\ 3)}\omega \tag{3.3.1}$$

for all $\omega \in \{1, 2, 3\}^\infty$.

Definition 3.3.2. Let s be the horizontal reflection of the Apollonian gasket. Symbolically, we have $s : \Omega_{AG} \longrightarrow \Omega_{AG}$ with

$$s(A\omega) = A\pi_{(2\ 3)}\omega, \quad s(B\omega) = B\pi_{(2\ 3)}\omega \tag{3.3.2}$$

for all $\omega \in \{1, 2, 3\}^\infty$.

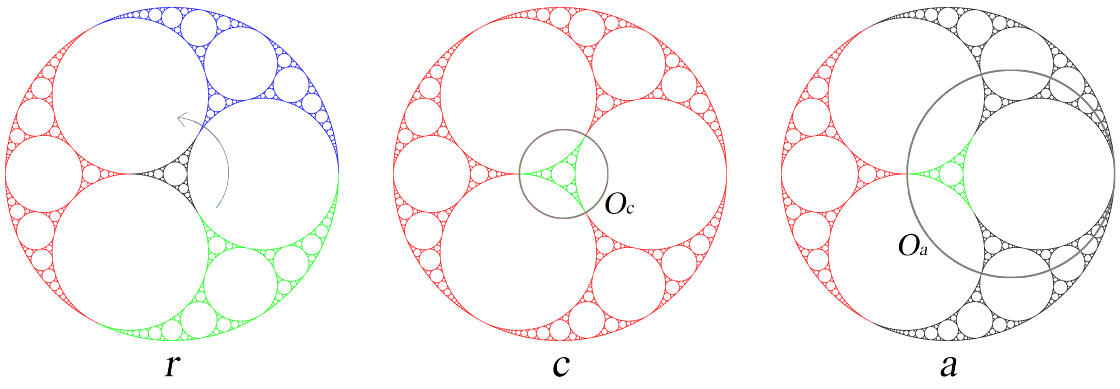

Figure 3.3.1: The Homeomorphisms r, c, and a of the Apollonian Gasket

It is clear that r and s are homeomorphisms of the Apollonian gasket and they generate the dihedral group D_3, and therefore, D_3 is a subgroup of Homeo(AG).

Definition 3.3.3. Let c be the circle inversion across the circle O_c. The map $c : \Omega_{AG} \longrightarrow \Omega_{AG}$ is symbolically defined by

$$\begin{aligned} &c(A\omega) = B11\pi_{(2\ 3)}\omega, \qquad c(B2\omega) = B12\pi_{(1\ 2)}\omega, \qquad c(B3\omega) = B13\pi_{(1\ 3)}\omega, \\ &c(B11\omega) = A\pi_{(2\ 3)}\omega, \qquad c(B12\omega) = B2\pi_{(1\ 2)}\omega, \qquad c(B13\omega) = B3\pi_{(1\ 3)}\omega, \end{aligned} \tag{3.3.3}$$

for all $\omega \in \{1, 2, 3\}^\infty$.

Definition 3.3.4. Let a be the circle inversion across the circle O_a. The map $a : \Omega_{AG} \longrightarrow \Omega_{AG}$ is symbolically defined by

$$\begin{aligned} &a(A\omega) = B1\pi_{(2\ 3)}\omega, \qquad a(B2\omega) = B2\pi_{(1\ 2)}\omega, \\ &a(B1\omega) = A\pi_{(2\ 3)}\omega, \qquad a(B3\omega) = B3\pi_{(1\ 3)}\omega, \end{aligned} \tag{3.3.4}$$

for all $\omega \in \{1, 2, 3\}^\infty$.

We need to verify that c and a are homeomorphisms of the Apollonian gasket. In order to do that, we need to show that both of them are bijective maps under which the identification rules 3.2.1 and 3.2.2 are invariant.

Lemma 3.3.5. *The maps c and a are homeomorphisms of the Apollonian gasket.*

Proof. The definitions of c and a gives well-defined homeomorphisms on Ω_{AG}. We need to show that the equivalence relations within Ω_{AG} specified by Proposition 3.2.2 are invariant under the maps c and a. Recall that the equivalence relations include

$$A\overline{1} = B\overline{1}, \qquad A\overline{2} = B\overline{3}, \qquad A\overline{3} = B\overline{2}, \tag{3.3.5}$$

and

$$\omega 1\overline{2} = \omega 2\overline{1}, \qquad \omega 2\overline{3} = \omega 3\overline{2}, \qquad \omega 1\overline{3} = \omega 3\overline{1}, \tag{3.3.6}$$

for any finite word $\omega \in \{A, B\} \times \{1, 2, 3\}^{k-1}$ of length k.

We first show that the rules in 3.3.5 are invariant under c and a. Apply the maps to the rules in 3.3.5, we get

$$c(A\overline{1}) = B\overline{1},\ c(B\overline{1}) = A\overline{1},\ c(A\overline{2}) = B11\overline{3},\ c(B\overline{3}) = B13\overline{1},\ c(A\overline{3}) = B11\overline{2},\ c(B\overline{2}) = B12\overline{1},$$

and

$$a(A\overline{1}) = B\overline{1},\ a(B\overline{1}) = A\overline{1},\ a(A\overline{2}) = B1\overline{3},\ a(B\overline{3}) = B3\overline{1},\ a(A\overline{3}) = B1\overline{2},\ a(B\overline{2}) = B2\overline{1}.$$

It follows from 3.3.5 and 3.3.6 that

$$c(A\overline{1}) = c(B\overline{1}), \quad c(A\overline{2}) = c(B\overline{3}), \quad c(A\overline{3}) = c(B\overline{2}),$$

and

$$a(A\overline{1}) = a(B\overline{1}), \quad a(A\overline{2}) = a(B\overline{3}), \quad a(A\overline{3}) = a(B\overline{2}).$$

Now we show that the rules in 3.3.6 are invariant under c and a. The proof is fairly mechanical. We show the proof for one case of a, the rest and the proof for c follows a similar argument. Let $\omega \in \{1, 2, 3\}^k$ be a finite word of length k. Then

$$a(A\omega 1\overline{2}) = B1\pi_{(2\ 3)}\omega 1\overline{3}, \quad a(A\omega 2\overline{3}) = B1\pi_{(2\ 3)}\omega 3\overline{2}, \quad a(A\omega 1\overline{3}) = B1\pi_{(2\ 3)}\omega 1\overline{2},$$

$$a(A\omega 2\overline{1}) = B1\pi_{(2\ 3)}\omega 3\overline{1}, \quad a(A\omega 3\overline{2}) = B1\pi_{(2\ 3)}\omega 2\overline{3}, \quad a(A\omega 3\overline{1}) = B1\pi_{(2\ 3)}\omega 2\overline{1}.$$

By 3.3.6, we have

$$a(A\omega 1\overline{2}) = a(A\omega 2\overline{1}), \quad a(A\omega 2\overline{3}) = a(A\omega 3\overline{2}), \quad a(A\omega 1\overline{3}) = a(A\omega 3\overline{1}).$$

Similarly, we are able to deduce that

$$a(B1\omega 1\overline{2}) = a(B1\omega 2\overline{1}), \quad a(B1\omega 2\overline{3}) = a(B1\omega 3\overline{2}), \quad a(B1\omega 1\overline{3}) = a(B1\omega 3\overline{1}),$$

$$a(B2\omega 1\overline{2}) = a(B2\omega 2\overline{1}), \quad a(B2\omega 2\overline{3}) = a(B2\omega 3\overline{2}), \quad a(B2\omega 1\overline{3}) = a(B2\omega 3\overline{1}),$$

$$a(B3\omega1\overline{2}) = a(B3\omega2\overline{1}), \quad a(B3\omega2\overline{3}) = a(B3\omega3\overline{2}), \quad a(B3\omega1\overline{3}) = a(B3\omega3\overline{1}).$$

Hence, we conclude that the identification rules 3.3.5 and 3.3.6 are invariant under a. With the same approach, we can prove the same argument for c. Therefore, both c and a are homeomorphisms of the Apollonian gasket. □

Lemma 3.3.6. *The group generated by r and a is isomorphic to the permutation group S_4.*

Proof. We consider the four cells $\alpha, \beta, \gamma, \delta$ shown in the figure below.

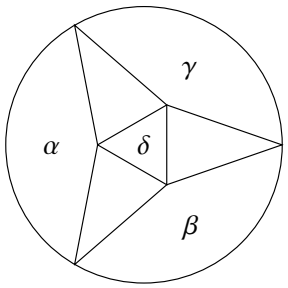

The map r cyclically permutes the cells α, β, and γ and preserves the cell δ, and a switches the cells α and δ and preserves the other two cells. Hence, a homomorphism $\varphi : \langle r, a\rangle \longrightarrow S_4$ can be defined by

$$\varphi : r \mapsto (\alpha\ \beta\ \gamma) \text{ and } a \mapsto (\alpha\ \delta).$$

Incidentally, $(\alpha\ \beta\ \gamma)$ and $(\alpha\ \delta)$ generate S_4, which makes φ an isomorphism. □

Therefore, S_4 is a subgroup of Homeo(AG). Furthermore, because $D_3 \cong S_3 \leq S_4$, it follows that $s \in \langle r, a\rangle$. We can figure out that $s = r^2ar^2arar$.

Definition 3.3.7. Let b be the map defined by the composition of maps $b = arcr^2a$.

By composing the symbolic definitions of r, c, and a, we may figure out that the symbolic interpretation of the map $b : \Omega_{AG} \longrightarrow \Omega_{AG}$ is described by

$$b(A\omega) = B\pi_{(2\ 3)}\omega, \quad b(B\omega) = A\pi_{(2\ 3)}\omega \tag{3.3.7}$$

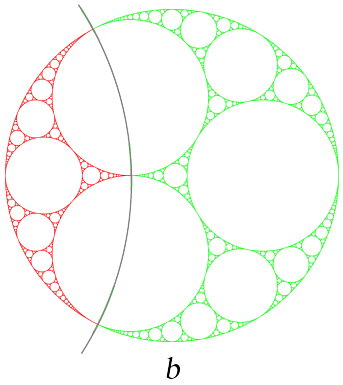

Figure 3.3.2: Geometric Presentation of the Map b

for all $\omega \in \{1,2,3\}^\infty$. Geometrically, the map b is the circle inversion that switches the A-cell with the B-cell as shown in Figure 3.3.2.

Definition 3.3.8. Let t be the map defined by the composition of maps $t = rar^2$.

The symbolic dynamics of the map $t : \Omega_{AG} \longrightarrow \Omega_{AG}$ is described by

$$t(A\omega) = A\pi_{(1\ 3)}\omega, \quad t(B\omega) = B\pi_{(1\ 2)}\omega \tag{3.3.8}$$

for all $\omega \in \{1,2,3\}^\infty$. Geometrically, the map t preserves both the A-cell and the B-cell but switches the $A1$-cell with the $A3$-cell as well as switching the $B1$-cell and the $B2$-cell.

Lemma 3.3.9. *$\langle s,t\rangle$ is isomorphic to the permutation group S_3.*

Proof. Both s and t preserves the location of the A-cell. The map s switches the labels 1 and 2 on the A-cell, and the map t switches the labels 1 and 3 on the A-cell. Hence, a homomorphism $\varphi : \langle s,t\rangle \longrightarrow S_3$ can be defined by

$$\varphi : s \mapsto (1\ 2) \text{ and } t \mapsto (1\ 3).$$

Incidentally, (1 2) and (1 3) generates S_3, which makes φ an isomorphism. □

Readers should keep in mind that both subgroups $\langle r,s\rangle$ and $\langle s,t\rangle$ of Homeo(AG) are isomorphic to S_3. These are two different copies of S_3 in Homeo(AG). In fact, there are countably many copies of S_3 inside of Homeo(AG).

3.4 Proof of Generation

In this section, we will show that the homeomorphism group of the Apollonian gasket is generated by a set of three generators, namely, $\{r, c, a\}$.

Corollary 3.4.1. *$\langle r, c, a\rangle$ is a subgroup of* Homeo(AG).

Proof. The argument follows directly from the fact that $r, c, a \in$ Homeo(AG) shown in Lemma 3.3.5. □

Lemma 3.4.2. *Let $S \subseteq AG$ be a cell. Then there exist $x \in \langle r, c, a\rangle$ such that $x(A) = S$.*

Proof. Because we have the map $b = arcr^2a$ that switches the A-cell with the B-cell, it suffices to show the argument for any subcell of the A-cell. We use proof by induction.

Base Case 1. The map $w_1 = ba$ maps the A-cell onto the $A1$-cell.

Let $\omega \in \{1, 2, 3\}^\infty$ be an infinite word. Then

$$w_1(A\omega) = b(a(A\omega)) = b(B1\pi_{(2\ 3)}\omega) = A1\omega$$

It is clear that $w_1(A) = A1$.

Base Case 2. The map $w_2 = br^2s$ maps the A-cell onto the $A2$-cell.

Let $\omega \in \{1, 2, 3\}^\infty$ be an infinite word. Then

$$w_2(A\omega) = b(r^2(s(A\omega))) = b(r^2(A\pi_{(2\ 3)}\omega)) = b(B3\pi_{(2\ 3)}\omega) = A2\omega.$$

It follows that $w_2(A) = A2$.

Base Case 3. The map $w_3 = brs$ maps the A-cell onto the $A3$-cell.

Let $\omega \in \{1, 2, 3\}^\infty$ be an infinite word. Then

$$w_2(A\omega) = b(r(s(A\omega))) = b(r(A\pi_{(2\ 3)}\omega)) = b(B2\pi_{(2\ 3)}\omega) = A3\omega.$$

It follows that $w_3(A) = A3$.

Inductive Step. Let $\sigma \in \{1,2,3\}^k$ be a finite word of length k. Suppose that there exist a map $x \in \langle r, c, a\rangle$ such that $x(A) = A\sigma$. Let $\omega \in \{1,2,3\}^\infty$ be an infinite word. Then $x(A\omega) = A\sigma\omega$. Thus $w_1x(A\omega) = w_1(A\sigma\omega) = A1\sigma\omega$. It follows that w_1x maps the A-cell onto the $A1\sigma$-cell. Similarly, w_2x and w_3x maps the A-cell onto the $A2\sigma$-cell and the $A3\sigma$-cell, respectively.

Hence, given any subcell S of the A-cell, there exist $x \in \langle r, c, a\rangle$ such that $x(A) = S$. The same result follows immediately for any cell of the Apollonian gasket. □

Corollary 3.4.3. *Let $S, T \subseteq AG$ be two cells. Then there exist $z \in \langle r, c, a\rangle$ such that $z(T) = S$.*

Proof. Lemma 3.4.2 ensures the existence of maps $x, y \in \langle r, c, a\rangle$ such that $x(A) = S$ and $y(A) = T$. Let $z = xy^{-1}$. Then $z(T) = x(y^{-1}(T)) = x(A) = S$. □

Lemma 3.4.4. *Let $\phi : AG \longrightarrow AG$ be a homeomorphism of the Apollonian gasket. The image of a cell in AG under the map ϕ is either a cell or the complement of a cell.*

Proof. Let $S \subseteq AG$ be a cell. Let $T = \phi(S)$ be the image of S. There exist a homeomorphism x such that $x(S)$ is the A-cell. Then $bx(S)$ is the B-cell. Thus $x(S) \cup bx(S) = AG$ and $x(S) \cap bx(S)$ is a set of three points $P = \{p_1, p_2, p_3\}$ with addresses $A\overline{1}$, $A\overline{2}$, and $A\overline{3}$. Notice that the removal of P from AG disconnects AG into two components. Because x and ϕ are homeomorphisms, it follows that $\phi x^{-1}(x(S)) \cup \phi x^{-1}(bx(S)) = AG$, and $\phi x^{-1}(x(S)) \cap \phi x^{-1}(bx(S))$ contains three points, whose removal disconnects AG into two components. But $\phi x^{-1}(x(S)) = \phi(S) = T$, and $\phi x^{-1}(bx(S))$ is the complement of T in AG. It follows from Claim 3.2.5 that T is either a cell or the complement of a cell. □

Theorem 3.4.5. $\text{Homeo}(AG) = \langle r, c, a\rangle$.

Proof. Let $\phi \in \text{Homeo}(AG)$. Then $\phi(A)$ is either a cell or the complement of a cell. If $\phi(A)$ is a cell, then there exist $x \in \langle r, c, a\rangle$ such that $x(A) = \phi(A)$. Since each cell of the Apollonian gasket is homeomorphic to the Sierpinski gasket, and the homeomorphism group of the Sierpinski gasket is isomorphic to S_3, it follows that there exist $u \in \langle s, t\rangle$ such that $xu = \phi$. If $\phi(A)$

is the complement of a cell, then $\phi(B)$ has to be a cell, and there exist $y \in \langle r, c, a \rangle$ such that $y(A) = \phi(B)$. There exist $v \in \langle s, t \rangle$ such that $yv = \phi$. Thus $\phi \in \langle r, c, a \rangle$. Hence, we have Homeo$(AG) \leq \langle r, c, a \rangle$. Together with Corollary 3.4.1, we conclude that Homeo$(AG) = \langle r, c, a \rangle$. □

4

The Eyes Julia Sets

Another fractal structure we investigated was the *Eyes Julia set* (Figure 4.0.1). The Eyes Julia set corresponds to the rational function $f(z) = (z^2+1)/(z^2-1)$. We also investigated a 3-piece modification of the Eyes Julia set, which corresponds to the algebraic function $g(z) = f(z^{3/4})^{4/3}$. In this chapter, we will construct fractals E_4 and E_3 according to the structure of these two Julia sets, respectively, and show finite generation of the homeomorphism group of E_3 by a set of four generators. Additionally, we will give preliminary arguments to showing that the homeomorphism group of the fractal E_4 is finite.

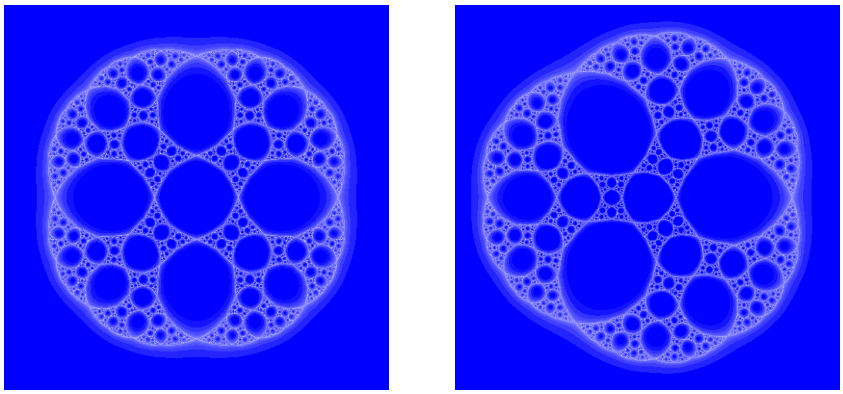

Figure 4.0.1: The 4-Piece and 3-Piece Eyes Julia Sets

4.1 Construction of the E_4 and E_3 Fractals

Similar to the approach for the Apollonian gasket, we use a hypergraph replacement system to construct the E_4 and E_3 fractals. In the next section, we will use an *address system*, according to the geometric structure of the E_3 fractal defined by this replacement system, to describe the location of points within the fractal.

The global structures of E_4 and E_3 are captured by two different *base graphs*, and their common local structure is described by a *replacement rule* shown in Figure 4.1.1. The replacement rule can be applied to each subcell the fractals, and the fractals can be obtained by taking the limit of all the graphs under such replacement rule. We notice that the only difference between the base graphs of E_4 and E_3 is the order of the labels $1, 2, 3, 4$ appearing on the boundary of the B-cell. We also notice that in the replacement rule, the order of the labels in subcells are different from that in the starting cell. However, if we apply the replacement rule once more, we are able to get the original order back to the next level of subcells, which is shown in Figure 4.1.2.

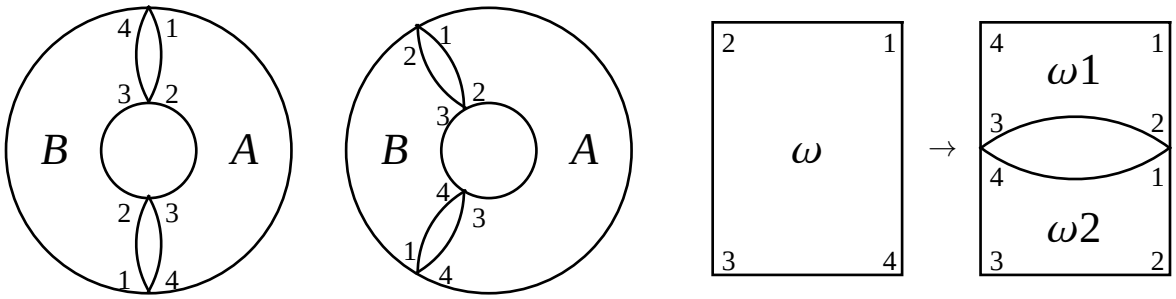

Figure 4.1.1: Base Graphs of E_4 and E_3 together with Their Replacement Rule

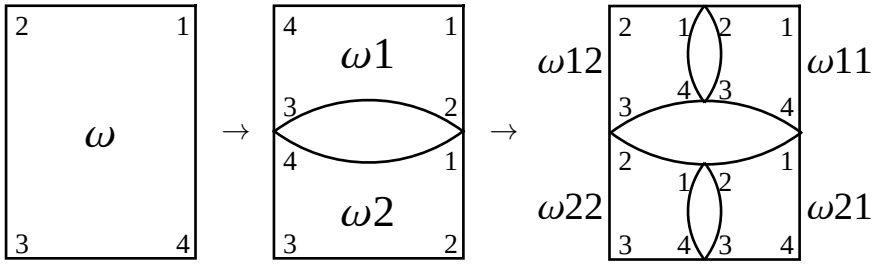

Figure 4.1.2: Applying the Replacement Rule Twice Retains the Order of Labels

4.2 Addresses and Cells of E_3

The definitions on addresses and cells in this section will be constructed in analogous to those of the Sierpinski gasket and Apollonian gasket given in Section 2.3 and 3.2, respectively. From now on, we will use the picture of the Julia set as a visualization of the E_3 fractal, but readers should keep in mind that the E_3 fractal only appear to be homeomorphic to the Julia set. We will not show homeomorphism relation between these two objects in this project.

In order to describe points in the E_3 fractal, we need an *address system*, based on the hypergraph replacement system defined in the previous section, to assign addresses to points inside of the fractal. The basic components of the E_3 fractal are *cells*, and each cell is divided into two *subcells*. The complete E_3 fractal is composed of two *main cells*, as shown in Figure 4.2.1

Based on the hypergraph replacement system, we assign symbols A and B to the main cells of the E_3 fractal. The replacement rule gives the way to assign symbols to subcells by concatenating 1 or 2 to the symbol of the starting cell. The replacement rule can be applied to each subcell of E_3, and E_3 can be obtained by taking the limit of all the graphs under such replacement rule. Similar to the case of the Apollonian gasket, every point in E_3 can be described by an *address*, which is an infinite sequence of $\{1, 2\}$ with one of $\{A, B\}$ at the beginning.

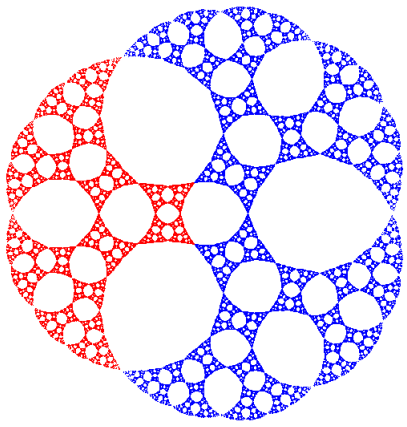

Figure 4.2.1: Main Cells of the E_3 Fractal

Definition 4.2.1. The **symbol space** of the E_3 fractal is the set of infinite sequences $\Omega_{E_3} = \{A, B\} \times \{1, 2\}^\infty$.

If we consider Ω_{E_3} as a topological space with product topology, it is homeomorphic to the Cantor set.

Definition 4.2.2. A cell of E_3 is the collection of all the points with the same initial n digits in their addresses. Formally, a set of points S is a **cell** if there exist $n \geq 1$ such that $S = \omega \times \{1, 2\}^\infty$ for some finite word $\omega \in \{A, B\} \times \{1, 2\}^{n-1}$. The integer n is the **depth** of the cell S, and the finite word ω is the **address** of the cell S. The cell S is referred to as the ω-cell, or simply cell ω when there is no confusion.

Definition 4.2.3. A cell of depth 1 is a **main cell** of E_3. There are two main cells of E_3, namely, the A-cell and the B-cell.

We observe that, unlike the case in the Sierpinski gasket or the Apollonian gasket, the order of labels on the edges of each cell is not preserved after applying the replacement rule. However, it is preserved under two applications of the replacement rule. Therefore, given the address of an ω-cell, we can write down the addresses of its four edges:

$$1 : \omega\overline{1}, \qquad 2 : \omega\overline{12}, \qquad 3 : \omega\overline{2}, \qquad 4 : \omega\overline{21}. \tag{4.2.1}$$

The addresses of points in the E_3 fractal are not uniquely determined. For example, the junction points between two adjacent cells may have two different addresses since they lie on the intersection of two different cells. The replacement rule tells us that, in each cell, there are two pairs of addresses, each pair referring to one single point of the cell. We provide the following proposition for these identified addresses.

Proposition 4.2.4. *The following addresses are identified*

$$A\overline{1} = B\overline{12}, \qquad A\overline{12} = B\overline{2}, \qquad A\overline{2} = B\overline{21}, \qquad A\overline{21} = B\overline{1}. \tag{4.2.2}$$

In addition, given any finite word $\omega \in \{A, B\} \times \{1, 2\}^{k-1}$ of length k, the following addresses are identified

$$\omega 1\overline{2} = \omega 2\overline{21}, \qquad \omega 1\overline{12} = \omega 2\overline{1}. \tag{4.2.3}$$

Definition 4.2.5. The **pinch points** in E_3 are points that correspond to two different addresses in Ω_{E_3} identified by Proposition 4.2.4.

Each boundary point of cells is a pinch point in E_3. Furthermore, the rules defined by Proposition 4.2.4 induces a quotient map $q : \Omega_{E_3} \longrightarrow E_3$. The E_3 fractal is homeomorphic to the quotient space of Ω_{E_3} with quotient topology induced by q.

Claim 4.2.6. *Each cell is path connected, and there exists a unique set of two points in each cell, whose removal disconnects the cell into two cells.*

The validity of this claim is fairly clear from the geometry of the cells. It helps in proving the following theorem.

Theorem 4.2.7. *The full homeomorphism group of a cell S is isomorphic to the Klein-4 group $\mathbb{Z}/2 \times \mathbb{Z}/2$.*

Proof. Notice that there is a Klein-4 group generated by the horizontal and vertical reflections within the homeomorphism group of S. We will refer to this Klein-4 group as D_2. Let $P = \{p_1, p_2\}$ be the set of two points according to Claim 4.2.6. Furthermore, we can have a unique set of four points $Q = \{q_1, q_2, q_3, q_4\}$, whose removal following the removal of P disconnects the cell into four subcells. Each subcell is then further partitioned into two sub-subcells. We denote these eight cells with labels **1** through **8**. Because P and Q have the topological property stated, both P and Q must be invariant under any homeomorphism of the cell. Let $\varphi : S \longrightarrow S$ be a homeomorphism. Then there exist a $\sigma \in D_2$ such that $(\sigma \circ \varphi)(p_i) = p_i$ for $i \in \{1, 2\}$. Let $\psi = \sigma \circ \varphi$. Then ψ is a homeomorphism of SG that fixes p_1 and p_2. We will first show that $\psi \in D_2$.

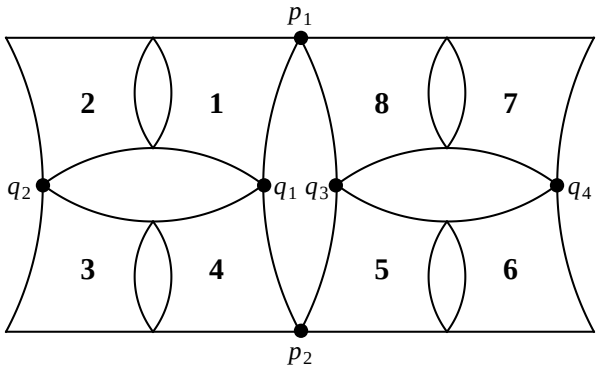

Each cell is path connected. Thus there exist a path lying entirely within cell **1** that connects from q_1 to p_1. If $\psi(q_1) = q_2$, there cannot be any paths lying entirely within one cell that connects from $\psi(q_1)$ to $\psi(p_1)$. Hence, $\psi(q_1) \neq q_2$. For the same reason, we have $\psi(q_1) \neq q_4$, $\psi(q_3) \neq q_4$, and $\psi(q_3) \neq q_2$. Furthermore, because ψ is a homeomorphism, we have $\psi(q_2) \neq q_1$, $\psi(q_4) \neq q_1$, $\psi(q_4) \neq q_3$, and $\psi(q_2) \neq q_3$. Therefore, there are only two candidates for ψ, namely, $\psi_1 : S \to S$, whose restriction on Q is the identity map, and $\psi_2 : S \to S$, whose restriction on Q is defined by

$$\psi_2 : q_1 \mapsto q_3,\ q_2 \mapsto q_4,\ q_3 \mapsto q_1,\ q_4 \mapsto q_2.$$

It then suffices to show that ψ_1 is the identity map on S.

Now we take a closer look at the cell composed of **1** and **2**. This cell has a unique set of two points $R = \{r_1, r_2\}$ whose removal disconnects the cell into **1** and **2**, and $\psi_1(R) = R$. Furthermore, each of **1** and **2** can be subdivided into two cells. We denote these four cells within this subcell TL, BL, TR, and BR.

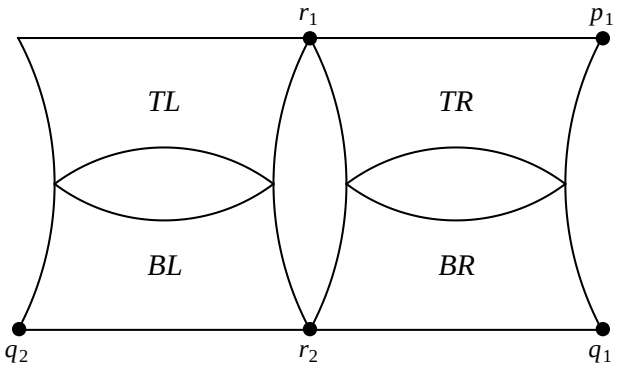

There exist a path lying entirely within the TR cell that connects r_1 with p_1. Suppose that $\psi_1(r_1) = r_2$, then any path connecting $\psi_1(r_1)$ and $\psi_1(p_1) = p_1$ cannot sit entirely in one of these four cells, and ψ_1 would not be a homeomorphism. Thus $\psi_1(r_1) = r_1$ and $\psi_2(r_2) = r_2$.

This process can be iterated to show that every point within a cell S where two subcells meet each other is fixed by ψ_1. Such points form a dense subset of S. Then ψ_1 agrees with the identity map on a dense subset of S. Because ψ_1 is a homeomorphism, it follows that ψ_1 is the identity map. We conclude that the full homeomorphism group of a cell S is $D_2 \cong \mathbb{Z}/2 \times \mathbb{Z}/2$. □

Claim 4.2.8. *The removal of a set of four points from the E_3 fractal disconnects E_3 if and only if at least one of the disconnected component is a cell.*

If we pick a cell with address ω, and we remove the boundary points of the cell, namely the ones with addresses $\omega\overline{1}$, $\omega\overline{12}$, $\omega\overline{2}$, and $\omega\overline{21}$, the ω-cell is naturally disconnected from its complement in E_3. The converse is rather clear from the geometry of E_3.

At the end of this section, we introduce two useful notations for manipulating the addresses of points in E_3.

Definition 4.2.9. Let $\omega \in \{1, 2\}^\infty$ be an infinite word. The **negation operation** on ω, denoted by ω^{-1}, is defined by replacing every letter 1 in ω by 2, and every 2 by 1.

Definition 4.2.10. Let $\omega \in \{1, 2\}^\infty$ be an infinite word. We can break ω into two-digit words by placing a break at every other digit. There are four possible two-digit words, namely 11, 12, 22, and 21. The **reflection operation** on ω, denoted by ω^*, is defined by replacing every word 11 by 12, 12 by 11, 22 by 21, and 21 by 22.

The following automata show the negation and the reflection operations on a word ω.

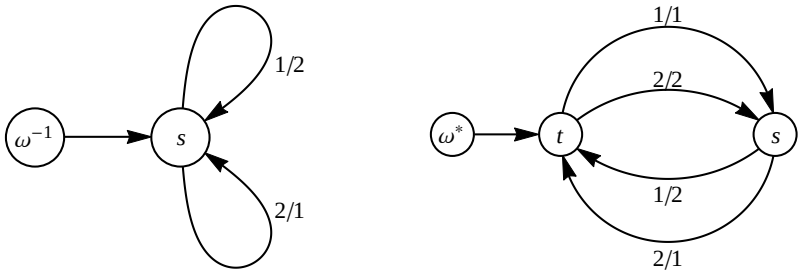

We notice that both the negation and reflection operations are inverses of themselves, *i.e.* $(\omega^{-1})^{-1} = \omega$, and $(\omega^*)^* = \omega$ for all $\omega \in \{1,2\}^\infty$. Moreover, these two operations commutes with each other, *i.e.* $(\omega^{-1})^* = (\omega^*)^{-1}$ for all $\omega \in \{1,2\}^\infty$. We shall denote the composition of these two operations on ω by ω^{*-1}, and the automaton for this composition is shown below.

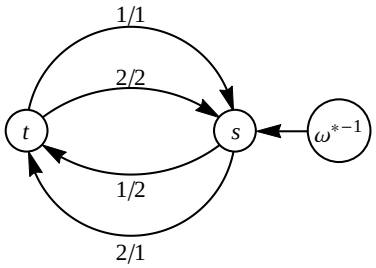

4.3 Generators

In this section, we present four homeomorphisms of E_3 in terms of the addresses. In the section following, we will show that these four homeomorphisms generate the homeomorphism group Homeo(E_3) of the E_3 fractal.

Definition 4.3.1. Let r be the counterclockwise 120-degree rotation of the E_3 fractal. Symbolically, we have $r : E_3 \longrightarrow E_3$ with

$$r(A1\omega) = B\omega, \quad r(A2\omega) = A1\omega, \quad r(B\omega) = A2\omega, \tag{4.3.1}$$

for all $\omega \in \{1,2\}^\infty$.

Definition 4.3.2. Let s be the horizontal reflection of the E_3 fractal. Symbolically, we have $s : E_3 \to E_3$ with

$$s(A1\omega) = A2\omega^*, \quad s(A2\omega) = A1\omega^*, \quad s(B\omega) = B\omega^*, \tag{4.3.2}$$

for all $\omega \in \{1,2\}^\infty$.

The following lemma verifies that r and s are homeomorphisms of E_3.

Lemma 4.3.3. *The maps r and s are homeomorphisms of the E_3 fractal.*

Proof. The definitions of r and s ensures that they give well-defined homeomorphisms o Ω_{E_3}. We need to show that the equivalence relations in Proposition 4.2.4 are invariant under r and s. Recall that the equivalence relations include

$$A\overline{1} = B\overline{12}, \qquad A\overline{12} = B\overline{2}, \qquad A\overline{2} = B\overline{21}, \qquad A\overline{21} = B\overline{1}, \tag{4.3.3}$$

and

$$\omega 1\overline{2} = \omega 2\overline{21}, \qquad \omega 1\overline{12} = \omega 2\overline{1}. \tag{4.3.4}$$

for any finite word $\omega \in \{A,B\} \times \{1,2\}^{k-1}$ of length k.

We first show that the rules in 4.3.3 are preserved under r and s. Applying the maps to the rules in 4.3.3 gives

$$r(A\overline{1}) = B\overline{1},\ r(B\overline{12}) = A\overline{21}, \quad r(A\overline{12}) = B\overline{21},\ r(B\overline{2}) = A\overline{2},$$

$$r(A\overline{2}) = A1\overline{2},\ r(B\overline{21}) = A2\overline{21}, \quad r(A\overline{21}) = A1\overline{12},\ r(B\overline{1}) = A2\overline{1},$$

and

$$s(A\overline{1}) = A\overline{21},\ s(B\overline{12}) = B\overline{1}, \quad s(A\overline{12}) = A\overline{2},\ s(B\overline{2}) = B\overline{21},$$

$$s(A\overline{2}) = A\overline{12},\ s(B\overline{21}) = B\overline{2}, \quad s(A\overline{21}) = A\overline{1},\ s(B\overline{1}) = B\overline{12}.$$

It then follows from 4.3.3 that

$$r(A\overline{1}) = r(B\overline{12}), \qquad r(A\overline{12}) = r(B\overline{2}), \qquad r(A\overline{2}) = r(B\overline{21}), \qquad r(A\overline{21}) = r(B\overline{1}),$$

and

$$s(A\overline{1}) = s(B\overline{12}), \qquad s(A\overline{12}) = s(B\overline{2}), \qquad s(A\overline{2}) = s(B\overline{21}), \qquad s(A\overline{21}) = s(B\overline{1}).$$

Now we show that the rules in 4.3.4 are invariant under r and s. Let $\omega \in \{1,2\}^k$ be a finite word of length k. Then

$$r(A1\omega1\overline{2}) = B\omega1\overline{2},\ r(A1\omega2\overline{21}) = B\omega2\overline{21}, \quad r(A1\omega1\overline{12}) = B\omega1\overline{12},\ r(A1\omega2\overline{1}) = B\omega2\overline{1},$$

$$r(A2\omega1\overline{2}) = A1\omega1\overline{2},\ r(A2\omega2\overline{21}) = A1\omega2\overline{21}, \quad r(A2\omega1\overline{12}) = A1\omega1\overline{12},\ r(A2\omega2\overline{1}) = A1\omega2\overline{1},$$

$$r(B\omega1\overline{2}) = A2\omega1\overline{2},\ r(B\omega2\overline{21}) = A2\omega2\overline{21}, \quad r(B\omega1\overline{12}) = A2\omega1\overline{12},\ r(B\omega2\overline{1}) = A2\omega2\overline{1},$$

By 4.3.4, we have

$$r(A1\omega1\overline{2}) = r(A1\omega2\overline{21}),\ r(A2\omega1\overline{2}) = r(A2\omega2\overline{21}),\ r(B\omega1\overline{2}) = r(B\omega2\overline{21}),$$

$$r(A1\omega1\overline{12}) = r(A1\omega2\overline{1}),\ r(A2\omega1\overline{12}) = r(A2\omega2\overline{1}),\ r(B\omega1\overline{12}) = r(B\omega2\overline{1}).$$

Hence, we conclude that the rules in 4.3.4 are preserved under the map r. The case for s is a little more complicated. Let $\omega \in \{1,2\}^{2k}$ be an arbitrary finite word of even length $2k$. Then both sets $\{\omega1, \omega2\}$ and $\{1\omega, 2\omega\}$ can represent the collection of arbitrary finite word of odd length. Now we investigate s in detail in three cases.

$$s(A1\omega1\overline{2}) = A2\omega^*1\overline{12}, \quad s(A1\omega11\overline{2}) = A2\omega^*12\overline{21}, \quad s(A1\omega21\overline{2}) = A2\omega^*22\overline{21},$$

$$s(A1\omega2\overline{21}) = A2\omega^*2\overline{1}, \quad s(A1\omega12\overline{21}) = A2\omega^*11\overline{2}, \quad s(A1\omega22\overline{21}) = A2\omega^*21\overline{2},$$

$$s(A1\omega1\overline{12}) = A2\omega^*1\overline{2}, \quad s(A1\omega11\overline{12}) = A2\omega^*12\overline{1}, \quad s(A1\omega21\overline{12}) = A2\omega^*22\overline{1},$$

$$s(A1\omega2\overline{1}) = A2\omega^*2\overline{21}, \quad s(A1\omega12\overline{1}) = A2\omega^*11\overline{12}, \quad s(A1\omega22\overline{1}) = A2\omega^*21\overline{12}.$$

By 4.3.4, we have $s(A1\omega1\overline{2}) = s(A1\omega2\overline{21})$ and $s(A1\omega1\overline{12}) = s(A1\omega2\overline{1})$ for any finite word $\omega \in \{1,2\}^k$ of any length k. Similarly, we can show $s(A2\omega1\overline{2}) = s(A2\omega2\overline{21})$, $s(A2\omega1\overline{12}) = s(A2\omega2\overline{1})$,

$s(B\omega 1\overline{2}) = s(B\omega 2\overline{21})$, and $s(B\omega 1\overline{12}) = s(B\omega 2\overline{1})$ with the same approach. The process is fairly technical, and we omit the details here.

Therefore, we can conclude that the rules in 4.3.4 and 4.3.3 are preserved by both r and s. Both r and s are homeomorphisms of the E_3 fractal. □

Definition 4.3.4. Let c be the inversion across the central circle. The map $c : E_3 \longrightarrow E_3$ is symbolically defined by

$$c(A\omega) = A\omega^*, \quad c(B1\omega) = B2\omega^*, \quad c(B2\omega) = B1\omega^*, \tag{4.3.5}$$

for all $\omega \in \{1, 2\}^\infty$.

Definition 4.3.5. Let $a : E_3 \longrightarrow E_3$ defined symbolically by

$$a(A\omega) = B\omega, \quad a(B\omega) = A\omega^{-1}, \tag{4.3.6}$$

for all $\omega \in \{1, 2\}^\infty$.

Lemma 4.3.6. *The maps r and s are homeomorphisms of the E_3 fractal.*

Proof. The proof for this lemma is very similar to the proof for Lemma 4.3.3 and it is very technical. We omit the detail of this proof here. □

The geometric interpretation of these homeomorphisms is shown in Figure 4.3.1.

The following theorems show some subgroups of the homeomorphism group of E_3 generated by part of $\{a, c, r, s\}$, all of which are useful in the next section for finding a presentation of Homeo(E_3). Theorem 4.3.10 is especially important in the following section for the proof of finite generation of Homeo(E_3).

Theorem 4.3.7. *$\langle c, r, s\rangle$ is isomorphic to the dihedral group D_6.*

Proof. We take a look at the geometric interpretation of c, r, and s. Generator c switches cells $B1$ with $B2$, $A11$ with $A12$, $A21$ with $A22$; generator r cyclically permutes cells $B1$, $A11$, $A21$

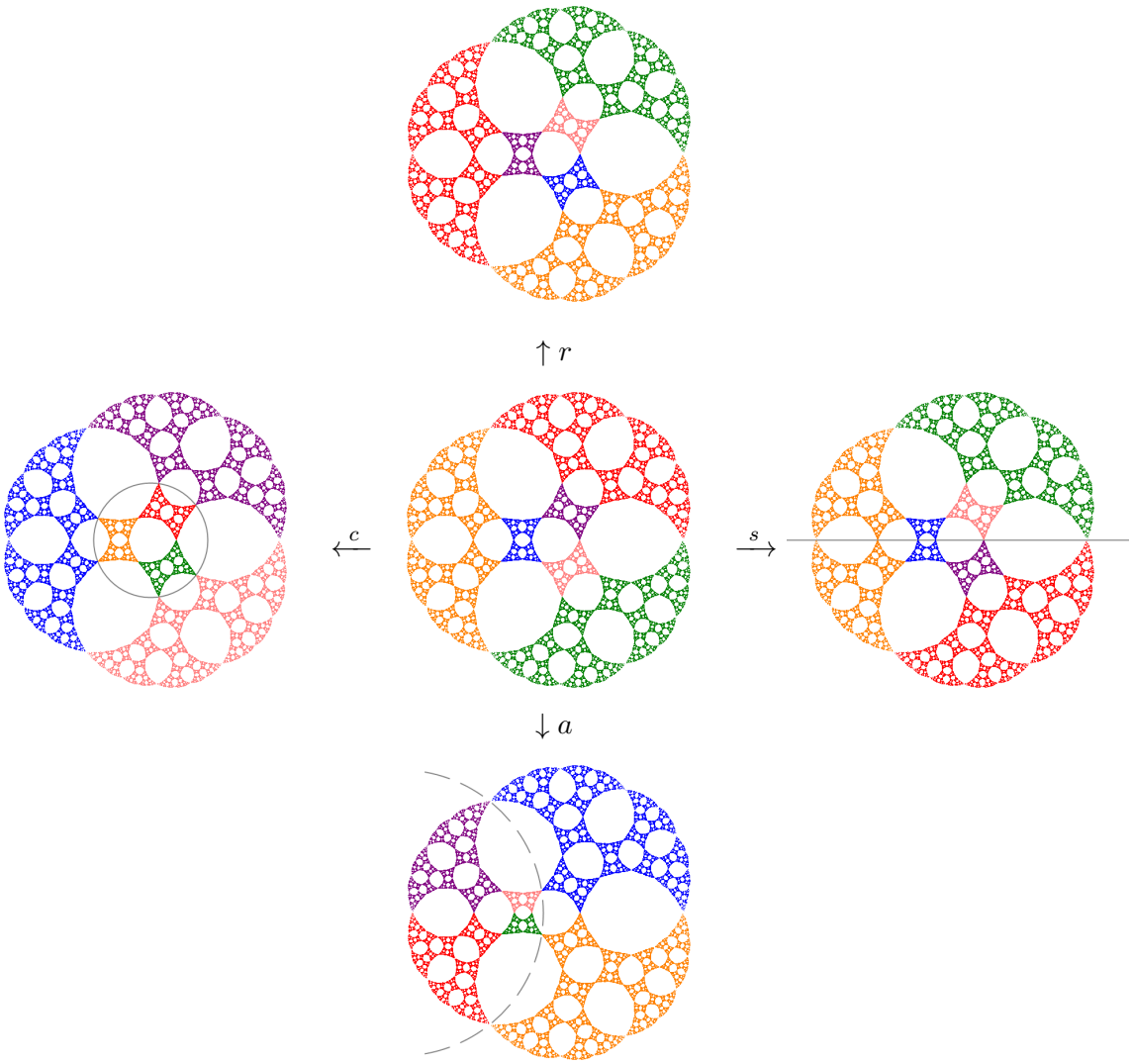

Figure 4.3.1: Four Homeomorphisms in Homeo(E_3)

and cells $B2$, $A12$, $A22$; generator s switches cells $A12$ with $A22$ and cells $A11$ with $A21$.

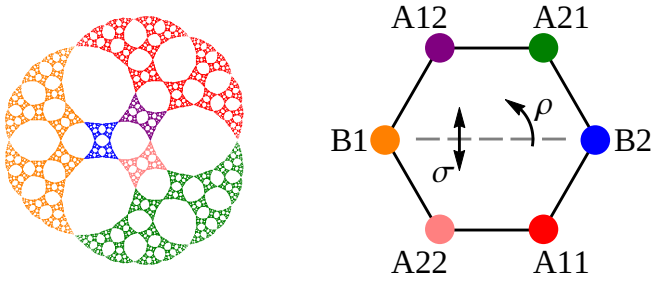

Hence, a homomorphism $\varphi : \langle c, r, s\rangle \longrightarrow D_6$ can be naturally defined by

$$\varphi : c \mapsto \rho^3,\ r \mapsto \rho^2,\ \text{and } s \mapsto \sigma.$$

We then have $\varphi(cr^2) = \rho$. Because ρ and σ generates the dihedral group D_6, it follows that $\langle c, r, s\rangle = \langle cr^2, s\rangle \cong D_6$ with φ as an isomorphism. □

Theorem 4.3.8. *$\langle a, c\rangle$ is isomorphic to the dihedral group D_4.*

Proof. We take a look at the geometric interpretation of a and c. Generator a cyclically permutes the cells $A1$, $B1$, $A2$, and $B2$, while generator c switches the $B1$-cell and the $B2$-cell, retaining the $A1$-cell and the $A2$-cell.

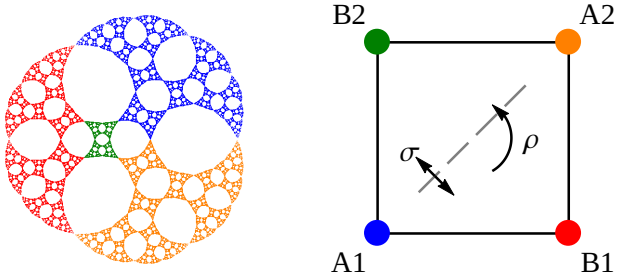

Hence, a homomorphism $\varphi : \langle a, c\rangle \longrightarrow D_4$ can be defined by

$$\varphi : a \mapsto \rho \text{ and } c \mapsto \sigma.$$

Incidentally, the rotation ρ and the reflection σ generates D_4, which makes φ an isomorphism. □

We notice that a^2c is a map that switches the $A1$-cell and the $A2$-cell, retaining the other two cells. The following lemma shows the symbolic equivalence between the maps s and a^2c.

Lemma 4.3.9. *The homeomorphism $s = a^2c$.*

Proof. Let $\omega \in \{1,2\}^\infty$ be an infinite word. Then

$$a^2c(A1\omega) = a^2(A1\omega^{*-1}) = a(B1\omega^{*-1}) = A2\omega^* = s(A1\omega),$$
$$a^2c(A2\omega) = a^2(A2\omega^{*-1}) = a(B2\omega^{*-1}) = A1\omega^* = s(A2\omega),$$
$$a^2c(B1\omega) = a^2(B2\omega^*) = a(A1\omega^{*-1}) = B1\omega^{*-1} = s(B1\omega),$$
$$a^2c(B2\omega) = a^2(B1\omega^*) = a(A2\omega^{*-1}) = B2\omega^{*-1} = s(B2\omega).$$

It then follows that $a^2c = s$ for all words in Ω_{E_3}. □

Theorem 4.3.10. *$\langle c, s\rangle$ is isomorphic to the Klein-4 group $\mathbb{Z}/2 \times \mathbb{Z}/2$.*

Proof. Let $\sigma \in \{A1, A2, B1, B2\}$, and let $\omega \in \{1,2\}^\infty$ be an infinite word. Then

$$s(\sigma\omega) = (\pi_{(A1\ A2)}\sigma)\omega^*, \quad \text{and} \quad c(\sigma\omega) = (\pi_{(B1\ B2)}\sigma)\omega^*.$$

Thus c and s commute, and

$$cs(\sigma\omega) = (\pi_{(A1\ A2)(B1\ B2)}\sigma)\omega.$$

It is clear that $\langle c, s\rangle = \{e, c, s, cs\}$, and all elements except the identity have order 2. Thus we conclude that $\langle c, s\rangle \cong \mathbb{Z}/2 \times \mathbb{Z}/2$. □

It is worth noticing that $\langle c, s\rangle$ is the maximal subgroup of Homeo(E_3) that fixes both the main cells, because, as Theorem 4.2.7 stated, the full homeomorphism group of an individual cell is isomorphic to the Klein-4 group.

4.4 Proof of Generation

In this section, we will show that the homeomorphism group Homeo(E_3) of the E_3 fractal is generated by the set of four generators $\{a, c, r, s\}$.

Corollary 4.4.1. *$\langle a, c, r, s\rangle$ is a subgroup of* Homeo(E_3).

Proof. This argument follows directly from the fact that $a, c, r, s \in \text{Homeo}(E_3)$ shown in Lemma 4.3.3 and 4.3.6. □

Lemma 4.4.2. *Let $S \subseteq E_3$ be a cell. Then there exist $x \in \langle a, c, r, s\rangle$ such that $x(A) = S$.*

Proof. Because we have the map a that switches the A-cell with the B-cell, it suffices to show the argument for any subcell of the A-cell. We use proof by induction.

Base Case 1. The map $w_1 = r^2a$ maps the A-cell onto the $A1$-cell.

Let $\omega \in \{1, 2\}^\infty$ be an infinite word. Then

$$w_1(A\omega) = r^2(a(A\omega)) = r^2(B\omega) = A1\omega.$$

It is then clear that $w_1(A) = A1$.

Base Case 2. The map $w_2 = ra$ maps the A-cell onto the A_2-cell.

Let $\omega \in \{1, 2\}^\infty$ be an infinite word. Then

$$w_2(A\omega) = r(a(A\omega)) = r(B\omega) = A2\omega.$$

It follows that $w_2(A) = A2$.

Inductive Step. Let $\sigma \in \{1, 2\}^k$ be a finite word of length k. Suppose that there exist a map $x \in \langle a, c, r, s\rangle$ such that $x(A) = A\sigma$. Let $\omega \in \{1, 2\}^\infty$ be an infinite word. Then $x(A\omega) = A\sigma\omega$. Thus $w_1x(A\omega) = w_1(A\sigma\omega) = A1\sigma\omega$. It follows that w_1x maps the A-cell onto the $A1\sigma$-cell. Similarly, we can show that w_2x maps the A-cell onto the $A2\sigma$-cell.

In conclusion, given any subcell S of the A-cell, there exist $x \in \langle a, c, r, s\rangle$ such that $x(A) = S$. The same result follows immediately for any cell of the E_3 fractal. □

Corollary 4.4.3. *Let $S, T \subseteq E_3$ be two cells. Then there exist $z \in \langle a, c, r, s\rangle$ such that $z(T) = S$.*

Proof. Lemma 4.4.2 ensures the existence of maps $x, y \in \langle a, c, r, s\rangle$ such that $x(A) = S$ and $y(A) = T$. Let $z = xy^{-1}$. Then $z(T) = x(y^{-1}(T)) = x(A) = S$. □

Lemma 4.4.4. *Let $\phi : E_3 \longrightarrow E_3$ be a homeomorphism of the E_3 fractal. The image of a cell in E_3 under the homeomorphism ϕ is either a cell or the complement of a cell.*

Proof. Let $S \subseteq E_3$ be a cell. Let $T = \phi(S)$ be the image of S. There exist a homeomorphism x such that $x(S)$ is the A-cell. Then $ax(S)$ is the B-cell. Thus $x(S) \cup ax(S) = E_3$ and $x(S) \cap ax(S)$ is a set of four points $P = \{p_1, p_2, p_3, p_4\}$ with addresses $A\overline{1}$, $A\overline{12}$, $A\overline{2}$, and $A\overline{21}$. Notice that the removal of these four points from E_3 disconnects E_3 into two components. Because x and ϕ are homeomorphisms, it follows that $\phi x^{-1}(x(S)) \cup \phi x^{-1}(ax(S)) = AG$, and $\phi x^{-1}(x(S)) \cap \phi x^{-1}(ax(S))$ is a set of four points whose removal disconnects E_3 into two components. But $\phi x^{-1}(x(S)) = \phi(S) = T$, and $x^{-1}(ax(S))$ is the complement of T in E_3. It then follows from Claim 4.2.8 that T is either a cell or the complement of a cell. □

Theorem 4.4.5. $\text{Homeo}(E_3) = \langle a, c, r, s \rangle$.

Proof. Let $\phi \in \text{Homeo}(E_3)$. Then $\phi(A)$ is either a cell or the complement of a cell. If $\phi(A)$ is a cell, then there exist $x \in \langle a, c, r, s \rangle$ such that $x(A) = \phi(A)$. Since the homeomorphism group of each individual cell is isomorphic to $\mathbb{Z}/2 \times \mathbb{Z}/2$, and the maximal subgroup of $\text{Homeo}(E_3)$ that fixes the main cells is $\langle c, s \rangle \cong \mathbb{Z}/2 \times \mathbb{Z}/2$, it follows that there exist $u \in \langle c, s \rangle$ such that $xu = \phi$. If $\phi(A)$ is the complement of a cell, then $\phi(B)$ must be a cell, and there exist $y \in \langle a, c, r, s \rangle$ such that $y(A) = \phi(B)$, and there exist $v \in \langle s, t \rangle$ such that $yv = \phi$. Thus $\phi \in \langle a, c, r, s \rangle$. Hence, we have $\text{Homeo}(E_3) \leq \langle a, c, r, s \rangle$. Together with the result from Corollary 4.4.1, we conclude that $\text{Homeo}(E_3) = \langle a, c, r, s \rangle$. □

4.5 E_4 Has Finite Homeomorphism Group

In this section, we will provide a primary observation on why the homeomorphism group of E_4 is finite. Section 5.7 will provide a more structured argument using Bass-Serre theory and a polyhedral complex associated with E_4. Eventually, we shall show that $\text{Homeo}(E_4) \cong D_4 \times \mathbb{Z}/2$.

We observe that the Julia set associated with the rational map $f(z) = (z^2+1)/(z^2-1)$ is invariant under negation, complex conjugation, and unit circle inversion on the complex plane because

$$f(-z) = f(z),$$
$$f(\overline{z}) = \overline{f(z)},$$
$$f(1/\overline{z}) = -\overline{f(z)}.$$

We shall expect the E_4 fractal to exhibit the same symmetries.

Lemma 4.5.1. $D_4 \times \mathbb{Z}/2 \leq \text{Homeo}(E_4)$.

Proof. The E_4 fractal has a clear D_4 symmetry. In addition, we observe that the "inversion" across the central circle also acts on the E_4 fractal as illustrated in Figure 4.5.1. Therefore, the full symmetry group $D_4 \times \mathbb{Z}_2$ of a square prism is a subset of the homeomorphism group of E_4. □

Lemma 4.5.2. Homeo(E_4) *is a finite group.*

Proof. From Claim 4.2.8, we know that the removal of four corner points on a cell of E_3 disconnects E_3 into two components. We observe that E_4 also has this property. Among all the choices of four points of disconnection in E_4, there are two special sets of points illustrated as the red

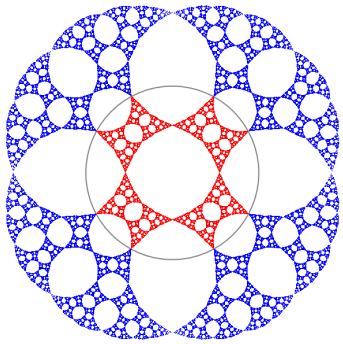

Figure 4.5.1: The "Circle Inversion" Acts on the E_4 Fractal

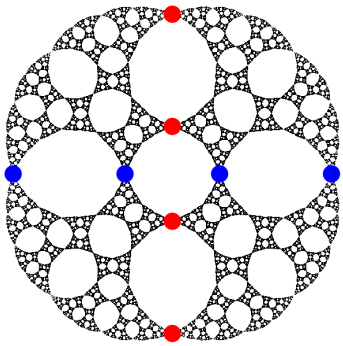

Figure 4.5.2: Two Sets of Special Points in E_4

points and blue points in Figure 4.5.2. The removal of each set disconnects E_4 into two components, and the subsequent removal of the other set further disconnects each of these two components into two smaller components. Because of the special topological property they posses, these eight points forms an invariant set under any homeomorphism of E_4. The four components resulted from the removal of these eight points are cells of E_4. Let $\phi\colon E_4 \to E_4$ be a homeomorphism. It then follows that ϕ permutes the eight special points. Let $\psi\colon \text{Homeo}(E_4) \to S_8$ be a homomorphism defined by the permutation of the eight special points by a homeomorphism of E_4. Theorem 4.2.7 has shown that the only homeomorphism with the four boundary points fixed is the identity map. Thus ψ has trivial kernel. It then follows that $|\text{Homeo}(E_4)| \leq |S_8| = 8!$. $\square$

5
Presentation of Homeo(E_3)

This chapter gives a presentation of the group Homeo(E_3) using the tools from *Bass-Serre Theory* provided in [18]. We only need a special case in Bass-Serre Theory, and we will present this special case with some examples in this chapter.

5.1 Graph Theoretic Preliminaries

In this preliminary section, we present some useful graph theoretic definitions as well as examples. Readers are assumed to have familiarity with basic definitions in graph theory.

Definition 5.1.1. A **tree** is an undirected connected graph without cycles.

Example 5.1.2. Two trees are shown here.

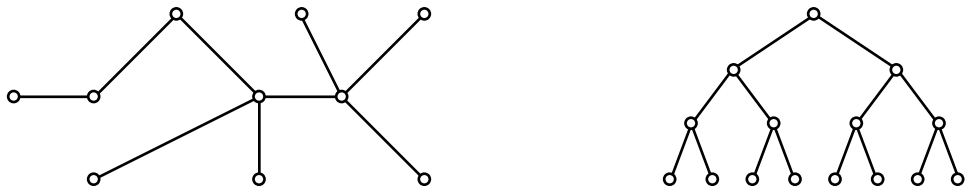

Definition 5.1.3. For a positive integer k, an **k-regular graph** is a graph whose vertices all have degree k.

Example 5.1.4. The only possible simple connected 1-regular graph is the graph with two vertices and an edge between them. For $k \geq 2$, the possible structures of k-regular graphs are much more varied. Examples of finite 2-regular, 3-regular, and 4-regular graphs are shown below.

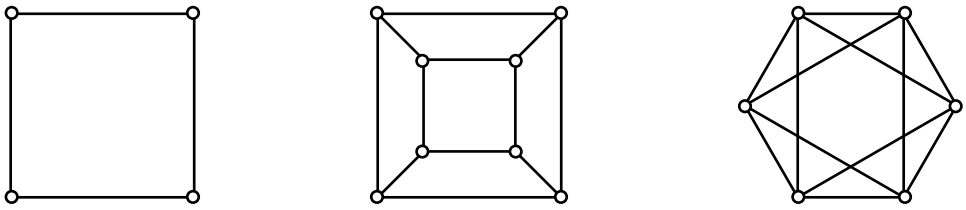

The following definition connects graph theory with group theory. It provides a method to construct a graph with respect to the structure of any given group.

Definition 5.1.5. Let G be a group and let X be a set of generators of G. The **Cayley graph** $\Gamma = \Gamma(G, X)$ is the graph with vertices the elements of G and with an edge between $g, h \in G$ if $h = gx$ or $g = hx$ for some $x \in X$.

In fact, there are several slightly different definitions of the Cayley graph. In [24], the definition requires the Cayley graph to be directed; in [5], the definition requires the edges to be directed and colored according to different generators. We do not require any of these additional structures, just to reveal the very basic structure of Cayley graphs.

It is important to specify the generating set of a group in order to construct its Cayley graph. Different choices of generators can result in different Cayley graphs for the same group.

Example 5.1.6. There are two different presentations for the dihedral groups with different generating sets:

$$D_n = \langle r, s \mid r^n, s^2, rsrs \rangle = \langle s, t \mid s^2, t^2, (st)^n \rangle.$$

We show the Cayley graphs of D_4 with respect to these two presentations below

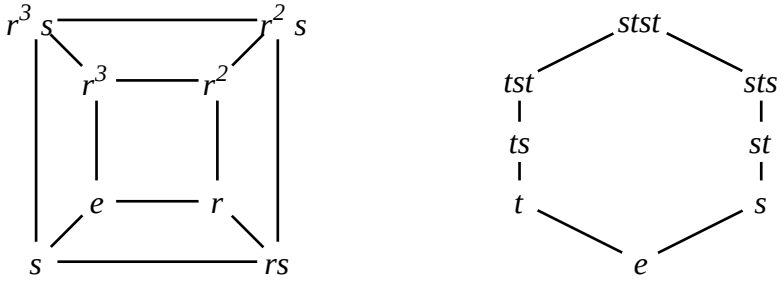

5.2 Free Groups

Definition 5.2.1. The **free group of rank** n, denoted by $\mathbb{F}_n$, is a group with presentation

$$\mathbb{F}_n = \langle x_1, x_2, \ldots, x_n \mid \varnothing \rangle.$$

A free group is free of non-trivial relations between its generators. The only relations that apply to the free groups are the group axioms (*e.g.* $xx^{-1} = e$ and $ex = xe = x$, where e refers to the identity element).

When $n = 1$, the free group of rank 1 has presentation $\mathbb{F}_1 = \langle x \mid \varnothing \rangle$. It follows immediately that $\mathbb{F}_1 \cong (\mathbb{Z}, +)$ by observing the presentation. For $n \geq 2$, the free group $\mathbb{F}_n$ has more than one generators, and there is no relations between the generators. In particular, for two generators x and y of the free group $\mathbb{F}_n$, there is no relation between x and y saying that $xy = yx$. Hence, $\mathbb{F}_1$ is the only free group that is abelian. Moreover, two words written with the generators as the alphabet are distinct elements of the free group $\mathbb{F}_n$ if and only if they cannot be reduced to the same word by only the group axioms. For example, the word $xyx^{-1}y^{-1}$ is the same element in $\mathbb{F}_2$ with $xy^2y^{-1}x^{-3}x^2y^{-1}$, while $xyxy^{-1}$ is a word different from the previous two in $\mathbb{F}_2$.

By Cayley's Theorem, a group acts faithfully and transitively on itself, and thus on its Cayley graph as a subgroup of the automorphism group of the Cayley graph. The Cayley graphs of $\mathbb{F}_1 = \langle x \rangle$ and $\mathbb{F}_2 = \langle x, y \rangle$ are shown in Figure 5.2.1.

In the action of $\mathbb{F}_1$ on its Cayley graph, the generator x acts on the graph so that each vertex shifts to its immediate neighbor on the right. Because $\mathbb{F}_1 \cong (\mathbb{Z}, +)$, this action can also be thought as the action of the additive group of integers $\mathbb{Z}$ on itself by addition.

The case for $\mathbb{F}_2$ is a lot more interesting. In the Cayley graph of $\mathbb{F}_2$, the vertex in the center corresponds to the identity element. Each vertex has a connected path starting from the identity vertex. The address along this path corresponds to the group element at the vertex. For example, vertices A and B shown in Figure 5.2.1b corresponds to the group elements xyx and $y^{-1}x^2$, respectively. The right action of the free group of rank 2 is simply the right concatenation of the acting word onto the word representing the group elements. In particular, the right action of the generator x acts on the graph so that each vertex shifts to its immediate neighbor on the right (along the red edges), and the other generator y right acts on the graph so that each

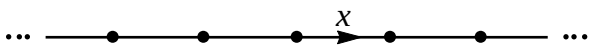

(a) Cayley Graph of $\mathbb{F}_1$

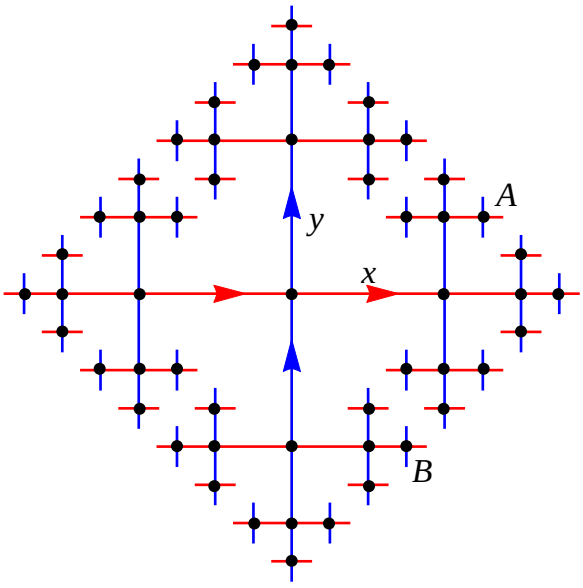

(b) Cayley Graph of $\mathbb{F}_2$

Figure 5.2.1: Cayley Graphs of Free Groups

vertex shifts to its immediate neighbor above it (along the blue edges). However, because $\mathbb{F}_2$ is not abelian, the left actions are different from the right actions, and it is the left action that is of more interest to us.

The Cayley graph of $\mathbb{F}_2$ has an intrinsic self-similar structure. It has four **branches**, and each branch consists of a **root** (black) and three branches (red, green, and blue).

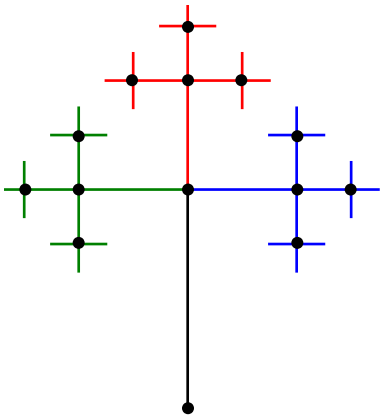

It is clear to see that the x-axis of the Cayley graph corresponds to the subgroup of $\mathbb{F}_2$ generated by x, and this subgroup is isomorphic to $\mathbb{F}_1$. Each vertex on the x-axis roots two branches, one upwards and one downwards, forming a vertical *vertex-branch system*. The left action of the generator x shifts every vertex-branch system on the x-axis to its immediate neighboring vertex-branch system on the right along the x-axis.

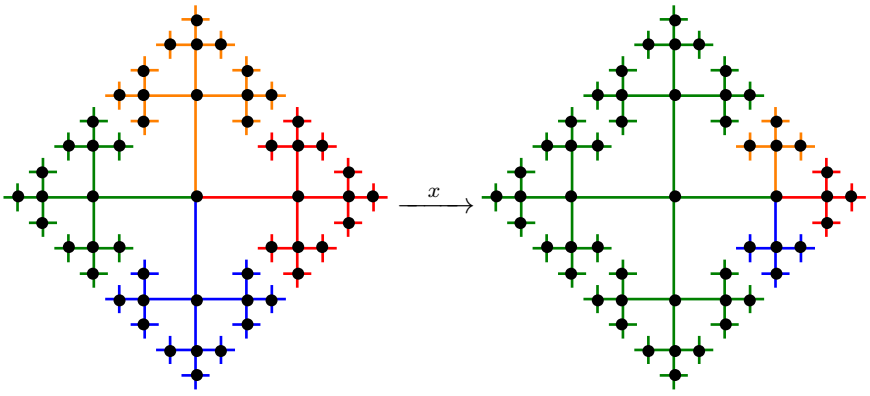

Similarly, the left action of y shifts each horizontal vertex-branch system on the y-axis to its immediate neighboring vertex-branch system above it.

5.3 Groups Acting on Trees

The Cayley graphs of $\mathbb{F}_1$ and $\mathbb{F}_2$ are examples of *regular trees*.

Definition 5.3.1. For a positive integer k, a **k-regular tree**, denoted by $\mathcal{T}_k$, is a tree whose vertices all have degree k.

Lemma 5.3.2. *For $k \geq 2$, a k-regular tree is infinite.*

Proof. We show this fact by contradiction. Suppose that G is a finite k-regular tree with n vertices for some $n \geq 1$. Because G is k-regular, there are a total of $nk/2$ edges. However, as a tree, G is supposed to have $n-1$ edges. Because $k \geq 2$, we have $nk/2 \geq n > n-1$, at which point we arrive at a contradiction. Thus when $k \geq 2$, a k-regular tree is always infinite. □

Example 5.3.3. The Cayley graph of $\mathbb{F}_1$ is the 2-regular tree $\mathcal{T}_2$; the Cayley graph of $\mathbb{F}_2$ is the 4-regular tree $\mathcal{T}_4$ (Figure 5.2.1, disregarding the arrows illustrating the direction of group action).

Example 5.3.4. Figure 5.3.1 shows the 3-regular tree $\mathcal{T}_3$. For clarity purpouse, the drawing of the vertices is removed, and a vertex is assumed at each junction of edges. We will show in the next section that the *modular group* acts on this tree.

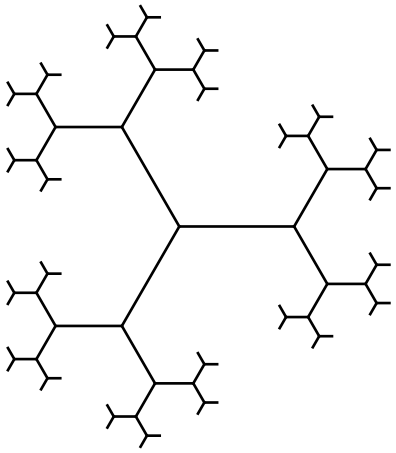

Figure 5.3.1: The 3-Regular Tree $\mathcal{T}_3$

Definition 5.3.5. Let $m, n \geq 2$ be distinct integers. A **biregular** tree $\mathcal{T}_{m,n}$ is a tree with vertices of degree m or n, connected in the way such that (i) each vertex of degree m is adjacent to m vertices of degree n, and (ii) each vertex of degree n is adjacent to n vertices of degree m.

Example 5.3.6. Figure 5.3.2 shows a biregular tree $\mathcal{T}_{3,4}$. The red vertices all have degree 4, and the blue vertices all have degree 3. Each edge connects a red vertex with a blue vertex.

Now that we have formulated the definitions of regular trees and biregular trees. We are ready to see some group actions on these trees.

Definition 5.3.7. Let Γ be a graph, and let G be a group. We say that the group G **acts on** the graph Γ if there exist a homomorphism $\varphi : G \longrightarrow \mathrm{Aut}(\Gamma)$.

Example 5.3.8. The free group $\mathbb{F}_1 = \langle x \rangle$ acts on $\mathcal{T}_2$ with the action by generator x shown in Figure 5.2.1a. The homomorphism $\varphi : \mathbb{F}_1 \longrightarrow \mathcal{T}_2$ is defined such that $\varphi(x)$ corresponds to shifting each vertex to its immediate neighbor on the right.

Example 5.3.9. The free group $\mathbb{F}_2 = \langle x, y \rangle$ acts on $\mathcal{T}_4$. The homomorphism $\varphi : \mathbb{F}_2 \longrightarrow \mathcal{T}_4$ is defined such that $\varphi(x)$ and $\varphi(y)$ correspond to the automorphisms shown in Figure 5.3.3.

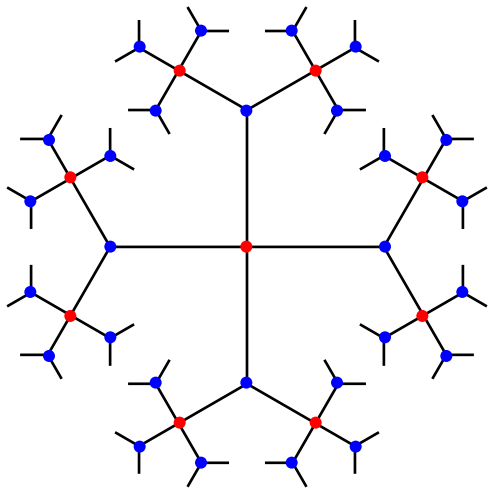

Figure 5.3.2: A Biregular Tree $\mathcal{T}_{3,4}$

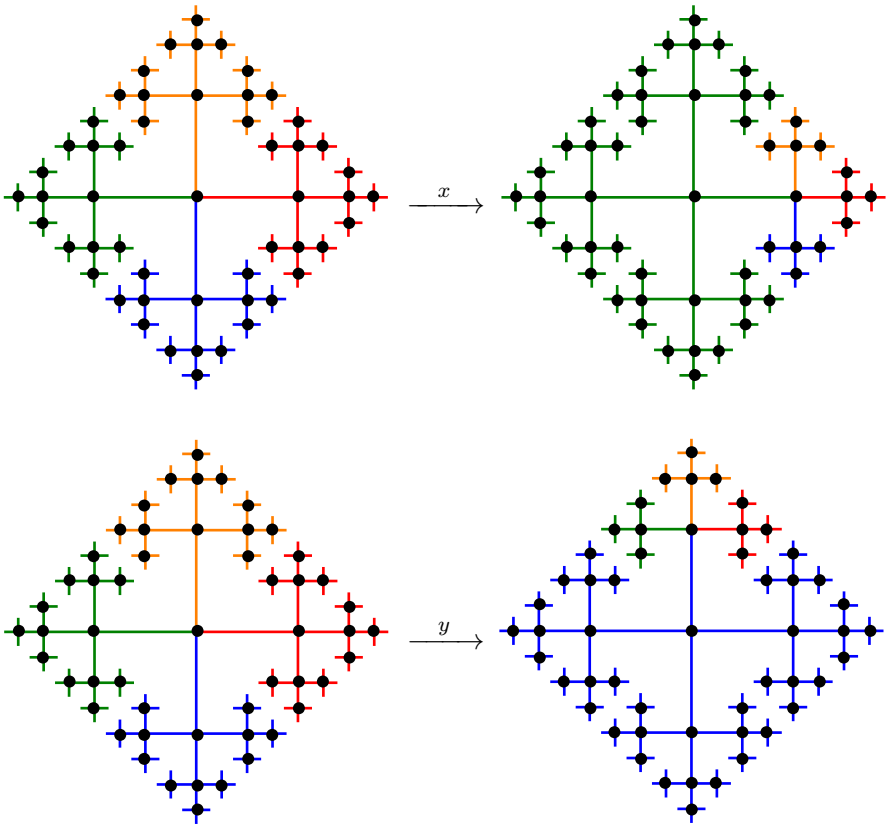

Figure 5.3.3: $\mathbb{F}_2$ Acting on $\mathcal{T}_4$

Example 5.3.10. The cyclic groups $\mathbb{Z}/4$ and $\mathbb{Z}/3$ both acts on the biregular tree $\mathcal{T}_{3,4}$ as rotations about vertices of the tree. Suppose that $\mathbb{Z}/4$ is generated by x, and $\mathbb{Z}/3$ is generated by y. The homomorphisms $\varphi_4 : \mathbb{Z}/4 \longrightarrow \mathcal{T}_{3,4}$ and $\varphi_3 : \mathbb{Z}/3 \longrightarrow \mathcal{T}_{3,4}$ are defined such that $\varphi_4(x)$ and $\varphi_3(y)$ corresponds to the rotations a and b, respectively, shown in Figure 5.3.4. The dihedral groups D_4 and D_3 also act on $\mathcal{T}_{3,4}$ so that the reflections in the dihedral groups correspond to the reflection actions along edges of $\mathcal{T}_{3,4}$. Furthermore, the symmetric groups S_4 and S_3 (isomorphic to D_3) act on $\mathcal{T}_{3,4}$ so that the branches extending from each vertex are permuted under the corresponding group actions. The actions by $\mathbb{Z}/4$ and $\mathbb{Z}/3$ are *orientation-preserving* because only rotations are allowed in the group actions. The actions by D_4 and D_3 are *geometry-preserving* since the group actions do not involve rearrangements of geometric structures of the graph. It follows immediately that orientation preserving actions are geometry-preserving.

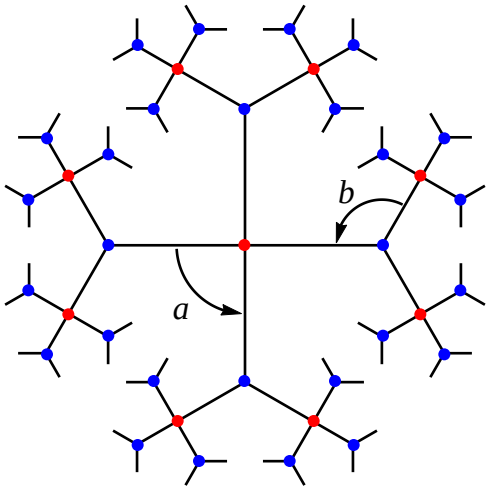

Figure 5.3.4: $\mathbb{Z}/4$ and $\mathbb{Z}/3$ Acting on $\mathcal{T}_{3,4}$

Example 5.3.11. The cyclic group $\mathbb{Z}/3$ acts on $\mathcal{T}_3$ as rotations around a vertex. Furthermore, the 180-degree rotation about the center of each edge is another orientation-preserving automorphism of $\mathcal{T}_3$, and thus the cyclic group $\mathbb{Z}/2$ acts on $\mathcal{T}_3$. Figure 5.3.5 shows the actions of $\mathbb{Z}/3$ and $\mathbb{Z}/2$ on $\mathcal{T}_3$. Notice that we have converted the 3-regular tree $\mathcal{T}_3$ to a biregular tree $\mathcal{T}_{2,3}$, and an orientation preserving group action on $\mathcal{T}_3$ naturally acts on $\mathcal{T}_{2,3}$, and *vice versa*.

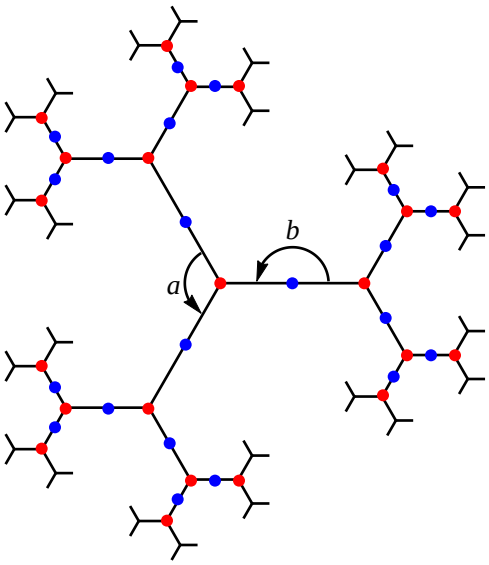

Figure 5.3.5: $\mathbb{Z}/3$ and $\mathbb{Z}/2$ Acting on $\mathcal{T}_3$

5.4 Free Products and Amalgamated Free Products

We will first investigate the group $\mathrm{Aut}_+(\mathcal{T}_{3,4})$ of orientation-preserving automorphisms on $\mathcal{T}_{3,4}$. Example 5.3.10 has shown that $a, b \in \mathrm{Aut}_+(\mathcal{T}_{3,4})$, with $|a| = 4$ and $|b| = 3$. What is the relation between a and b? In particular, is there a finite composition of a and b that can give rise to the identity automorphism?

The subgroup $\langle a \rangle \leq \mathrm{Aut}_+(\mathcal{T}_{3,4})$ acts on $\mathcal{T}_{3,4}$ so that it stabilizes the center red vertex. Similarly, $\langle b \rangle$ stabilizes the blue vertex around which the action of b rotates the tree. We shall call these two vertices the *basic vertices*, and the edge connecting them the *basic edge*. In fact, we can assign a coset of $\langle a \rangle$ to each red vertex, and a coset of $\langle b \rangle$ to each blue vertex. For each red vertex, the group actions in the corresponding coset map the basic red vertex to it, and the same thing applies to each blue vertex. For example, the cosets corresponding to the blue vertices around the center red vertex are, respectively, $\langle b \rangle$, $a\langle b \rangle$, $a^2\langle b \rangle$, and $a^3\langle b \rangle$, and the coset corresponding to the blue vertex on the bottom left corner of the tree (shown in Figure 5.4.1) is $a^3ba^2\langle b \rangle$. Furthermore, there is an edge between two vertices if and only if the intersection of the cosets corresponding to the vertices is not empty. In this case, the intersection is always a singleton

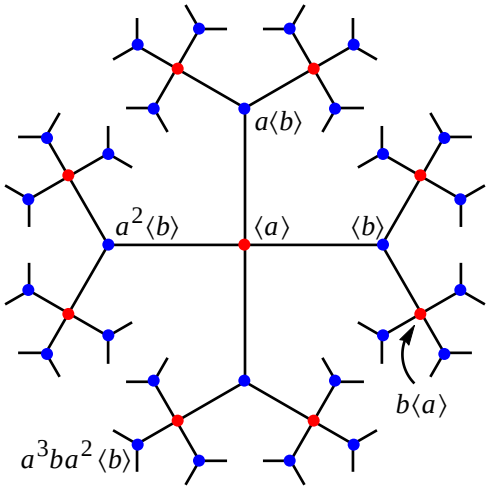

Figure 5.4.1: Vertex Labeling of $\mathcal{T}_{3,4}$ by Cosets of $\langle a \rangle$ and $\langle b \rangle$

set that sends the basic edge to this edge. It is clear to see that the cosets of the basic vertices are the only ones that contain the identity element. Hence, there does not exist any composition involving both a and b that results in the identity element, and it follows that there is no relation between a and b. We can write down a presentation of the group

$$\mathrm{Aut}_+(\mathcal{T}_{3,4}) = \langle a, b \mid a^4, b^3 \rangle.$$

Notice that a and b have the same relation with the generators of $\mathbb{Z}/4$ and $\mathbb{Z}/3$, respectively. The group $\mathrm{Aut}_+(\mathcal{T}_{3,4})$ is generated by an isomorphic copy of $\mathbb{Z}/4$ and an isomorphic copy of $\mathbb{Z}/3$, where there is no interaction between the subgroups $\langle a \rangle$ and $\langle b \rangle$. In the following definition, we define this method of combining two groups into a new one through group presentations.

Definition 5.4.1. Let G and H be groups. Suppose that

$$G = \langle S_1 \mid R_1 \rangle, \text{ and } H = \langle S_2 \mid R_2 \rangle$$

are presentations of G and H, where S_1 and S_2 are disjoint sets of generators, and R_1 and R_2 are sets of relations within S_1 and S_2, respectively. The **free product** of G and H, denoted by $G * H$, is the group with presentation

$$\langle S_1 \cup S_2 \mid R_1 \cup R_2 \rangle.$$

Example 5.4.2. Now we look at the orientation-preserving automorphisms of $\mathcal{T}_3$. As mentioned in Example 5.3.11, the orientation preserving automorphisms on $\mathcal{T}_3$ are the same as those on the biregular tree $\mathcal{T}_{2,3}$. The assignment of cosets to vertices of $\mathcal{T}_{2,3}$ is shown in Figure 5.4.2. Thus the subgroup $\langle a \rangle \cong \mathbb{Z}/3$ stabilizes the basic red vertex, and the subgroup $\langle b \rangle \cong \mathbb{Z}/2$ stabilizes the basic blue vertex. Only the identity automorphism (which forms the trivial subgroup) stabilizes the basic edge. The orientation-preserving automorphism group $\mathrm{Aut}_+(\mathcal{T}_3)$ is then presented as

$$\mathrm{Aut}_+(\mathcal{T}_3) = \mathbb{Z}/3 * \mathbb{Z}/2 = \langle a, b \mid a^3, b^2 \rangle.$$

It was shown in [2] that $\mathbb{Z}/3 * \mathbb{Z}/2 \cong \mathrm{PSL}_2(\mathbb{Z})$. The latter is usually referred to as the *modular group*.

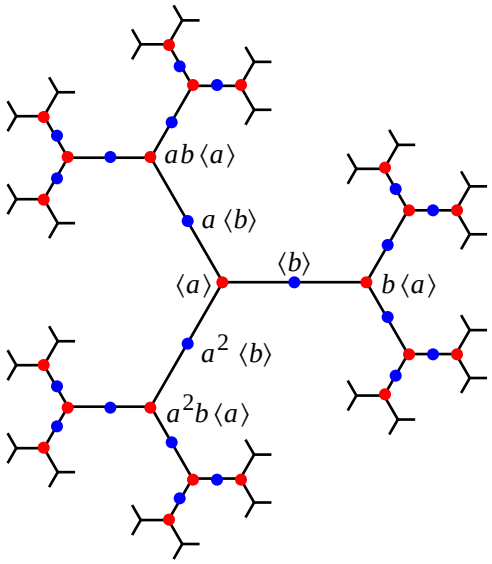

Figure 5.4.2: Vertex Labeling of $\mathcal{T}_{2,3}$ by Cosets of $\langle a\rangle$ and $\langle b\rangle$

Both of the examples shown here have trivial stabilizer of the basic edge. A more general construction is to allow nontrivial automorphisms that fixes the basic edge. This generalization corresponds to allowing common generator and relation in the presentation of two groups for the product. We will give the definition of the *amalgamated free product* and shown an example of this generalized version of free product.

Definition 5.4.3. Let G and H be groups whose intersection is a common subgroup K. Suppose that

$$G = \langle S_1 \mid R_1\rangle, \text{ and } H = \langle S_2 \mid R_2\rangle$$

are presentations of G and H, where $S = S_1 \cap S_2$ is not empty, and the subgroup generated by S is K. The **amalgamated free product** of G and H, denoted by $G *_K H$ is the group with presentation

$$\langle S_1 \cup S_2 \mid R_1 \cup R_2\rangle.$$

It is clear that the free product is a special case where the amalgamation is achieved with respect to the trivial group.

We now present some useful results in [18] without giving proofs. For a rigorous deduction of the following theorems, see Chapter 3 of [18].

Theorem 5.4.4. *The group $\mathbb{Z}/m * \mathbb{Z}/n$ acts transitively on the edges of $\mathcal{T}_{m,n}$.*

Theorem 5.4.5. *Every free product of groups $A * B$ can be realized as a group of symmetries of a biregular tree. If A and B are both finite, the tree is $\mathcal{T}_{|A|,|B|}$.*

Corollary 5.4.6. *The stabilizers of the vertices of the tree associated to a free product $A * B$ are conjugates of A and B.*

Corollary 5.4.7. *The stabilizer of an edge of the tree associated to a free product $A * B$ is trivial.*

Theorem 5.4.8. *Let $\mathcal{T}$ be a tree, and let G be a subgroup of the automorphism group of $\mathcal{T}$. Suppose that T has exactly two orbits of vertices and one orbit of edges. Let e be an edge of $\mathcal{T}$ with endpoints v and w. Let V, W, and E be the stabilizer subgroups of v, w, and e, respectively. Then*

$$G \cong V *_E W.$$

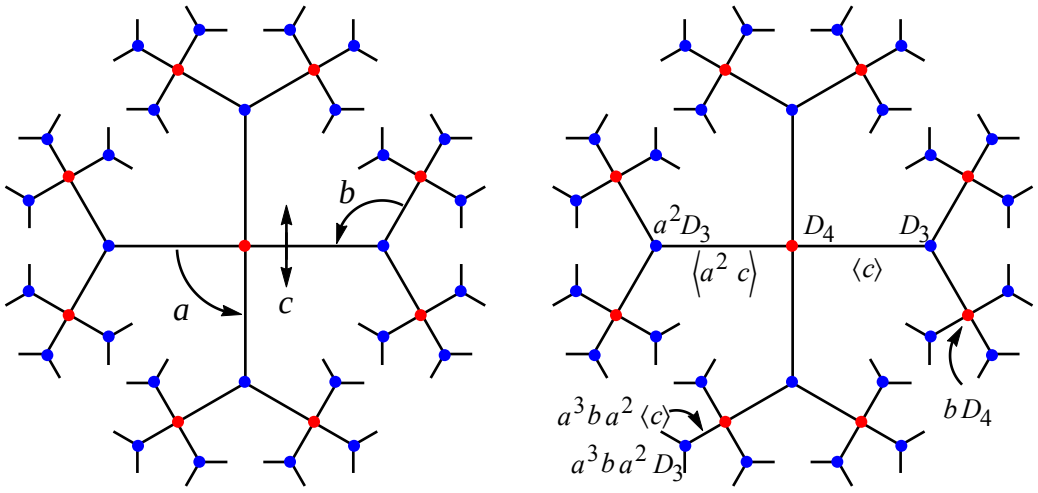

(a) Generators of the Group (b) Cosets on Vertices and Edges

Figure 5.4.3: Geometry-Preserving Automorphism Group of $\mathcal{T}_{3,4}$

Example 5.4.9. We consider the group of geometry-preserving automorphisms of $\mathcal{T}_{3,4}$. We will call the reflection across the basic edge c (Figure 5.4.3a). Thus the subgroup $\langle a, c\rangle \cong D_4$ acts on $\mathcal{T}_{3,4}$ so that it stabilizes the basic red vertex, and $\langle b, c\rangle \cong D_3$ stabilizes the blue basic vertex. The stabilizer for the basic edge is the intersection of these two subgroups $\langle c\rangle \cong \mathbb{Z}/2$. Similar with the previous cases, we can assign cosets to each vertex of $\mathcal{T}_{3,4}$, and there is an edge between two vertices if and only if the intersection of their corresponding cosets is not empty. In particular, the intersection is a coset of $\langle s\rangle$, which can be assigned to the edge. Figure 5.4.3b shows some of the cosets: each red vertex gets a coset of D_4 assigned; each blue vertex gets a coset of D_3 assigned, and every edge gets a coset of $\langle c\rangle$ assigned. This group is obtained by the amalgamated free product of the dihedral groups D_4 and D_3 with respect to the subgroup generated by the basic reflection $\langle c\rangle$:

$$D_4 *_{\mathbb{Z}/2} D_3 = \langle a, b, c \mid a^4, b^3, c^2, acac, bcbc\rangle.$$

5.5 A Tree Representation of the Apollonian Gasket

We presented the construction of the Apollonian gasket using an octahedron in Chapter 3. It can be constructed by placing four Sierpinski gaskets on alternating faces of an octahedron. There is a similar construction of the Apollonian gasket using a tetrahedron, which will be useful in this context. We can place four Sierpinski gaskets on the center of the faces of a tetrahedron to obtain the Apollonian gasket. Figure 5.5.1 shows the equivalence of these two constructions.

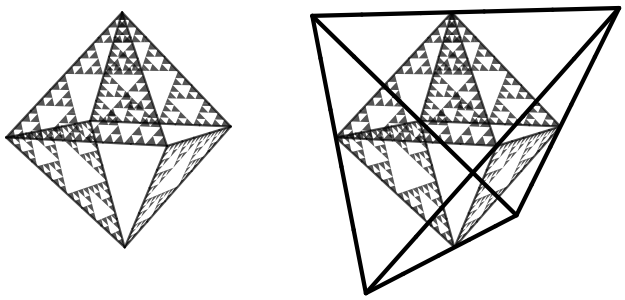

Figure 5.5.1: The Octahedral and Tetrahedral Constructions of the Apollonian Gasket

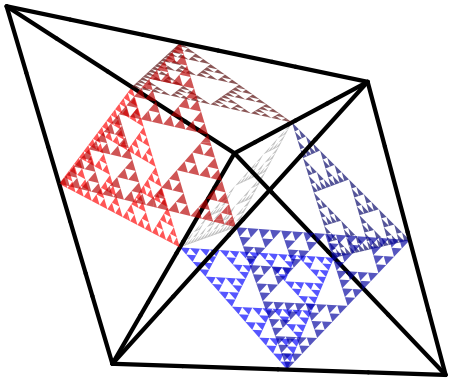

Figure 5.5.2: Pasting Two Apollonian Gaskets

There is a Sierpinski gasket on each face of the tetrahedron. Additionally, we know from Lemma 3.4.4 that the complement of each face is also a Sierpinski gasket. Therefore, we can paste two of these tetrahedrons together so that the resulting structure is still an Apollonian gasket (Figure 5.5.2). By doing this pasting, three subcells on the same face of the Apollonian tetrahedron becomes a face of the resulting polyhedron. We can repetitively paste Apollonian tetrahedrons together (disregarding spatial overlap) so that every cell of the Apollonian gasket can eventually become a face during the pasting process. In the next few paragraphs, we will use the background set-up in [11] to define a *simplicial complex* and to describe the resulting structure of the pasting process.

Definition 5.5.1. A **k-simplex** is a k-dimensional polytope which is the convex hull of $k+1$ affinely independent vertices.

The notion of simplices is a generalization of triangles and tetrahedrons into higher dimensions. A single point, a line segment, a triangle, and a tetrahedron are examples of 0-simplex, 1-simplex, 2-simplex, and 3-simplex, respectively.

Definition 5.5.2. A **simplicial complex** is a set V together with a collection Δ of finite subsets of V (the simplices) such that

(1) For all $v \in V$, we have $\{v\} \in \Delta$, and

(2) If $S \in \Delta$ and $T \subseteq S$ is nonempty, then $T \in \Delta$.

The definition of a simplicial complex we give here is purely combinatorial. We provide a geometric insight into simplicial complexes. A simplicial complex can be realized by gluing simplices together. The set V is the set of vertices in the simplices, and the collection Δ of finite subsets specifies the simplices in the simplicial complex.

Definition 5.5.3. A **simplicial k-complex** is a simplicial complex $\mathcal{K}$ where the largest dimension of any simplex in $\mathcal{K}$ equals k.

A graph is a collection of vertices (0-simplices) and edges (1-simplices). Thus graphs are examples of simplicial 1-complexes.

We take the resulting structure of the infinite pasting of Apollonian tetrahedrons, and define a simplicial complex for the Apollonian gasket.

Definition 5.5.4. Let V be the collection of complementary disks in the Apollonian gasket, and let Δ be subsets of V for which the disks are mutually tangent. The **structural complex of the Apollonian gasket**, denoted by $\mathcal{K}_{AG}$ is defined by the set of vertices V and the collection Δ of subsets of V.

We notice that there cannot be more than four disks on $\hat{\mathbb{C}}$ that are mutually tangent. It is then clear that $\mathcal{K}_{AG}$ is a simplicial 3-complex. The simplices in K_{AG} are described as follows.

0**-simplices:** complementary disks of the Apollonian gasket;

1**-simplices:** choices of two tangent complementary disks, or equivalently, all points with two different addresses in the Apollonian gasket;

2**-simplices:** choices of three mutually tangent complementary disks, or equivalently, choices of three points on the Apollonian gasket whose removal disconnects the Apollonian gasket into two components;

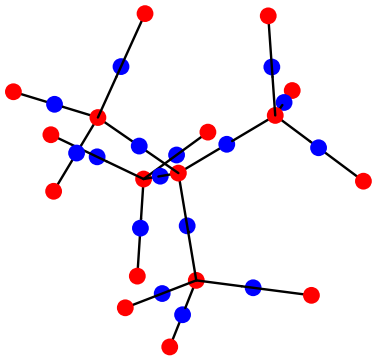

Figure 5.5.3: The Structural Tree $\mathcal{T}_{AG}$ of the Apollonian Gasket

3-simplices: choices of four mutually tangent complementary disks of the Apollonian gasket, or equivalently, choices of six points on the Apollonian gasket whose removal disconnects the Apollonian gasket into four components.

Notice that two 3-simplices share a common 2-simplex if and only if their corresponding choices of disks have three in common. Analogously, two 2-simplices share a common 1-simplex if and only if their corresponding choices of disks have two in common.

From the structural complex of the Apollonian gasket, we can construct its **structural tree**, denoted by $\mathcal{T}_{AG}$ with the following rules. Each 3-complex is assigned a red vertex; each 2-complex is assigned a blue vertex. An edge can only connect between a red vertex and a blue vertex precisely when the 2-simplex corresponding to the blue vertex belongs to the 3-simplex corresponding to the red vertex. It is then clear that $\mathcal{T}_{AG}$ is a biregular tree with vertices of degree 2 and 4 as illustrated in Figure 5.5.3.

Readers should keep in mind that the red vertices are at the center of tetrahedrons, and the blue vertices are at the center of the faces. The graph has a tetrahedral structure because the dual polyhedron of a tetrahedron is a tetrahedron.

An example of the correspondence between the vertices of $\mathcal{T}_{AG}$ and parts of the Apollonian gasket is illustrated in Figure 5.5.4. The degree-2 vertex labeled in blue corresponds to a 2-

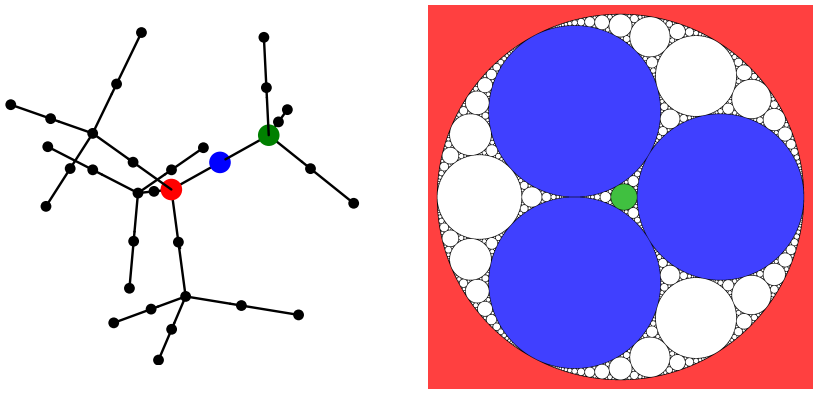

Figure 5.5.4: A Correspondence between $\mathcal{T}_{AG}$ and the Apollonian Gasket

simplex of $\mathcal{K}_{AG}$, or three mutually tangent complementary disks, and thus the blue part in the planar presentation. The degree-4 vertex labeled in red corresponds to a 3-simplex, or the choice of four mutually tangent disks labeled in blue and red in the planar presentation, while the other degree-4 vertex labeled in green corresponds to the choice of blue disks and the green disk. The red and green vertices corresponds to two 3-simplices that share a common 2-simplex. Their common choice of tangent disks are the blue ones shown in Figure 5.5.4.

We have shown that there is an isomorphic copy of S_4 as a subgroup of Homeo(SG) that acts on the Apollonian gasket so that the four cells shown in Lemma 3.3.6 are permuted. We have also shown in Corollary 3.4.3 that there exist $g \in$ Homeo(SG) that maps any cell to any other cell. Hence, the desired group acting on $\mathcal{T}_{AG}$ should include all geometry-preserving actions, *i.e.*, rotations, reflections, translations, and any compositions of these actions.

The degree-4 and degree-2 vertices, respectively, form exactly two orbits of vertices, and all the edges are in one orbit under the action of Homeo(AG). We pick the red and blue vertices in Figure 5.5.4 together with the edge connecting them for further analysis.

The stabilizer of the red vertex is supposed to preserve the four disks in blue and red. The isomorphic copy of S_4 generated by r and a shown in Lemma 3.3.6 permutes the cells as well as these four circles. Furthermore, we know that $s \in \langle r, a \rangle$ with $s = r^2ar^2arar$. Notice that

$s = s^{-1}$. Thus this vertex stabilizer is S_4 with presentation $\langle a, r \mid a^2, r^3, (ar)^4 \rangle$, or equivalently,

$$S_4 \cong \langle a, r, s \mid a^2, r^3, (ar)^4, sr^2ar^2arar \rangle.$$

The stabilizer for the blue vertex is supposed to preserve the three disks in blue. The isomorphic copy of D_3 generated by r and s preserves these three disks. However, the circle inversion c also preserves these disks, but c is not in $\langle r, s \rangle$. Hence, the vertex stabilizer for the blue vertex is $\langle r, s \rangle \rtimes \langle c \rangle \cong D_6$ with presentation

$$D_6 \cong \langle r, s, c \mid r^3, s^2, c^2, rsrs, crcr^{-1}, cscs \rangle.$$

The edge stabilizer is the intersection of these two groups, and it preserves the disks in blue as well as fixes the red disk. It is easily verified that the edge stabilizer is D_3 with presentation

$$D_3 \cong \langle r, s \mid r^3, s^2, rsrs \rangle.$$

Now we are ready to use Theorem 5.4.8 to find a presentation for Homeo(AG). The amalgamated free product $S_4 *_{D_3} D_6$ gives the isomorphic type of the group Homeo(AG). The presentation of the product is

$$S_4 *_{D_3} D_6 \cong \langle a, c, r, s \mid a^2, c^2, r^3, s^2, (ar)^4, sr^2ar^2arar, rsrs, crcr^{-1}, cscs \rangle.$$

Hence, a presentation of Homeo(AG), written in terms of the generators a, c, r, s presented in Section 4.3, can be

$$\text{Homeo}(AG) = \langle a, c, r, s \mid a^2, c^2, r^3, s^2, (ar)^4, sr^2ar^2arar, rsrs, crcr^{-1}, cscs \rangle. \tag{5.5.1}$$

5.6 A Tree Representation of E_3

Similar to the approach of the Apollonian gasket, we shall embed the E_3 fractal on a polyhedron, paste the polyhedra in a specific pattern to mimic the self-similar structure of E_3. We shall again use the results from Bass-Serre theory to find a presentation of Homeo(E_3).

As we mentioned in Section **??**, there is an isomorphic copy of the symmetry group D_6 of a triangular prism as a subgroup of Homeo(E_3). It is then natural to embed the E_3 fractal on a triangular prism with equilateral triangular bases and square sides. Each side of the triangular prism has a copy of a cell defined in Definition 4.2.2 and illustrated in the replacement system in Figure 4.1.1. Adjacent cells have two points in common, represented by two vertices on the adjacent edge of two side faces of the triangular prism.

Each cell of E_3 is composed of two subcells, whoso intersection is a set of two points. However, the orientation of these two subcells is different from their immediate supercell. We need a clever way of pasting the triangular prisms to realize the decomposition of E_3 into smaller and smaller cells.

One way of pasting the prisms together is shown in Figure 5.6.1. When the second prism is attached, it is orientated "perpendicular" to its adjacent prism so that the resulting structure is still an E_3 fractal. By doing such pasting, two subcells on one face of the triangular prism become a face of the resulting polyhedron. We can repetitively paste E_3 prisms together (disregarding spacial overlap) so that every cell of the E_3 fractal can eventually become a face during the pasting process. Notice that the boundary points of each cell are pinch points in E_3, and they

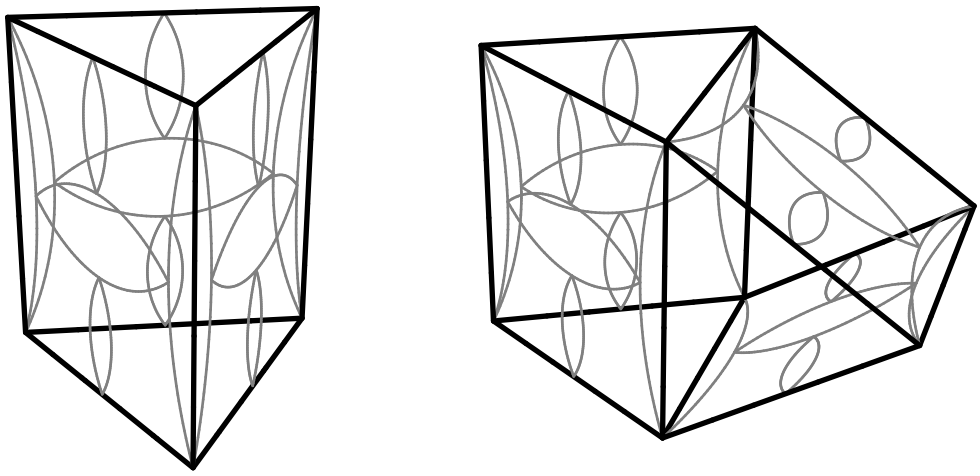

Figure 5.6.1: A Triangular Prism Embedding of E_3 and Its Pasting Method

are arranged in a circular order. We will use adjacency of boundary points on one cell specified by this circular order.

We construct a *polyhedral complex* for the result of the infinite pasting of E_3 prisms in analogous to the simplicial complex for the Apollonian gasket. We will skip the rigorous definition of a polyhedral complex but provide a construction of the polyhedral complex by specifying the vertices, edges, faces, and polyhedra.

Vertices: all pinch points in E_3;

Edges: there is one edge between each pair of pinch points that are adjacent boundary points of the same cell;

Triangular faces: any 3-cycles of edges;

Square faces: choices of four pinch points that are the boundary points of the same cell, or equivalently, choices of four points on E_3 whose removal disconnects E_3 into two components;

Triangular prisms: choices of six points in E_3 whose removal disconnects E_3 into three components, at least two of which are cells of E_3.

We call the polyhedral complex defined above the **structural complex of the E_3 fractal**, and we denote it by $\mathcal{K}_{E_3}$.

From the structural complex of the E_3 fractal, we can construct the **structural tree** of E_3, denoted by $\mathcal{T}_{E_3}$ with the following rules. Each triangular prism is assigned a red vertex; each square face is assigned a blue vertex. An edge can only connect between a red vertex and a blue vertex precisely when the square face corresponding to the blue vertex belongs to the triangular prism corresponding to the red vertex. It is then clear that $\mathcal{T}_{E_3}$ is a biregular tree with vertices of degree 2 and 3 as shown in Figure 5.6.2.

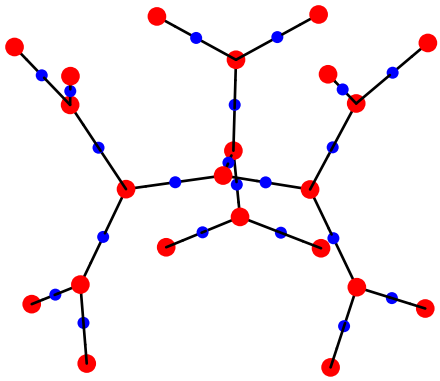

Figure 5.6.2: The Structural Tree $\mathcal{T}_{E_3}$ of the E_3 Fractal

Here we show an example of the correspondence between the structural tree $\mathcal{T}_{E_3}$ and the E_3 fractal in Figure 5.6.3. The degree-2 vertex labeled in blue corresponds to a square face of $\mathcal{K}_{E_3}$, and thus the blue points in the planar presentation of E_3. The central degree-3 vertex labeled in red corresponds to the choice of six points labeled in red and blue in E_3, while the degree-3 vertex labeled in green corresponds to the choice of points labeled in green and blue. It is clear that the removal of either sets of points corresponding to the red and green vertices, respectively, can disconnect the E_3 fractal into three separate piece, and at least two of them are cells.

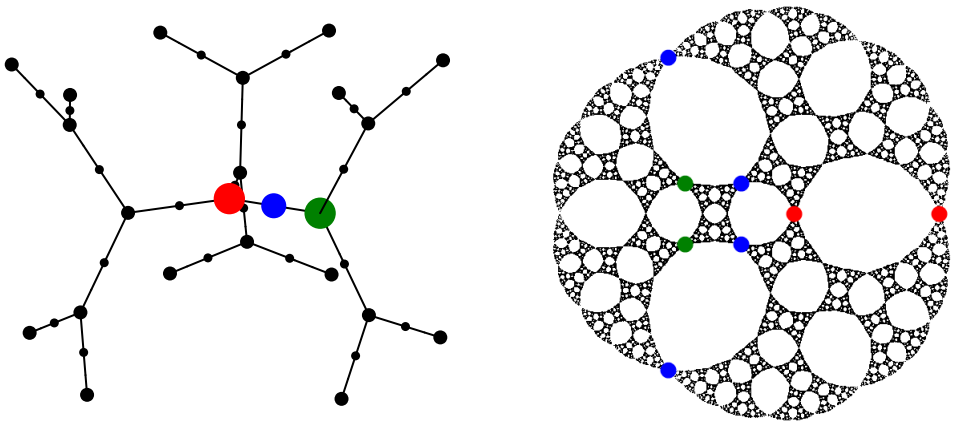

Figure 5.6.3: A Correspondence between $\mathcal{T}_{E_3}$ and the E_3 Fractal

Analogous to the case for the Apollonian gasket, the the desired group, which is expected to be isomorphic with Homeo(E_3), acting on $\mathcal{T}_{E_3}$ should include all geometry-preserving actions, *i.e.*, rotations, reflections, translations, and any compositions of these actions. We use Theorem 5.4.8 to show a representation of this group.

The degree-3 and degree-2 vertices, respectively, form exactly two orbits of vertices, and all the edges are in one orbit under the action of Homeo(E_3). If we take a look at the pink and purple vertices and the edge connecting them in Figure 5.6.3, we can see that the stabilizer subgroup of the degree-3 red vertex is isomorphic to D_6, and the stabilizer subgroup of the degree-2 blue vertex is isomorphic to D_4. The edge stabilizer is the intersection of these two subgroups, which is isomorphic to the Klein-4 group $\mathbb{Z}/2 \times \mathbb{Z}/2$.

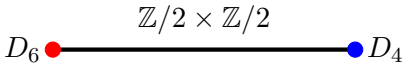

It follows that the group Homeo(E_3) acting on the biregular tree $\mathcal{T}_{E_3}$ is given by the amalgamated free product $D_6 *_{\mathbb{Z}/2\times\mathbb{Z}/2} D_4$.

We have shown in Section 4.3 the generation of D_6, D_4, and $\mathbb{Z}/2 \times Z/2$ with generators of Homeo(E_3). The presentations of these groups can be written as

$$\begin{aligned} D_6 &\cong \langle c, r, s \mid c^2, r^3, s^2, rsrs, crcr^{-1}, cscs \rangle, \\ D_4 &\cong \langle a, c \mid a^4, c^2, acac \rangle = \langle a, c, s \mid a^4, c^2, s^2, acac, a^2cs \rangle, \\ \mathbb{Z}/2 \times \mathbb{Z}/2 &\cong \langle c, s \mid c^2, s^2, cscs \rangle. \end{aligned}$$

The generators c, r, s all stabilize the red vertex, and the generators a and c stabilize the blue vertex. Hence, a presentation of Homeo(E_3), written in terms of the generators a, c, r, s presented in Section 4.3, can be

$$\text{Homeo}(E_3) = \langle a, c, r, s \mid a^4, c^2, r^3, s^2, rsrs, crcr^{-1}, cscs, acac, a^2cs \rangle. \tag{5.6.1}$$

5.7 E_4 Has $D_4 \times \mathbb{Z}/2$ Homeomorphism Group

In this section, we will show that the full homeomorphism group of the E_4 fractal is isomorphic to $D_4 \times \mathbb{Z}/2$.

We construct the structural complex $\mathcal{K}_{E_4}$ of E_4 in analogous to the structural complex of E_3. However, instead of a triangular prism, we need to start from a square prism (more precisely, a cube) because E_4 has four cells to start with. Subsequently, we paste triangular prisms onto the starting polyhedron, and we construct our desired structure complex. The vertices, edges, faces, and polyhedra of this structural complex are specified as follows.

Vertices: all pinch points in E_4;

Edges: there is one edge between each pair of pinch points that are adjacent boundary points of the same cell;

Triangular faces: any 3-cycles of edges;

Square faces (triangular prisms): choices of four pinch points that are the boundary points of the same cell, or equivalently, choices of four points on E_4 whose removal disconnects E_3 into two components;

Triangular prisms: choices of six points in E_4 whose removal disconnects E_3 into three components, at least two of which are cells of E_3.

A visualization of the first stage of pasting on this structural complex is shown in Figure 5.7.1. Notice that all but one of the polyhedra in this structural are triangular prisms. Only the starting polyhedron is a cube. This fact is very useful in showing the group structure of Homeo(E_4).

Theorem 5.7.1. Homeo(E_4) $\cong D_4 \times \mathbb{Z}/2$.

Proof. The construction of the structural complex $\mathcal{K}_{E_4}$ of E_4 naturally defines a homeomorphism $\varphi : \mathcal{K}_{E_4} \to E_4$. Thus Homeo($E_4$) $\cong$ Aut($\mathcal{K}_{E_4}$). Let $\psi : \mathcal{K}_{E_4} \to \mathcal{K}_{E_4}$ be an automorphism.

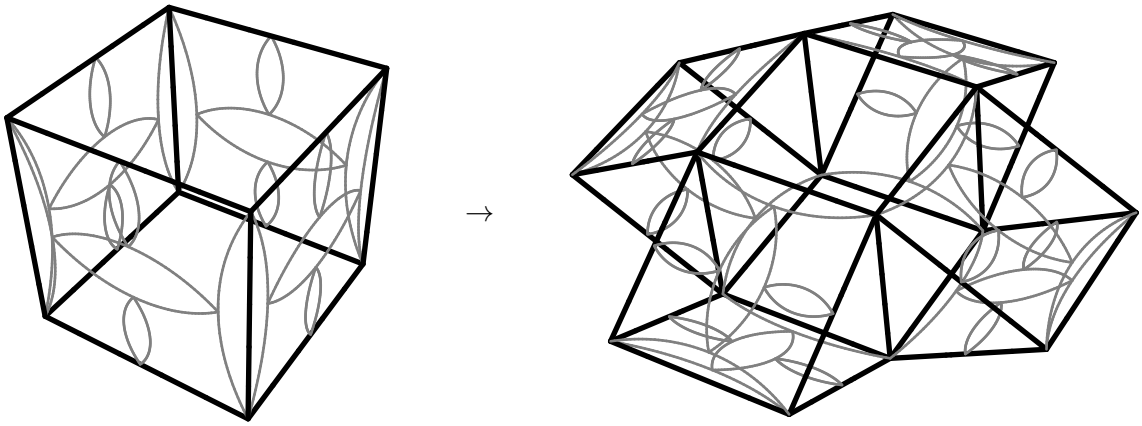

Figure 5.7.1: The Starting Cube and Subsequent Pasting of Triangular Prisms on $\mathcal{K}_{E_4}$

Because there is only one cube in the polyhedron complex $\mathcal{K}_{E_4}$, the automorphism ψ must fix the cube. Furthermore, because the top and the bottom of the cube has different geometric meanings with its sides, ψ must act on the cube so that either both the top and the bottom are preserved or they switch position. In another word, the only possible actions on the cube are the full symmetry group $D_4 \times \mathbb{Z}/2$ of a square prism. Thus we have $\mathrm{Aut}(\mathcal{K}_{E_4}) \leq D_4 \times \mathbb{Z}/2$. Lemma 4.5.1 has shown that $D_4 \times \mathbb{Z}/2 \leq \mathrm{Homeo}(E_4)$. We can conclude that $\mathrm{Homeo}(E_4) \cong \mathrm{Aut}(\mathcal{K}_{E_4}) \cong D_4 \times \mathbb{Z}/2$. $\square$

6
E_3 as a Limit Set

The previous chapter has given a nice presentation of the group Homeo(E_3) with four generators a, c, r, s. Three of these generators have clear geometric interpretations. Generator c is the inversion across the unit circle; generator r is the 120-degree rotation about the origin; generator s is the complex conjugation function, which reflects everything across the real axis. All of these three maps are well-defined Möbius transformations or anti-Möbius transformations on the complex plane. However, we are not sure about the geometric meaning of the map a. All we know from Section 4.3 is that a is an inversion composed with a rotation of the Riemann sphere. In this chapter, we will develop a geometric interpretation of the generators of Homeo(E_3). The first section will focus on the orientation-preserving subgroup of Homeo(E_3) and find a presentation of this subgroup. In Section 6.2, we will show that this orientation-preserving subgroup is isomorphic to a Kleinian group. The limit set of this Kleinian group is homeomorphic to the E_3 fractal. In Section 6.3, we will use *Tietze transformation* to change the generator r into an anti-Möbius transformation so that the group can be generated by four anti-Möbius transformations. We will investigate the geometric meaning of these four maps and present a conjugated limit set that has the same structure with E_3 as well as the limit set shown in Section 6.2.

6.1 Orientation-Preserving Homeomorphisms in Homeo(E_3)

The homeomorphism group Homeo(E_3) of the E_3 fractal contains orientation-preserving and orientation-reversing homeomorphisms. The orientation-preserving transformations in Homeo(E_3) form an index-2 normal subgroup of Homeo(E_3), and it should act on the structural tree $\mathcal{T}_{E_3}$ of E_3 as the orientation-preserving automorphisms, which include rotations, translations, and compositions of these two types of automorphisms, but not reflections. We denote this group by Homeo$_+$(E_3), and apply the method used in Sections 5.5 and 5.6 to find a presentation of Homeo$_+$(E_3).

We will use the specification of edges and vertices shown in Figure 5.6.3, and focus only on the orientation-preserving actions on $\mathcal{T}_{E_3}$. We isolate the pink and purple vertices and the edge connecting them from the tree, and find the orientation-preserving stabilizing actions. It then follows that the stabilizer subgroup of the pink vertex is isomorphic to D_3, and the stabilizer subgroup of the purple vertex is isomorphic to $\mathbb{Z}/2 \times \mathbb{Z}/2$. The edge stabilizer is the intersection of these two subgroups, which is isomorphic to $\mathbb{Z}/2$.

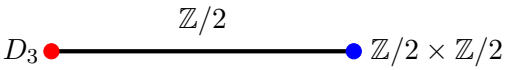

The stabilizer subgroups are subgroups of D_6, D_4, and $\mathbb{Z}/2 \times \mathbb{Z}/2$, respectively, presented at the end of Section 5.6. We enumerate the group elements of D_3, and $\mathbb{Z}/2 \times \mathbb{Z}/2$, and $\mathbb{Z}/2$ in terms of the generators for the former.

$$D_3 = \{1, r, r^2, cs, rcs, r^2cs\},$$
$$\mathbb{Z}/2 \times \mathbb{Z}/2 = \{1, a^2, ac, a^3c\} = \{1, cs, ac, as\},$$
$$\mathbb{Z}/2 = \{1, cs\}.$$

We define the transformations $x = cs$ and $y = ac$, and write down the presentation of the groups listed above. Notice that a, c, s are orientation-reversing homeomorphisms, but both x and y are

orientation-preserving.

$$D_3 = \langle r, x \mid r^3, x^2, rxrx \rangle,$$
$$\mathbb{Z}/2 \times \mathbb{Z}/2 = \langle x, y \mid x^2, y^2, xyxy \rangle,$$
$$\mathbb{Z}/2 = \langle x \mid x^2 \rangle.$$

Therefore, a presentation of Homeo$_+(E_3)$, written in terms of generators r, x, and y, can be

$$\text{Homeo}_+(E_3) = \langle r, x, y \mid r^3, x^2, y^2, rxrx, xyxy \rangle. \tag{6.1.1}$$

6.2 Homeo$_+(E_3)$ as a Kleinian Group

Because The E_3 fractal appears to have tangent complimentary regions, just like the Apollonian disks in the Apollonian gasket, we attempt to find a Kleinian group that is isomorphic to Homeo$_+(E_3)$. We first define a homomorphism $\xi : \text{Homeo}_+(E_3) \longrightarrow \text{Mob}$ by specifying where to map the generators of Homeo$_+(E_3)$ into the group of Möbius transformations. In this chapter, the symbols r, x, y are used as orientation-preserving homeomorphisms of E_3. The symbols r_ξ, x_ξ, y_ξ stand for the images of r, x, y, respectively, under the homomorphism ξ. They are all Möbius transformations.

By the presentation in 6.1.1, the homeomorphism x is an order-2 element. Thus its image x_ξ shall be a Möbius transformation of order-2. All Möbius transformations of order-2 are conjugates with each other. For convenience, we shall pick one order-2 Möbius transformation as x_ξ.

$$x_\xi(z) = 1/z, \tag{6.2.1}$$

On the other hand, we know that the homeomorphism r is an order-3 element, and $\langle r, s \rangle$ forms a subgroup isomorphic to D_3. Thus r_ξ must be an order-3 Möbius transformation that forms a D_3 subgroup with x_ξ. We shall pick the following Möbius transformation as r_ξ.

$$r_\xi(z) = ze^{2i\pi/3}. \tag{6.2.2}$$

The following lemma shows the validity of picking these two Möbius transformations as the images of x and r under the homomorphism ξ.

Lemma 6.2.1. *There exist a Möbius transformation y_ξ such that the map*

$$\xi\colon \mathrm{Homeo}_+(E_3) \longrightarrow \mathrm{Mob}$$

is a homomorphism.

Proof. To show that ξ is a homomorphism, we need to find a Möbius transformation y_ξ such that r_ξ, x_ξ, y_ξ satisfies the relations specified in 6.1.1. Let y_ξ be a Möbius transformation

$$y(z) = \frac{Az + B}{Cz + D},$$

with undetermined coefficients $A, B, C, D \in \mathbb{C}$. There are two relations that y_ξ needs to satisfy. First of all, y_ξ is an order-2 Möbius transformation by the relation y^2. Iterating y_ξ on any value $z \in \mathbb{C}$ should get z back. We use 0 and ± 1 as the input values of z to solve for the relation between the undetermined coefficients, and we get the equations

$$\frac{A\cdot(B/D)+B}{C\cdot(B/D)+D} = 0, \quad \frac{A\cdot\frac{A+B}{C+D}+B}{D\cdot\frac{A+B}{C+D}+D} = 1, \quad \text{and} \quad \frac{A\cdot\frac{B-A}{D-C}+B}{D\cdot\frac{B-A}{D-C}+D} = -1. \tag{6.2.3}$$

Secondly, y_ξ has to commute with x_ξ by the relation $xyxy$ and the fact that both x_ξ and y_ξ are order-2 Möbius transformations. Thus $y_\xi(x_\xi(z)) = x_\xi(y_\xi(z))$ for all $z \in \mathbb{C}$. Again, we use 0 and ± 1 as the input values of z to solve for another relation between the undetermined coefficients (for the equation with $z = 0$, we take the limit as $z \to 0$), and we get the equations

$$\frac{A}{C} = \frac{B}{D}, \quad \frac{A+B}{C+D} = \frac{C+D}{A+B} \quad \text{and} \quad \frac{B-A}{D-C} = \frac{D-C}{B-A}. \tag{6.2.4}$$

Combine Equations 6.2.3 and 6.2.4 and solve, we get two sets of solutions

$$\begin{cases} D = -A, \\ C = -B, \end{cases} \quad \text{and} \quad \begin{cases} A = D = 0, \\ B = C. \end{cases}$$

The second set yields the map x_ξ. It is clear that x_ξ is order-2 and commutes with x_ξ, but it is not the map we want. We want the other one with coefficients $D = -A$ and $C = -B$ as the map y_ξ. Let $q = B/A$, the closed-form expression for y_ξ can then be written as

$$y_\xi(z) = -\frac{z+q}{qz+1}, \tag{6.2.5}$$

with an arbitrary value $q \in \mathbb{C}$. Now we have made ξ a homomorphism. □

We notice that this is a one-parameter family of Kleinian groups isomorphic to Homeo$_+(E_3)$ with a parameter $q \in \mathbb{C}$. For different values of q, we computed the orbit of points on the complex plane, and plot them to approximate the associated limit set. For different values of q, we obtain different structures for the associated limit set. The structures of the resulting limit sets include space-filling orbits, circles, Cantor dusts, carpets, and post-critically finite fractals in which we are interested. We show some of the resulting limit sets in Figure 6.2.1. When $q = 0.66 + 0.75i$, the resulting limit set appears to have similar structure with the E_3 fractal. To find out the exact value of q for this limit set that resembles E_3, we need to understand how the map y, as a homeomorphism, acts on the E_3 fractal.

Theorem 6.2.2. *Let* $\xi\colon \text{Homeo}_+(E_3) \longrightarrow \text{Mob}$ *be the homomorphism defined above, where*

$$r_\xi(z) = ze^{2i\pi/3},\ x_\xi(z) = 1/z,\ \textit{and}\ y_\xi(z) = -\frac{z+q}{qz+1}$$

for an undetermined coefficient $q \in \mathbb{C}$. *Suppose that there exist a homeomorphism* $f\colon E_3 \longrightarrow \Lambda(\langle r_\xi, x_\xi, y_\xi\rangle)$ *that commutes with the action of* Homeo$_+(E_3)$, *then* q *is a root of the polynomial* $4q^4 + q^2 + 4$.

Proof. In Homeo(E_3), the map y is defined to be the composition of a and c. The sequential action of c followed by a on the E_3 fractal is shown in Figure 6.2.2. We focus on four special points on the E_3 fractal, namely, the points labeled p_1, p_2, p_3, p_4 in Figure 6.2.2. These four points form an invariant set under the actions of both c and a. The image of each point under

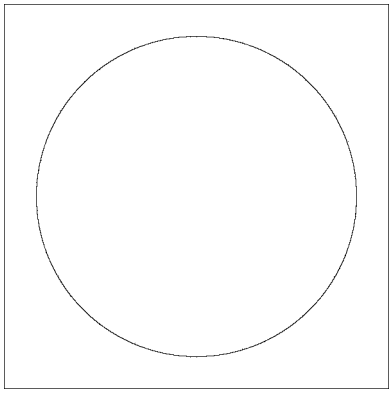

$q = 5$

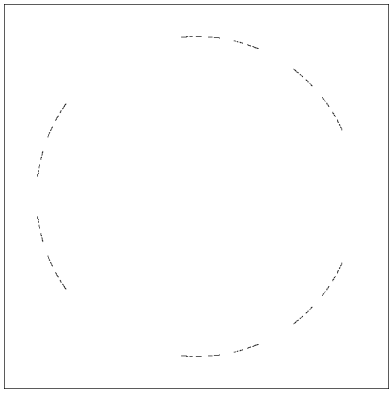

$q = 0.55$

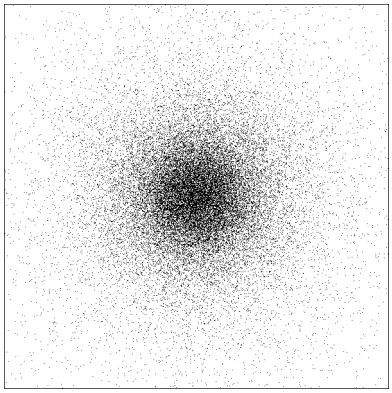

$q = i$

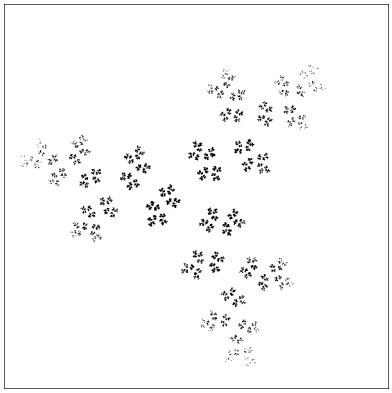

$q = 1 + i$

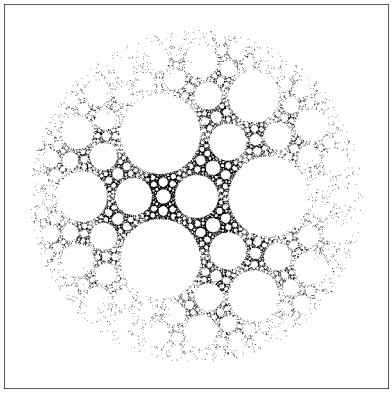

$q = 0.6 + 0.8i$

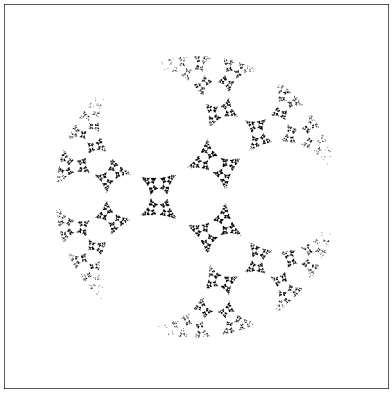

$q = 0.66 + 0.75i$

Figure 6.2.1: Orbit-Approximated Limit Sets with Different Parameter q

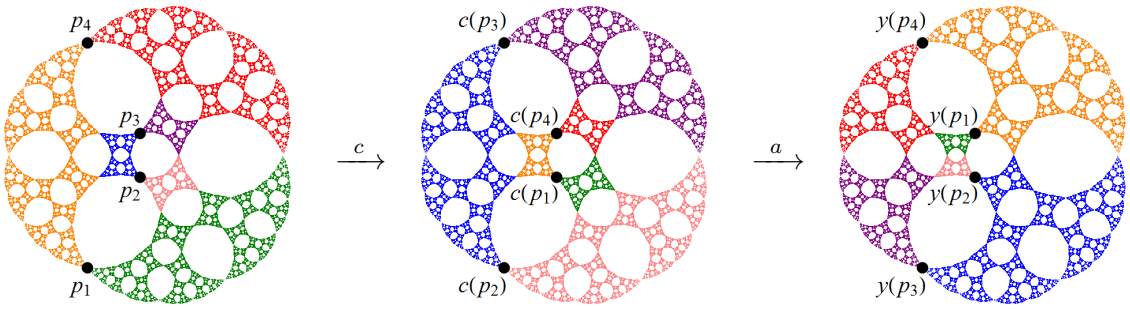

Figure 6.2.2: Action of y on E_3

the actions is also shown in the figure. Points p_2 and p_4 are fixed under the action of y, while points p_1 and p_3 switch their positions.

Now we return to our desired Kleinian group and its limit set. We denote the corresponding points permuted by y_ξ with $q_1, q_2, q_3, q_4 \in \mathbb{C}$. By D_3 symmetry of the limit set, we know that the argument of q_1 and q_2 is $-2\pi/3$, and the argument of q_3 and q_4 is $2\pi/3$. By the unit circle inversion as a symmetry operation, we know that the norm of q_2 and q_3 is inverse of the norm of q_1 and q_4. We suppose that q_1 corresponds to the complex number $Re^{-2i\pi/3}$, where $R > 1$ is an undetermined coefficient. Then q_2, q_3, and q_4 correspond to $e^{-2i\pi/3}/R$, $e^{2i\pi/3}/R$, and $Re^{2i\pi/3}$, respectively. Hence, we have the following equations

$$y(Re^{-2i\pi/3}) = e^{2i\pi/3}/R, \tag{6.2.6}$$

$$y(e^{-2i\pi/3}/R) = e^{-2i\pi/3}/R, \tag{6.2.7}$$

$$y(e^{2i\pi/3}/R) = Re^{-2i\pi/3}, \tag{6.2.8}$$

$$y(Re^{2i\pi/3}) = Re^{2i\pi/3}. \tag{6.2.9}$$

We can solve this system of equations for the undetermined coefficients q and R, and we get

$$q \approx 0.6614 + 0.75i \quad \text{and} \quad R \approx 2.189, \tag{6.2.10}$$

with minimal polynomials $4q^4 + q^2 + 4$ and $R^4 - 5R^2 + 1$, respectively. Hence, we are able to write the map y_ξ as

$$y_\xi(z) = -\frac{z+q}{qz+1}, \tag{6.2.11}$$

where q is the root of the quartic polynomial $4q^4 + q^2 + 4$ with approximated value $0.6614 + 0.75i$. □

The limit set of the Kleinian group generated by r_ξ, x_ξ, and y_ξ appears to be homeomorphic to E_3. Figure 6.2.3 shows part of the orbit of an arbitrary complex number on the complex plane under this Kleinian group. We can clearly see the structure of E_3 in the orbit. In the next section, we will show another Kleinian group whose limit set has the same structure. However, the Kleinian group in the next section is conjugate to the Kleinian group generated by r_ξ, x_ξ, y_ξ. In fact, up to conjugacy, there is only one Kleinian group with limit set homeomorphic to E_3.

Definition 6.2.3. Let K_+ be the Kleinian group generated by r_ξ, x_ξ, and y_ξ. Let K be the group $K_+ \rtimes \langle s_\xi \rangle$, where s_ξ is the complex conjugation function.

The group K contains Möbius transformations and anti-Möbius transformations. The anti-Möbius transformations in K forms a coset of K_+ in K. The following lemma shows the relation between the groups K_+ and K.

Lemma 6.2.4. *The limit set of K is the same as the limit set of K_+.*

Proof. The statement follows immediately from the fact that the limit set of K_+ is invariant under the complex conjugation function s_ξ. □

Lemma 6.2.5. *The homomorphism* $\xi\colon \mathrm{Homeo}_+(E_3) \longrightarrow \mathrm{Mob}$ *extends to an onto homomorphism*

$$\xi_\pm\colon \mathrm{Homeo}(E_3) \longrightarrow K.$$

Proof. Let $\xi_\pm\colon \mathrm{Homeo}(E_3) \longrightarrow K$ be a homomorphism defined by

$$\xi_\pm\colon s \mapsto s_\xi, r \mapsto r_\xi, c \mapsto x_\xi s_\xi^{-1}, a \mapsto y_\xi s_\xi x_\xi^{-1}.$$

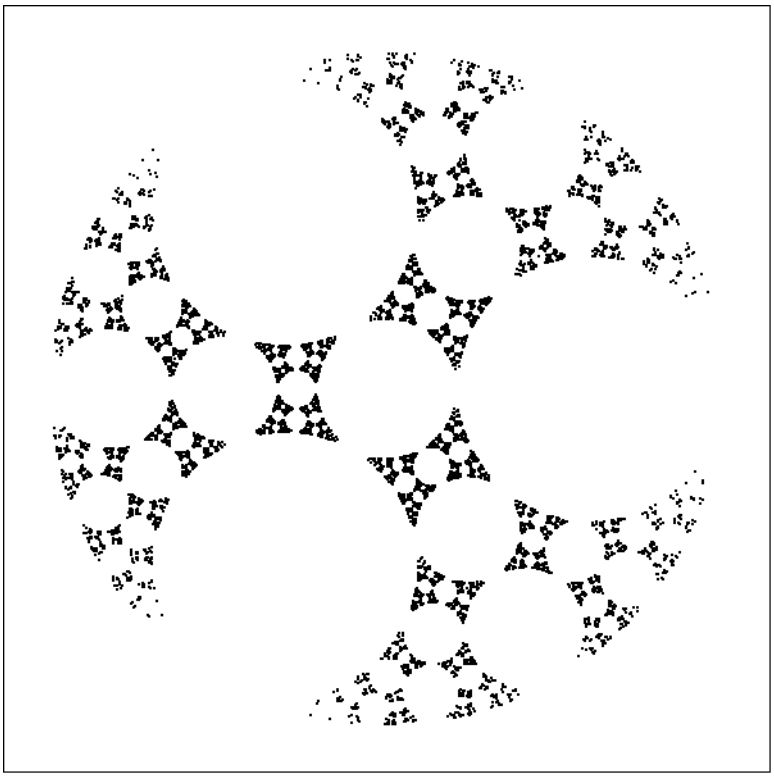

Figure 6.2.3: K_+-Orbit of an Arbitrary Point on the Complex Plane

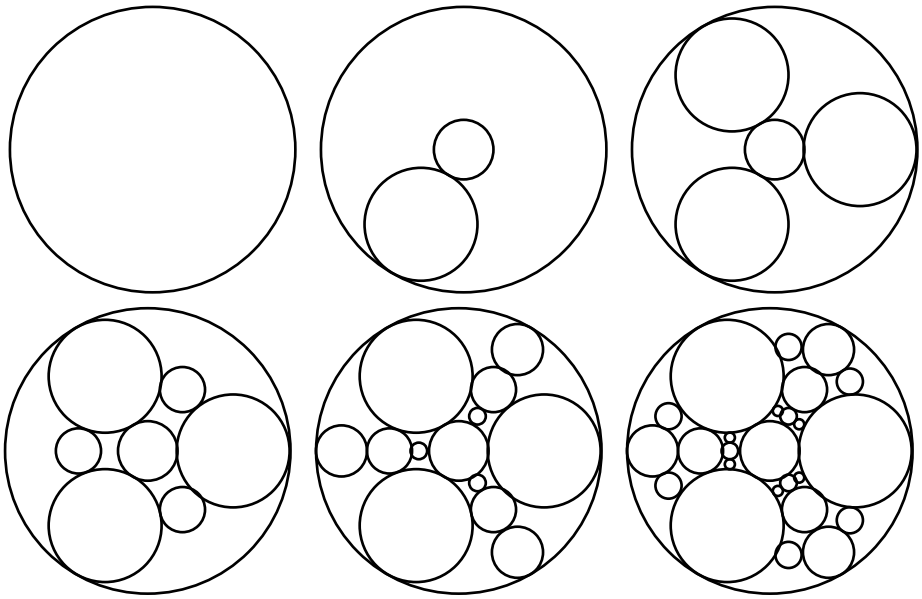

Figure 6.2.4: Complementary Disks in the Limit Set of K_+

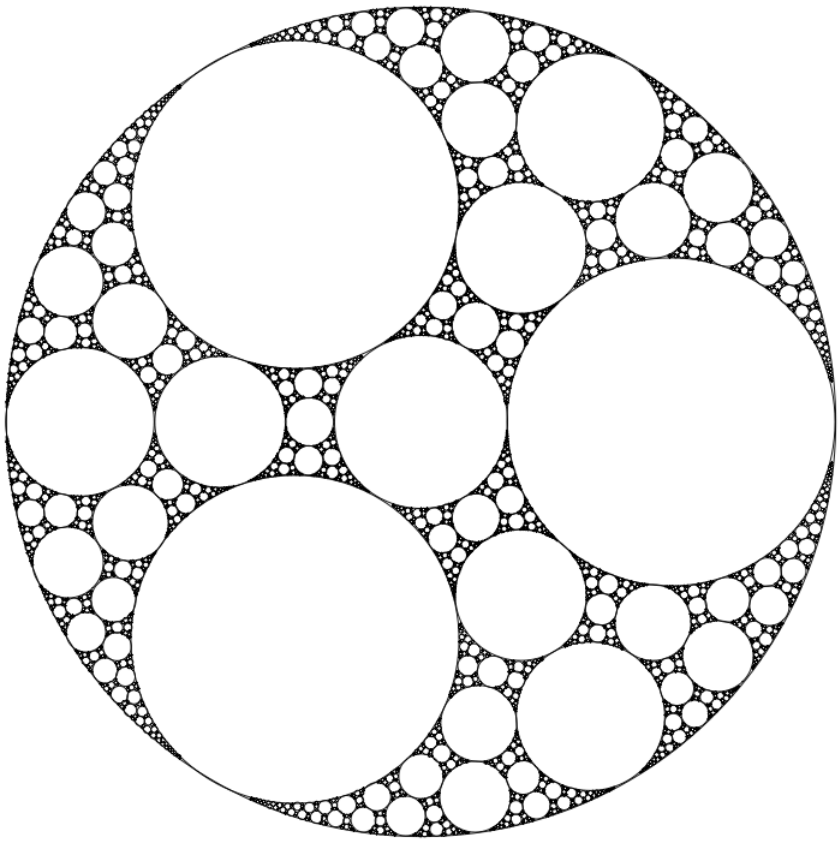

Figure 6.2.5: Limit Set of K_+

It then follows that

$$\xi_{\pm}(x) = \xi_{\pm}(cs) = \xi_{\pm}(c)\xi_{\pm}(s) = x_{\xi}s_{\xi}^{-1}s_{\xi} = x_{\xi},$$

and

$$\xi_{\pm}(y) = \xi_{\pm}(ac) = \xi_{\pm}(a)\xi_{\pm}(c) = y_{\xi}s_{\xi}x_{\xi}^{-1}x_{\xi}s_{\xi}^{-1} = y_{\xi}.$$

Thus $\xi_{\pm}$ is an extension of ξ. Furthermore, because K contains all finite words written with the alphabet $\{r_{\xi}, x_{\xi}, y_{\xi}, s_{\xi}\}$, it follows that $\xi_{\pm}$ is onto K. □

Because $\xi_{\pm}$ is an extension of ξ, we shall extend our notation for the anti-Möbius transformations under the map of $\xi_{\pm}$. The images of a and c shall be denoted by a_{ξ} and c_{ξ}, respectively.

Unlike the Julia set, the limit set has disks as its complementary regions. From the solution we obtain in 6.2.10, we know the circle that encloses the whole limit set as the circle C centered at the origin with radius $R \approx 2.189$. The limit set is an invariant set under the action of K_+, so is the complement of the limit set. Hence, the complementary disks of the limit set maps to complementary disks under the action of K_+. A sequential application of the generators $r_{\xi}, x_{\xi}, y_{\xi}$ on the circle C, as shown in Figure 6.2.4, will give us all the complementary regions of the limit set, hence providing another way of visualizing the limit set. Figure 6.2.5 shows a visualization of the limit set using this method, and it surely appears homeomorphic to the E_3 fractal.

6.3 Geometric Interpretation of K

Recall that Homeo(E_3) has the presentation

$$\text{Homeo}(E_3) = \langle a, c, r, s \mid a^4, c^2, r^3, s^2, rsrs, crcr^{-1}, cscs, acac, a^2cs \rangle. \tag{6.3.1}$$

Lemma 6.2.5 has shown that there exist an onto homomorphism $\xi_{\pm}\colon \text{Homeo}(E_3) \to K$. It follows that K is a quotient of Homeo(E_3), and it is generated by a_{ξ}, c_{ξ}, r_{ξ}, and s_{ξ} with presentation

$$\langle a_{\xi}, c_{\xi}, r_{\xi}, s_{\xi} \mid R \cup \{a_{\xi}^4, c_{\xi}^2, r_{\xi}^3, s_{\xi}^2, r_{\xi}s_{\xi}r_{\xi}s_{\xi}, c_{\xi}r_{\xi}c_{\xi}r_{\xi}^{-1}, c_{\xi}s_{\xi}c_{\xi}s_{\xi}, a_{\xi}c_{\xi}a_{\xi}c_{\xi}, a_{\xi}^2c_{\xi}s_{\xi}\}\rangle, \tag{6.3.2}$$

where R is an additional set of relations on the generating set $\{a_\xi, c_\xi, r_\xi, s_\xi\}$. We suspect that R is the empty set, in which case we would have $K \cong \text{Homeo}(E_3)$. Furthermore, K would act on the polyhedral complex associated with E_3 embedded in hyperbolic 3-space $\mathbb{H}^3$.

Among these four generators, we understand the geometric interpretations of c_ξ, r_ξ, and s_ξ on the Riemann sphere. Generator c_ξ has the equation $c_\xi(z) = 1/\overline{z}$ for all $z \in \hat{\mathbb{C}}$, and it is the inversion across the unit circle; generator r_ξ is the 120-degree rotation about the origin; generator s_ξ is the complex conjugation function, which corresponds to a reflection across the real axis. However, the geometric interpretation of a_ξ is limited to Figure 4.3.1 and its permutation on the points $\{q_1, q_2, q_3, q_4\}$ in the proof for Theorem 6.2.2 by the rule

$$q_1 \xrightarrow{a_\xi} q_2 \xrightarrow{a_\xi} q_3 \xrightarrow{a_\xi} q_4 \xrightarrow{a_\xi} q_1.$$

The actual geometric meaning of a_ξ is still a mystery. In order to obtain a better understanding of a_ξ, we conjugate a_ξ with a Möbius transformation m so that the transformation $\alpha = ma_\xi m^{-1}$ has a better-understood geometric interpretation.

Lemma 6.3.1. *There exist a Möbius transformation m such that $\alpha = ma_\xi m^{-1}$ acts on the complex plane as an inversion across the unit circle followed by a 90-degree rotation around the origin.*

Proof. We know that given two sets of points $\{z_1, z_2, z_3\}$ and $\{w_1, w_2, w_3\}$ on the Riemann sphere $\hat{\mathbb{C}}$, there exist a unique Möbius transformation under which z_1, z_2, z_3 map to w_1, w_2, w_3, respectively. In this case, m is the conjugator Möbius transformation that maps q_1, q_2, q_3 to i, i^2, i^3, respectively.

Let $R \approx 2.189$ be the solution in 6.2.10. Let $\omega = e^{2i\pi/3}$. Suppose that m is the Möbius transformation with expression

$$m(z) = \frac{Az + B}{Cz + D},$$

where $A, B, C, D \in \mathbb{C}$ are undetermined coefficients. According to the mapping conditions, we get the system of equations

$$m(\omega^2 R) = i, \tag{6.3.3}$$

$$m(\omega^2/R) = i^2 = -1, \tag{6.3.4}$$

$$m(\omega/R) = i^3 = -i. \tag{6.3.5}$$

Because Mob $\cong \mathrm{PSL}_2(\mathbb{C})$, we can force the condition

$$A = 1. \tag{6.3.6}$$

Solving this system of four equations gives the undetermined coefficients

$$A = B = 1,\ C = -D \approx 0.475 - 0.475i, \tag{6.3.7}$$

where C and D both have minimal polynomial $9x^8 + 46x^4 + 9$. Hence, we can write m with the expression

$$m(z) = \frac{z+1}{C(z-1)}, \tag{6.3.8}$$

where C is a constant with minimal polynomial $9x^8 + 46x^4 + 9$ and approximated value $0.475 - 0.475i$. It is then easy to verify that $\alpha(z) = i/\overline{z}$ for all $z \in \hat{\mathbb{C}}$. □

Now we are ready to change the generators of K. We hereby introduce *Tietze transformations* as the tool for doing the change of generators. The definition we adopt here is from [12].

Definition 6.3.2. Let G be a group with presentation $G = \langle S \mid R \rangle$. We define four types of **Tietze transformations** as follows:

R^+: If r is a word in X and $r = e$ is a relation that holds in G, then

$$G \cong \langle S \mid R \cup \{r\} \rangle.$$

R^-: If $r \in R$ is a relation such that $r = e$ holds in the group $\langle S \mid R - \{r\} \rangle$, then

$$G \cong \langle S \mid R - \{r\} \rangle.$$

S^+: If w is a word in S and s is a symbol not in S, then

$$G \cong \langle S \cup \{s\} \mid R \cup \{sw^{-1}\}\rangle.$$

S^-: If $s \in S$ and w is a word in $S - \{s\}$ such that $sw^{-1} = e$, then substitute w for s in every other relation of R to get $\tilde{R}$, and

$$G \cong \langle S - \{s\} \mid \tilde{R}\rangle.$$

Theorem 6.3.3. *Two finite presentations define isomorphic groups if and only if it is possible to pass from one to the other by a finite sequence of Tietze transformations.*

Proof. See proofs for Theorem 1 and 2 in Chapter 4 of [12]. □

We first apply Tietze transformations S^+ and S^- to substitute the generator r_ξ with $t_\xi = r_\xi s_\xi$. The map t_ξ is an anti-Möbius transformation, and it corresponds to a circle inversion on the Riemann sphere $\hat{\mathbb{C}}$. The purpose of changing this generator is to simplify the geometric interpretation of generators because a nice geometric interpretation of a Möbius is not always guaranteed, but a circle inversion conjugated by a Möbius transformation is always another circle inversion. The presentation of K after applying the transformations then becomes

$$K = \langle a_\xi, c_\xi, s_\xi, t_\xi \mid \tilde{R} \cup \{a_\xi^4, c_\xi^2, s_\xi^2, t_\xi^2, (s_\xi t_\xi)^3, c_\xi t_\xi s_\xi c_\xi s_\xi t_\xi, c_\xi s_\xi c_\xi s_\xi, a_\xi c_\xi a_\xi c_\xi, a_\xi^2 c_\xi s_\xi\}\rangle, \quad (6.3.9)$$

where $\tilde{R}$ is the result of Tietze transformations S^+ and S^- on the set of relations R.

Now we apply Tietze transformations S^+ and S^- again to substitute each generator with its conjugate under the map m. Notice that this set of transformation does not change the presentation in 6.3.9. We define the group

$$CE = \langle \alpha, \gamma, \sigma, \tau \mid m\tilde{R}m^{-1} \cup \{\alpha^4, \gamma^2, \sigma^2, \tau^2, (\sigma\tau)^3, \gamma\tau\sigma\gamma\sigma\tau, \gamma\sigma\gamma\sigma, \alpha\gamma\alpha\gamma, \alpha^2\gamma\sigma\}\rangle,$$

where $\alpha = ma_\xi m^{-1}$, $\gamma = mc_\xi m^{-1}$, $\sigma = ms_\xi m^{-1}$, and $\tau = mt_\xi m^{-1}$ as anti-Möbius transformations, and $m\tilde{R}m^{-1}$ is the set of relations $\tilde{R}$ under the conjugation of m. Hence, CE is a group

isomorphic to K. We can also reason that CE contains an index-2 Kleinian subgroup CE_+, which contains all Möbius transformations in CE, with presentation

$$CE_+ = \langle \rho, \phi, \psi \mid R' \cup \{\rho^3, \phi^2, \psi^2, \rho\phi\rho\phi, \phi\psi\phi\psi\}\rangle,$$

where $\rho = mr_\xi m^{-1}$, $\phi = mx_\xi m^{-1}$, and $\psi = my_\xi m^{-1}$ as Möbius transformations, and R' is a set of additional relations on the generating set $\{\rho, \phi, \psi\}$. We would also expect the limit set $\Lambda(CE_+)$ of CE_+ to be homeomorphic to the limit set $\Lambda(K_+)$ of K_+.

Finally, we analyze the geometric meaning of the other three generators γ, σ, and τ of CE. Readers should keep in mind that all of c_ξ, s_ξ and t_ξ are circle inversions on the Riemann sphere, thus their conjugation under m shall also be circle inversions. The mapping relation of some of the points in the limit sets are shown in Figure 6.3.1. The image of the circles (lines) about which the anti-Möbius transformations reflect is also shown in Figure 6.3.2.

It is then clear that α is the reflection across the unit circle followed by a 90-degree rotation; γ and σ are reflections across the lines $\mathrm{Re}(z)+\mathrm{Im}(z) = 0$ and $\mathrm{Re}(z)-\mathrm{Im}(z) = 0$, respectively. But what is the circle associated with τ? We use the conformal property of Möbius transformations to answer this question.

We denote the circle associated with a Möbius transformation labeled h_ξ by C_h. Notice that C_t intersects C_c twice at right angle, and C_t intersects C_s twice (once at infinity) with a 60° angle. Additionally, C_t intersects C_a twice with an unknown angle. We notice that the intersection points between C_t and C_a are the points q_1 and q_2. There exist a unique circle that intersects C_γ at right angle, intersects C_σ at 60-degrees, and passes through $m(q_1) = i$ and $m(q_2) = -1$, namely the circle C_τ associated with the circle inversion τ. The center of C_τ is

$$\Big(\frac{1+\sqrt{7}}{6}, -\frac{1+\sqrt{7}}{6}\Big),$$

and the radius of C_τ is

$$\frac{\sqrt{2}+\sqrt{14}}{3}.$$

Figure 6.3.3 shows the limit set of CE_+ generated with the same method as the limit set of K_+. It indeed appears to be homeomorphic to the limit set of K_+ as well as the E_3 fractal. The relatively simple geometric interpretation of CE_+ possibly provides a pathway to showing homeomorphic relations between $\Lambda(CE_+)$, $\Lambda(K_+)$, and the E_3 fractal.

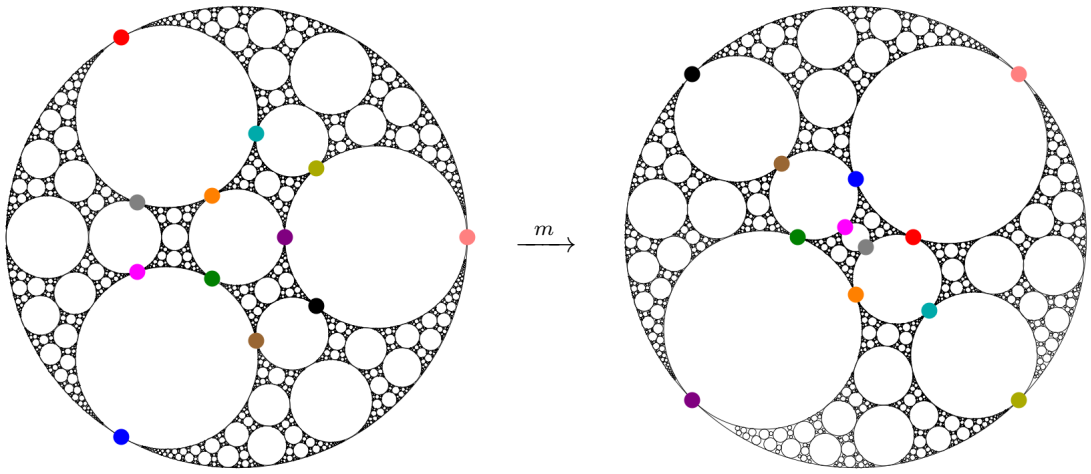

Figure 6.3.1: Mapping Relation of Points under Conjugator m

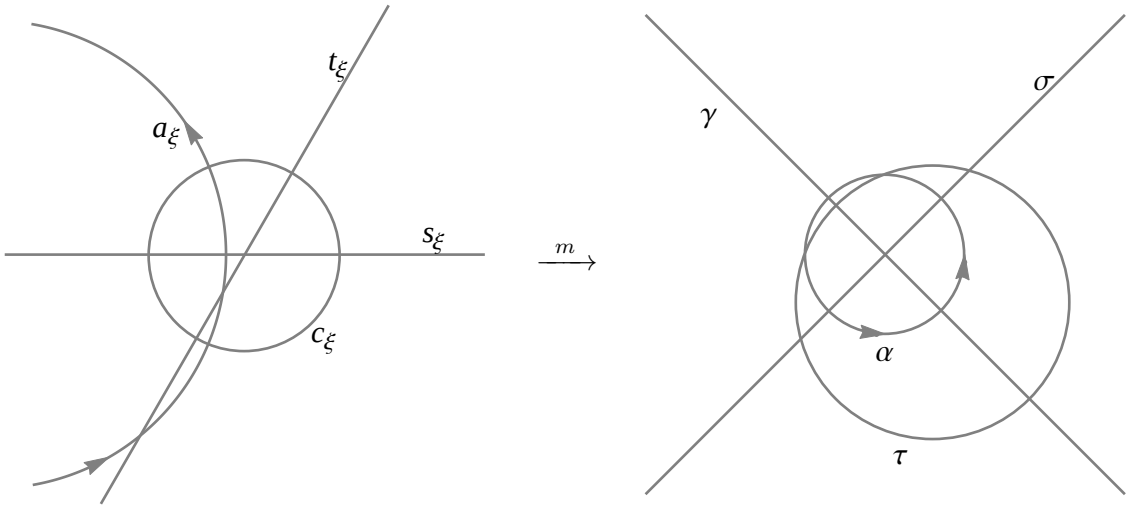

Figure 6.3.2: Mapping Relation of Circles under Conjugator m

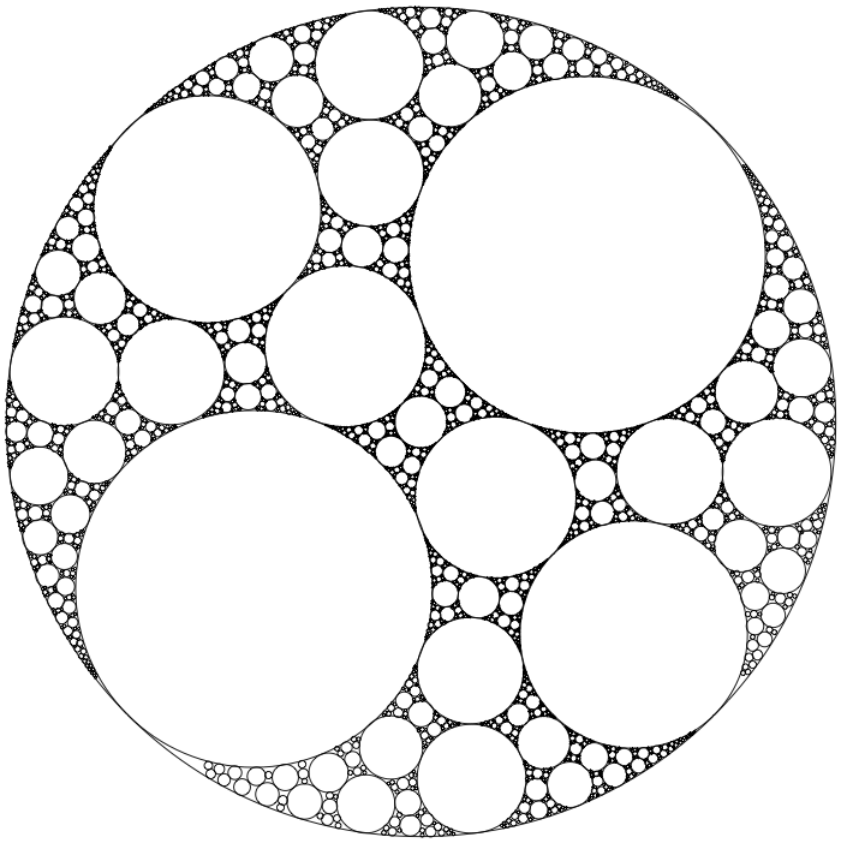

Figure 6.3.3: Limit Set of CE_+

Bibliography

[1] Kathleen T. Alligood, Tim D. Sauer, and James A. Yorke, *Chaos: An Introduction to Dynamical Systems*, Springer, New York, 1996.

[2] Roger C. Alperin, $\mathrm{PSL}_2(\mathbb{Z}) = \mathbb{Z}_2 * \mathbb{Z}_3$, Am. Math. Mon. **100** (1993), no. 4, 385–386.

[3] James Belk, *Thompson's Group F*, Cornell University, 2004.

[4] James Belk and Bradley Forrest, *A Thompson Group for the Basilica* (2012). preprint, arXiv:1201.4225 [math.GR].

[5] B. Bollobás, *Graph theory: an introductory course*, Graduate texts in mathematics, Springer Verlag, 1979.

[6] Francis Bonahon, *Low-Dimensional Geometry: From Euclidean Surfaces to Hyperbolic Knots*, AMS, Providence, 2009.

[7] J. W. Cannon, W. J. Floyd, and W. R. Parry, *Introductory notes on Richard Thompson"s groups* (1996).

[8] Robert L. Devaney, *Complex Dynamical Systems: The Mathematics Behind the Mandelbrot and Julia Sets*, Proceedings of Symposia in Applied Mathematics, vol. 49, American Mathematical Society, 1995.

[9] Robert L. Devaney, Monica Moreno Rocha, and Stefan Siegmund, *Rational maps with generalized Sierpinski gasket Julia sets*, Topology and its Applications **154** (2007), no. 1, 11-27, DOI 10.1016/j.topol.2006.03.024.

[10] K. Falconer, *Techniques in Fractal Geometry*, Wiley, 1997.

[11] F. Harary, *Graph Theory*, Addison-Wesley Series in Mathematics, Perseus Books, 1994.

[12] D. L. Johnson, *Presentations of Groups*, Lecture Note Series, vol. 22, Cambridge University Press, 1976.

[13] Atsushi Kameyama, *Julia sets of postcritically finite rational maps and topological self-similar sets*, Nonlinearity **13** (2000), no. 1, 165-188.

[14] A. A. Kirillov, *A Tale of Two Fractals*, Birkhauser, 2010.

[15] Daniel M. Look, *The Dynamics of Two and Three Circle Inversion*, Fund. Math **199** (2008), 227–247.

[16] Joel Louwsma, *Homeomorphism Groups of the Sierpinski Carpet and Sierpinski Gasket*, 2004. preprint, University of Michigan REU project.

[17] Benoît Mandelbrot, *How Long Is the Coast of Britain? Statistical Self-Similarity and Fractional Dimension.*

[18] John Meier, *Groups, Graphs and Trees*, Cambridge University Press, 2008. Cambridge Books Online.

[19] John Milnor, *Dynamics in One Complex Variable*, Princeton University Press, Princeton, 2006.

[20] D. Mumford, C. Series, and D. Wright, *Indra's Pearls: The Vision of Felix Klein*, Indra's Pearls: The Vision of Felix Klein, Cambridge University Press, 2002.

[21] James Munkres, *Topology*, Pearson Prentice Hall, New Jersey, 2000.

[22] Richard S Palais, *A simple proof of the Banach contraction principle*, Journal of Fixed Point Theory and Applications **2** (2007), no. 2, 221–223.

[23] C.C. Pugh, *Real Mathematical Analysis*, Undergraduate Texts in Mathematics, Springer New York, 2013.

[24] Joseph J. Rotman, *An Introduction to the Theory of Groups*, Graduate Texts in Mathematics, Springer, 1995.

[25] Will Smith, *Thompson-Like Groups for Dendrite Julia Sets* (2013). senior thesis.

[26] Jasper Weinrich-Burd, *A Thompson-Like Group for the Bubble Bath Julia Set* (2013). senior thesis.